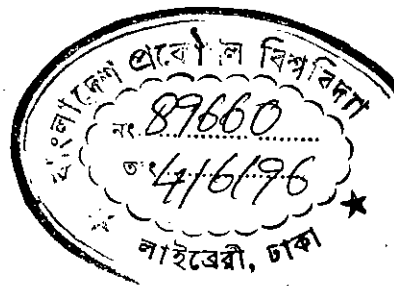


PERFORMANCE STUDY OF OPTICAL TRANSMISSION SYSTEM WITH FIBER NON-LINEARITIES

NAROTTAM KUMAR DAS



DEPARTMENT OF ELECTRICAL AND ELECTRONIC ENGINEERING
BANGLADESH UNIVERSITY OF ENGINEERING AND TECHNOLOGY (BUET),
DHAKA - 1000, BANGLADESH.



#89660#

PERFORMANCE STUDY OF OPTICAL TRANSMISSION SYSTEM WITH FIBER NON-LINEARITIES

A Thesis submitted to the Department of
Electrical and Electronic Engineering,
Bangladesh University of Engineering and
Technology (BUET), Dhaka, Bangladesh,
in partial fulfillment of the
requirements for the degree of
Master of Science in Engineering
(Electrical and Electronic)

NAROTTAM KUMAR DAS

May 1996

Dedicated to

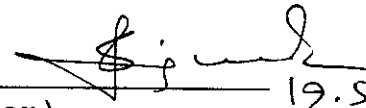
My Parents

APPROVAL

The thesis titled **"Performance Study Of Optical Transmission System With Fiber Non-Linearities"** submitted by Narottam Kumar Das, Roll no. 911350F, session 1989-90 to the Department of Electrical and Electronic Engineering, Bangladesh University of Engineering and technology (B.U.E.T.) has been accepted as satisfactory for partial fulfillment of the requirements for the degree of Master of Science in Engineering (Electrical and Electronic).

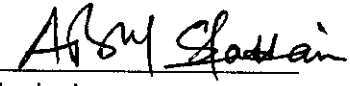
Board of Examiners

1. Dr. Satya Prasad Majumder
Associate Professor
Department of E.E.E.
B.U.E.T., Dhaka 1000.

Chairman 
(Supervisor)

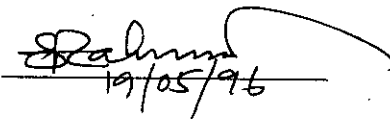
19.5.96

2. Dr. A. B. M. Siddique Hossain
Professor and Head
Department of E.E.E.
B.U.E.T., Dhaka 1000.

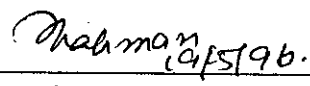
Member 
(Ex-officio)

19/05/96

3. Dr. Md. Saifur Rahman
Assistant Professor
Department of E.E.E.
B.U.E.T., Dhaka 1000.

Member 
19/05/96

4. Md. Mujibur Rahman
Divisional Engineer
BTTB Gulshan, Dhaka.

Member 
(External)

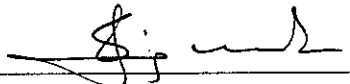
19/5/96

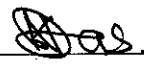
DECLARATION

This work has been done by me and it has not been submitted elsewhere for the award of any degree or diploma.

Counter-signed

Signature of the student


17.5.96
(Dr. Satya Prasad Majumder)


19.05.96
(Narottam Kumar Das)

CONTENTS

DEDICATION	(ii)
APPROVAL	(iii)
DECLARATION	(iv)
CONTENTS	(v)
ACKNOWLEDGEMENT	(vii)
ABSTRACT	(viii)
LIST OF FIGURES	(ix)
LIST OF PRINCIPAL SYMBOLS	(xv)
LIST OF ABBREVIATIONS	(xix)

Chapter I: INTRODUCTION

1.1 Introduction and Historical Background of Fiber Optic Communication	1
1.2 Advantages of Optical Fiber Communication	3
1.3 Detection Schemes	4
1.4 Limitations of Optical Fiber Communication Systems	6
1.5 The Objective of this Thesis	12
1.6 Brief Introduction to this Thesis	13

Chapter II: PERFORMANCE ANALYSIS OF MULTIWAVELENGTH OPTICAL TRANSPORT NETWORK

2.1 Introduction	14
2.2 System Architecture	16

2.3	Transmitter and Receiver Models	18
2.4	Theoretical Analysis of Coherent Optical Multiwavelength Transmission System	22
2.4.1	The Optical Signal	22
2.4.2	Output Phase of IF Filter	25
2.4.3	Data Decision	31
2.4.4	Probability of Bit Error	34

Chapter III: RESULTS AND DISCUSSIONS 37

Chapter IV: CONCLUSIONS AND SUGGESTIONS

4.1	Conclusions	78
4.2	Suggestions	79

REFERENCES 81

APPENDIX - A	A-1
APPENDIX - B	B-1
APPENDIX - C	C-1
APPENDIX - D	D-1

ACKNOWLEDGEMENT

The Author expresses his sincere and profound gratitude to Dr. Satya Prasad Majumder, Associate Professor, Department of Electrical and electronic Engineering, Bangladesh University of Engineering and Technology (BUET), Dhaka for his incessant and meticulous guidance in completing this work. The author thanks him for his outstanding suggestions and help during vital phases of the work.

The author wishes to express his thanks and regards to Dr. A. B. M. Siddique Hossain, Professor and Head, Department of Electrical and Electronic Engineering, Bangladesh University of Engineering and Technology (BUET), for his encouragement and cooperation to complete this work successfully.

The author also wishes to express his thanks to Dr. Mohammad Ali Choudhury, Associate Professor, Department of Electrical and Electronic Engineering for his helpful suggestions. Sincerest thanks to Dr. Md. Bashir Uddin, Associate Professor, Department of Electrical and Electronic Engineering, Bangladesh Institute of Technology (BIT), Chittagong and all other friends and colleagues for their cooperation and encouragement.

Finally, the author would like to thank all the members of his family for their inspiration and encouragement and moral support.

ABSTRACT

A theoretical analysis for optical wavelength division multiplexed transmission system is presented considering a single building block of an optical mesh network consisting of optical amplifiers, optical multiplexers and demultiplexers, splitters, fiber protection switch etc. Continuous phase frequency shift keying (CPFSK) modulation of the transmitting laser is considered with heterodyne delay-demodulation reception. The analysis is carried out to evaluate the degrading effect of fiber non-linearities, viz. chromatic dispersion and four-wave mixing (FWM) on the overall system performance. The expressions for the probability density functions for the random phase fluctuations due to above non-linear effects at the output of the IF filter are analytically formulated.

The bit error rate (BER) performance of the system is evaluated at a bit rate of 2.5 Gb/s for practical values of the receiver and system parameters and the optimum system parameters viz. optimum channel separation, maximum number of nodes for a mesh network, optimum input transmitter power etc are also determined for reliable system performance.

LIST OF FIGURES

- Fig.2.1 Optical mesh network.
- Fig.2.2 Schematic of optical path between two consecutive nodes.
- Fig.2.3a Schematic diagram of a typical CPFSK-DD optical heterodyne receiver.
- Fig.2.3b Block diagram of an optical transmitter.
- Fig.3.1 Bit error rate (BER) performance of optical multiwavelength transport network (MWTN) at a bit rate of 2.5 Gb/s as a function of the number of nodes M when number of channels $N=11$, fiber span $L=20$ Km, optical bandwidth $B_o=6B_r=15$ GHz and $P_{FWM}=0.0$ for three different values of the optical transmitter power P_{in} (dBm).
- Fig.3.2 Bit error rate (BER) performance of optical MWTN at a bit rate of 2.5 Gb/s as a function of the number of nodes M when number of channels $N=11$, fiber span $L=50$ Km, optical bandwidth $B_o=6B_r=15$ GHz and $P_{FWM}=0.0$ for three different values of the optical transmitter power P_{in} (dBm).
- Fig.3.3 Bit error rate (BER) performance of optical MWTN at a bit rate of 2.5 Gb/s as a function of the number of nodes M when number of channels $N=11$, fiber span $L=100$ Km, optical bandwidth $B_o=6B_r=15$ GHz and $P_{FWM}=0.0$ for three different values of the optical transmitter power P_{in} (dBm).
- Fig.3.4 Bit error rate (BER) performance of optical MWTN at a bit rate of 2.5 Gb/s as a function of the number of nodes M when number of channels $N=11$, fiber span $L=100$ Km, $B_o=10B_r=25$ GHz and $P_{FWM}=0.0$ for three different values of the optical transmitter power P_{in} (dBm).

Fig.3.5 Bit error rate (BER) performance of optical MWTN at a bit rate of 2.5 Gb/s as a function of the number of nodes M when number of channels $N=11$, fiber span $L=100$ Km, $B_o=20Br=50$ GHz and $P_{\text{FWM}}=0.0$ for three different values of the optical transmitter power P_{in} (dBm).

Fig.3.6 Plots of allowable maximum number of nodes M corresponding to BER of 10^{-9} as a function of the input transmitter power P_{in} (dBm) at a bit rate of 2.5 Gb/s and optical bandwidth $B_o=6Br=15$ GHz for three values of the fiber span $L=20$ Km, $L=50$ Km and $L=100$ Km, and $P_{\text{FWM}}=0.0$.

Fig.3.7 Plots of allowable maximum number of nodes M corresponding to BER of 10^{-9} as a function of the input transmitter power P_{in} (dBm) at a bit rate of 2.5 Gb/s and optical bandwidth $B_o=10Br=25$ GHz for three values of the fiber span $L=20$ Km, $L=50$ Km and $L=100$ Km, and $P_{\text{FWM}}=0.0$.

Fig.3.8 Plots of allowable maximum number of nodes M corresponding to BER of 10^{-9} as a function of the input transmitter power P_{in} (dBm) at a bit rate of 2.5 Gb/s and optical bandwidth $B_o=20Br=50$ GHz for three values of the fiber span $L=20$ Km, $L=50$ Km and $L=100$ Km, and $P_{\text{FWM}}=0.0$.

Fig.3.9 Variation of the allowable maximum number of nodes M as a function of optical bandwidth B_o for three values of the transmitter power P_{in} (dBm) at BER= 10^{-9} , $P_{\text{FWM}}=0.0$ and fiber span $L=20$ Km.

Fig.3.10 Variation of the allowable maximum number of nodes M as a function of optical bandwidth B_o for three values of the transmitter power P_{in} (dBm) at BER= 10^{-9} , $P_{\text{FWM}}=0.0$ and fiber span $L=50$ Km.

Fif.3.11 Variation of the allowable maximum number of nodes M as a function of optical bandwidth B_o for three values of the transmitter power P_{in} (dBm) at BER= 10^{-9} , $P_{\text{FWM}}=0.0$ and fiber span $L=100$ Km.

- Fig.3.12 Bit error rate (BER) performance of optical MWTN versus number of nodes M , at a bit rate of 2.5 Gb/s for transmitter power $P_{in} = -5$ dBm and number of channels $N=11, 51, 101$ with $L=20$ Km and $B_o=6Br=15$ GHz.
- Fig.3.13 Bit error rate (BER) performance of optical MWTN versus number of nodes M , at a bit rate of 2.5 Gb/s for transmitter power $P_{in} = -2.5$ dBm and number of channels $N=11, 51, 101$ with $L=20$ Km and $B_o=6Br=15$ GHz.
- Fig.3.14 Bit error rate (BER) performance of optical MWTN versus number of nodes M , at a bit rate of 2.5 Gb/s for transmitter power $P_{in} = -5$ dBm and number of channels $N = 11$ and 51 with $L=50$ Km and $B_o=6Br=15$ GHz.
- Fig.3.15 Bit error rate (BER) performance of optical MWTN versus number of nodes M , at a bit rate of 2.5 Gb/s for transmitter power $P_{in} = -2.5$ dBm and number of channels $N = 11$ and 51 with $L=50$ Km and $B_o=6Br=15$ GHz.
- Fig.3.16 Plots of maximum allowable number of nodes M corresponding to BER of 10^{-9} as a function of the input transmitter power P_{in} (dBm) in the presence of four-wave mixing (FWM) effect at a bit rate of 2.5 Gb/s with optical bandwidth $B_o=6Br=15$ GHz and fiber span $L=20$ Km for number of channels $N = 11, 51, 101$ and channel separation $\Delta f=10$ GHz.
- Fig.3.17 Plots of maximum allowable number of nodes M corresponding to BER of 10^{-9} as a function of the input transmitter power P_{in} (dBm) in the presence of four-wave mixing (FWM) effect at a bit rate of 2.5 Gb/s with optical bandwidth $B_o=6Br=15$ GHz and fiber span $L=50$ Km for number of channels $N=11$ and 51 and channel separation $\Delta f=10$ GHz.

- Fig.3.18 Plots of maximum allowable number of nodes M corresponding to BER of 10^{-9} as a function of the input transmitter power P_{in} (dBm) in the presence of four-wave mixing (FWM) effect at a bit rate of 2.5 Gb/s with optical bandwidth $B_o=6Br=15$ GHz and fiber span $L=100$ Km for number of channels $N=11, 51, 101$ and channel separation $\Delta f=10$ GHz.
- Fig.3.19 Plots of maximum allowable number of nodes M corresponding to BER of 10^{-9} as a function of the input transmitter power P_{in} (dBm) in the presence of four-wave mixing (FWM) effect at a bit rate of 2.5 Gb/s with optical bandwidth $B_o=10Br=25$ GHz and fiber span $L=50$ Km for number of channels $N=11, 51, 101$ and channel separation $\Delta f=10$ GHz.
- Fig.3.20 Plots of maximum allowable number of nodes M corresponding to BER of 10^{-9} as a function of the input transmitter power P_{in} (dBm) in the presence of four-wave mixing (FWM) effect at a bit rate of 2.5 Gb/s with optical bandwidth $B_o=20Br=50$ GHz and fiber span $L=50$ Km for number of channels $N=11, 51, 101$ and channel separation $\Delta f=10$ GHz.
- Fig.3.21 Variation of the allowable number of nodes M at $BER=10^{-9}$ versus the transmitter power P_{in} (dBm) in the presence of FWM effect when the number of channels $N=11$ and 51 and channel separation $\Delta f=50$ GHz, $B_o=15$ GHz and fiber span, $L=20$ Km.
- Fig.3.22 Plots of maximum allowable number of nodes M in presence of FWM effect at a bit error rate (BER) of 10^{-9} as a function of the number of WDM channels, N when channel separation is 10 GHz and $L=20$ Km for different values of transmitter power P_{in} (dBm).

- Fig.3.23 Plots of maximum allowable number of nodes M in presence of FWM effect at a bit error rate (BER) of 10^{-9} as a function of the number of WDM channels, N when channel separation is 10 GHz and $L=100$ Km for different values of transmitter power P_{in} (dBm).
- Fig.3.24 Plots of maximum allowable number of nodes M in presence of FWM effect at a bit error rate (BER) of 10^{-9} as a function of the number of WDM channels, N when channel separation is 10 GHz and $L=50$ Km and $B_o=10B_r=25$ GHz for different values of transmitter power P_{in} (dBm).
- Fig.3.25 Plots of the allowable maximum number of nodes M_{max} at $BER=10^{-9}$ as a function of channel separation Δf in the presence of FWM effect when the number of WDM channels $N=11$ and fiber span $L=50$ Km for $P_{in} = -2.5, -5.0, -7.5$ dBm.
- Fig.3.26 Plots of the allowable maximum number of nodes M_{max} at $BER=10^{-9}$ as a function of channel separation Δf in the presence of FWM effect when the number of WDM channels $N=51$ and fiber span $L=50$ Km for $P_{in} = -2.5, -5.0, -7.5$ dBm.
- Fig.3.27 Plots of the ultimate maximum number of nodes M_{max} , versus optical bandwidth B_o (GHz) at $BER=10^{-9}$ in the presence of FWM effect for three different values of the number of WDM channels $N=11, 51, 101$ when fiber span $L=50$ Km and channel separation $\Delta f=25$ GHz.
- Fig.3.28 Plots of maximum allowable laser transmitter power $P_{in(max)}$ corresponding to the ultimate maximum number of nodes M_{max} at $BER=10^{-9}$ versus optical bandwidth B_o (GHz) in the presence of FWM effect when fiber span $L=50$ Km for the number of WDM channels $N=11, 51, 101$ and channel separation $\Delta f=25$ GHz.

- Fig.3.29 Plots of maximum allowable laser transmitter power $P_{in(max)}$ versus number of WDM channels N for three values of optical bandwidth $B_o=15, 25, 50$ GHz at $BER=10^{-9}$ in the presence of FWM effect and fiber span $L=50$ Km and channel separation $\Delta f=25$ GHz.
- Fig.3.30 Plots of maximum allowable ultimate number of nodes M_{max} versus number of WDM channels N for three values of optical bandwidth $B_o=15, 25, 50$ GHz at $BER=10^{-9}$ in the presence of FWM effect and fiber span $L=50$ Km and channel separation $\Delta f=25$ GHz.
- Fig.3.31 Plots of the ultimate maximum number of nodes M_{max} , versus number of WDM channels N at $BER=10^{-9}$ for fiber span $L=20$ Km, 50 Km and 100 Km when optical bandwidth $B_o=15$ GHz and channel separation $\Delta f=25$ GHz.
- Fig.3.32 Plots of maximum allowable laser transmitter power P_{in} (dBm) corresponding to the ultimate maximum number of nodes M_{max} at $BER=10^{-9}$ versus number of WDM channels N for fiber span $L=20$ Km, 50 Km and 100 Km when optical bandwidth $B_o=15$ GHz and channel separation $\Delta f=25$ GHz.

LIST OF PRINCIPAL SYMBOLS

nm = Nano meter

dB = Decibel

μm = Micro meter

$e_s(t)$ = Output of the laser transmitter signal

P_s = Optical signal power

ω_s = Angular frequency of the optical carrier

ϕ_s = Angle modulation

$e_o(t)$ = Optical amplifier output signal

$e_{\text{ASE}}(t)$ = Optical amplifier's spontaneous emission

$e_{\text{FWM}}(t)$ = FWM output signal

P_{pqr} = FWM power generated within the fiber

f_{pqr} = FWM frequency

f_p = Carrier frequency of the p-th channel

f_q = Carrier frequency of the q-th channel

f_r = Carrier frequency of the r-th channel

$E(t)$ = Total optical field at the output of the fiber

$h(t)$ = Low-pass equivalent impulse response of the fiber

F^{-1} = Inverse Fourier transform

$H(f)$ = Transfer function of the optical fiber span

D_c = Fiber chromatic dispersion factor

L = Fiber length / span

λ = Optical wavelength of the desired channel

C = Velocity of light

$E_{LO}(t)$ = Local oscillator signal
 P_{LO} = Local oscillator power
 f_{LO} = Local oscillator frequency
 R_L = Receiver load resistance
 K = Boltzmann's constant
 T = Receiver temperature
 B = Receiver bandwidth
 $n(t)$ = Total noise
 $\phi_d(t)$ = Additive phase noise due to fiber chromatic dispersion
 $\Psi(t)$ = Output phase
 $n_o(t)$ = Filtered additive noise
 σ^2 = Variance of total noise power
 $\Theta_t(t)$ = Total phase noise
 $\Delta\Psi_t$ = Accumulated phase over the demodulation interval
 $\Delta\Psi_T$ = Total accumulated phase over the demodulation interval
 h = Modulation index
 τ = Delay time
 $*$ = Complex conjugate
 K^2 = Correlation co-efficient
 $E[.]$ = Mathematical expectation
 B_{eq} = Equivalent bandwidth
 $I_0(.)$ = Zero-order modified Bessel function
pdf = Probability density function
 $P(\Delta\Psi_t)$ = The pdf of $\Delta\Psi_t$
 \otimes = Convolution

$P_e | \Delta \Psi_T$ = Error probability condition on $\Delta \Psi_T$
 β = Linewidth of laser
 $f_i (i=p,q,r)$ = Optical frequency of the i -th channel
 χ = Nonlinear susceptibility
 A_{eff} = Effective core area
 r = Modified radius
 W = Modified diameter
 α = Attenuation of fiber
 l = Fiber length
 L_{eff} = Effective fiber length
 Δf = Frequency separation between two adjacent channels
 B_e = Bandwidth of IF filter
 B_0 = Bandwidth of optical amplifier
 I_{sp} = Spontaneous emission current
 I_{FWM} = Detector current due to FWM power
 R_d = Responsivity of photodetector (A/W)
 N_0 = Power spectral density of spontaneous emission
 N_{sp} = Spontaneous emission factor
 G = Gain of optical amplifier
 h = Plank's constant
 ν = Frequency of optical carrier
 P_{sp} = Optical amplifiers spontaneous emission (ASE) power
 I_{LO} = Detector current due to P_{LO}
 I_s = Signal current due to P_{in}
 N_{0-LOSP} = PSD of optical oscillator-ASE beat noise

$N_{0\text{-ssp}}$ = PSD of optical signal-ASE beat noise

$G_{\text{LO-PN}}(f)$ = Phase noise corrupted spectrum of LO signal

$G_{\text{PN}}(f-f_{\text{IF}})$ = Phase noise corrupted spectrum of LO signal

$G_{\text{FSK-PN}}(f)$ = Spectrum of phase noise corrupted FSK signal

$N_{\text{LO-FWM}}$ = PSD of LO-FWM beat noise

N_{FWM} = PSD of FWM power

$N_{\text{s-FWM}}$ = PSD of signal-FWM beat noise

$P_{\text{s-FWM}}$ = Signal FWM beat noise power

$P_{\text{sp-sp}}$ = ASE-ASE beat noise power

LIST OF ABBREVIATIONS

LASER = Light Amplification by Stimulated Emission of
Radiation

LD = Laser Diode

LED = Light Emitting Diode

LO = Local Oscillator

PIN = Positive Intrinsic Negative

PD = Photodiode

APD = Avalanche Photodiode

th = Thermal

FWM-sp = FWM Spontaneous Emission

LO-sp = LO Spontaneous Emission

ssp = Signal Spontaneous Emission

LO-FWM = Local Oscillator FWM

s-FWM = Signal FWM

sp-sp = Spontaneous-Spontaneous

WDM = Wavelength Division Multiplexing

IM/DD = Intensity Modulation Direct Detection

FDM = Frequency Division Multiplexing

FCD = Fiber Chromatic Dispersion

FWM = Four-Wave Mixing

DFWM = Degenerate FWM

SBS = Stimulated Brillouin Scattering

SRS = Stimulated Raman Scattering
RIN = Relative Intensity Noise
SPM = Signal Phase Modulation
ASE = Amplifier's Spontaneous Emission
DFWM = Degenerate Four-Wave Mixing
OFCD = Optical Frequency Division Multiplexing
ASK = Amplitude Shift Keying
DPSK = Differential Phase Shift Keying
FSK = Frequency Shift Keying
CPFSK = Continuous Phase FSK
BER = Bit Error Rate
Km = Kilometer
MUX = Multiplexer
DMUX = Demultiplexer
W = Fiber Core Diameter
MWTN = Multiwavelength Transport Network.

CHAPTER - I

INTRODUCTION



1.1 Introduction and Historical Background of Fiber Optic Communication:

Since the early seventies, optical fibers have been seriously considered as a long range communication medium. Several fabrication techniques and specialized optical sources and detectors have been developed. Huge reductions in material attenuation have been obtained. It has been established that as compared to metal conductors / waveguides, size for size, optical fibers offer greater information capacity arising from a higher carrier frequency and lower material costs. Because of these reasons, during the last two decades there have been considerable advancements in the field of optical communication both in theory and practice [1]. The period 1965 to 1975 was devoted to the development of graded index systems operating at bit rates in the range of 8-140 Mbits and at wavelengths of 850-900 nm. However, the shortcomings of graded index fibers were soon apparent and by 1978 research had commenced on single mode fiber technology. This rapidly led to the establishment

of 1300 nm single mode fiber design and system specifications for 140 Mbit/s operation. Recently, the scientists have started working at 1500 nm range for long haul systems and coherent detection systems [1-2].

Optical fiber communication technology has today permeated almost every field of modern society. In less than three decades, it has emerged from a mere theoretical concept to a commercial viability. Today, there is hardly any communication field where fiber optics has not left its mark. The need for and means of communication have always existed in human society. What we are observing today is a kind of communication revolution where information is created, managed, processed and distributed. This revolution is leading the society to an integrated global network that will carry the information in the form of video, data and voice channels across national boundaries, transferring the globe into a local network, overcoming time and distance and changing the overall concept of communication, business and ways of life.

The development of LASER in 1960 was a landmark for optical fiber communication using coherent light signal. Discovery of gas and solid state lasers gave impetus for fiber optic communication technology developments. Though these initial lasers had poor life times and were required to work

at low temperature, today lasers have projected lifetimes of up to 10 years at room temperature and above. Accessibility of light emitting diodes (LED) to transfer an electrical signal into light energy, and PIN and avalanche photodiode (APD) to detect light signals and turn them back into electrical information have made fiber optic communication system simple and efficient [3].

1.2 Advantages of Optical Fiber Communication:

In addition to the advantages of having extra information bandwidth using light as a carrier signal, the optical fiber communication systems have several other advantages over the conventional systems.

(a) Extra advantages of having low weight and small in size.

(b) The immunity to ambient electrical noise, ringing echoes or electromagnetic interference.

(c) No hazards of short circuits as in metal wires.

(d) No problems when used in explosive environments.

(e) Immunity to adverse temperature and moisture conditions.

(f) Lower cost of cables per unit length compared to that

of metal counter-part.

(g) No need for additional equipment to protect against grounding and voltage problems.

(h) Very nominal shipping, handling and installation costs.

Because of these advantages fiber optic communication is being currently utilized in telephones such as loops, trunks, terminals and exchanges, etc., computers, cable television, space vehicles, avionics, ships, submarine cable and security and dark systems, electronic instrumentation systems, medical systems, satellite ground stations and industrial automation and process controls. The coming development of integrated optic technology is hoped to play a bigger part in influencing further departures from existing concepts of electronic systems for communication, control and instrumentation.

1.3 Detection Schemes:

In optical communication system, there are two important detection schemes employed, viz, the intensity modulation direct detection (IM/DD) and coherent detection [4-5]. In the direct detection scheme, the intensity of received optical field is directly converted to a current by a photodetector. The sensitivity of an ideal direct detection

receiver is determined by the statistical distribution of the detected photons. At higher data rates the performance of the practical direct detection receiver deviates further from the quantum limited case since the electronic preamplifier usually has a rising noise versus frequency characteristic. Therefore, coherent detection will be beneficial for high capacity systems working at the longer wavelengths.

Coherent optical (light) detection is the optical analogy of superheterodyne radio detection. Thus a coherent light receiver first converts the incoming signal from the optical regime down to the radio regime and then uses conventional electronic circuitry to perform various signal processing operations such as amplification and demodulation. This technique has been able to provide large increases in receiver sensitivity (>20 dB) compared to what one could get with direct detection systems using avalanche photodiodes [4]. This technique is quite suitable in the wavelength range of 1.3 to 1.6 μm and capable of providing the 'quantum limit' of receiver sensitivity (10 photons/bit at 10^{-9} error rate). Since here the detection is shot noise limited rather than thermal noise limited, repeater spacing can be increased. It allows for the use of frequency and phase modulation of light. Also the generation of large number of closely spaced optical frequency division multiplexed (FDM) channels is possible [6].

The advantages of coherent detection system can be expressed in terms of improved receiver sensitivity. The performance of a coherent detection system is seriously affected by three important parameters, viz; (i) phase noise of transmitting and local oscillator laser (ii) extinction ratio of LD and (iii) the state of polarization of the received signal [4-7].

1.4 Limitations of Optical Fiber Communication Systems:

Though optical communication system is more advantageous, there are some limitations of optical fiber communication systems.

The important limit in optical communication is that the sensitivity of optical receiver is dictated by quantum effects. Other factors such as background light, dark current, post detection amplifier noise and transmitter imperfections also affect considerably the receiver sensitivity. The limits on channel are related to input coupling, loss and delay distortions.

Other limitations of optical transmission systems are due to the fiber chromatic dispersion (FCD), four-wave mixing (FWM) [7-16], Stimulated Brillouin Scattering (SBS), Stimulated Raman Scattering (SRS), phase noise of laser, Relative intensity noise (RIN), Signal phase modulation (SMP), Optical Amplifier's Spontaneous Emission (ASE), etc., [17-21].

Dispersion will play an increasing role on the overall system performance in future high-speed systems. Dispersion is an important characterization factor of optical fiber as it determines the distortion of the output signals launched into the fiber. These in effect modifies the actual information carrying capacity or bit rate of the optical fiber. The dispersion in optical fiber may arise due to various reasons and in practice three main factors have been analyzed [9,15] namely:-

- (i) material dispersion,
- (ii) waveguide dispersion and
- (iii) differential group delay or intermodal (or simply modal) dispersion.

The effect of chromatic dispersion can be overcome to some extent by dispersion compensation device which is based on differential time delay for the upper and the lower side band of the modulated signal [19].

Four-wave mixing (FWM) phenomenon is one of the important limiting factors in multichannel transmission systems. Four-wave mixing (FWM) refers to the process in which three input optical waves interact in a medium and generate a fourth wave [7-16]. The combined interference and diffraction effect therefore corresponds to four wave mixing (FWM) in the language of non-linear optics. The process is called degenerate if the frequencies of the three incident waves and the generated wave are equal. Degenerate four-wave mixing (DFWM) is a simple method to achieve phase conjugation i.e., to generate a wave with a phase which is the complex conjugate of one of the incident waves. In optical fiber transmission lines with optical in-line amplifiers, the generated FWM light accumulates and seriously influences system performance [10-11,13]. Several studies have been reported on the influence of fiber four-wave mixing effect on multichannel systems [7-16]. FWM process, as well as Stimulated Brillouin Scattering (SBS) has the potential to influence significantly the operation of optical transmission systems using narrow-linewidth single frequency laser. In the coherent transmission systems employing frequency division multiplexing (FDM), it is necessary to determine the channel frequency separation at the operating wavelength of the system. FWM process depends on the channel frequency separation, fiber chromatic dispersion and the fiber length.

Dense wavelength division multiplexing (WDM) or optical frequency division multiplexing (FDM) techniques have been intensely studied for future lightwave communications systems, including subscriber and trunk transmission networks. The theoretical and experimental results of the effects of FWM in OFDM system were reported by Maeda et al [8]. The theoretical expression for FWM power was presented to demonstrate the dependence of FWM power on various system parameters and the experimental results were provided and the system performance degradation due to FWM crosstalk in a 16-channel coherent system were described.

Litchman [11] has reported the bit-rate distance product limitations due to fiber non-linearities viz. SBS, FWM and dispersion limits in multichannel coherent optical communication system.

The theoretical performance limitations due to fiber chromatic dispersion on coherent ASK and DPSK system was reported by Elrefaie et al [9]. The experimental results of chromatic dispersion limitations on direct detection FSK and DPSK system was also reported [15].

The effect of FWM on direct detection FSK and FDM system is reported by Toba et al [6] with some experimental

demonstrations. The amount of crosstalk due to FWM is evaluated both theoretically and experimentally.

The traditional way of compensating for optical loss in lightwave communication systems has been the rather cumbersome procedure of regeneration. Regeneration includes photon-electron conversion, electrical amplification, retiming, pulse shaping and finally electron-photon conversion. In many applications, direct optical amplification of the light signal would be advantageous. Optical amplifiers can be used in any system that is loss limited: i.e., dispersion effects are a limiting factor. This is the case for most systems operating near the dispersion minimum at $1.3\mu\text{m}$, and the coherent lightwave systems with local area networks (LAN), where the main losses are from branching and taps, are also loss limited and can benefit from simple optical amplifiers.

Er^{3+} -doped fiber amplifiers are essentially promising because of their inherent matching to fiber lines, high output power, and insensitive to interchannel crosstalk compared to semiconductor laser amplifier (SLA) [20]. To date, several works have been reported for multichannel amplification using fiber amplifiers, such as investigations on interchannel modulation and mutual signal-gain saturation as well as demonstrations of 16-channel common amplification [20-21]. They

studied an Er^{3+} -doped fiber amplifier for multichannel systems, from the point of clarifying the ultimate capacity and the applicable number of channels.

Semiconductor laser amplifiers have been studied for a number of years. Significant work at 0.8- μm wavelength was done in the early 80's. Recently major progress has been made in long wavelength devices. Optical amplifiers with high gain, low gain ripple, low noise, and high saturation output power have been reported. Optical amplifier system applications have also been reported, both applications for preamplifiers and in-line amplifiers[20-21].

As optical amplifiers have advanced to the stage that actual system use might be possible in the near future, it is important to know the system consequences, its advantages and limitations. The theoretical as well as experimental investigations of optical amplifier lightwave systems are already reported [20-21]. Noise levels, bit-error-rate characteristics (BER), receiver sensitivities, and power penalties are calculated functions of the relevant optical amplifier parameters.

1.5 The objective of this Thesis:

The objectives of this thesis work are:

- (1) To develop a novel theoretical analysis for multiwavelength optical transmission system with CPFSK modulation and delay-demodulation heterodyne reception.
- (2) To carry out the analysis to include the effect of fiber non-linear effects, viz. four-wave mixing (FWM), chromatic dispersion etc. in the presence of receiver noise and photodetector shot noise.
- (3) To evaluate the system performance at a bit rate of 2.5 Gb/s and determine the optimum system parameters, viz. optimum fiber span, optimum number of nodes, optimum bandwidth and channel separation, maximum allowable transmitter power and maximum number of channels that can be transmitted for reliable system performance.

1.6 Brief Introduction to this Thesis:

In chapter 1, a brief introduction and historical background of optical communication systems are discussed. The main features of optical communication systems are presented. A review of recent works in the related field, limitations of optical fiber communication systems are also presented.

In chapter 2, a novel theoretical analysis for multiwavelength optical transmission system is presented which accounts for the nonlinear effects of optical fibers on the system performance in the presence of receiver noise and photodetector shot noise.

Chapter 3 provides the performance results of multiwavelength optical transmission system for different sets of values of receiver and system parameters at a bit rate of 2.5 Gb/s.

A brief conclusion and suggestions for future work are presented in chapter 4.

CHAPTER - II

PERFORMANCE ANALYSIS OF MULTIWAVELENGTH OPTICAL TRANSPORT NETWORK

2.1 Introduction:

Telecommunication networks of the future must be capable of adapting to rapid changes in the network traffic requirements. This is a consequence of the introduction of a new narrowband and broadband services with, at present, uncertain demands of bitrates, signal formats, etc.. Today, the development of telecommunication networks is constrained by the influencible interference between the optical high-speed fiber interconnection networks, and the electronic terminals at switch nodes. The vast bandwidth potential of the optical fiber cannot be exploited easily since the existing electronic interface is designed for specific multiplexing schemes and bitrates. Therefore, post installation changes will be required which is expensive. Optical technologies may be employed to provide the required capacity and flexibility. Until now, advanced optical techniques for time switching and frequency switching are still immaturred compared to the electronic counterparts, whereas optical space switching and wavelength division multiplexing (WDM) [22] provide attractive solutions to some of the improved networking functions required.

The dimension of an optical network is limited by a number of effects, such as laser phase noise, Stimulated Brillouin Scattering (SBS), Stimulated Raman Scattering (SRS), Amplifier's Spontaneous Emission (ASE), laser saturation, reflection, jitter accumulation, signal bandwidth narrowing caused by filter concatenation and more prominently due to the fiber four-wave mixing (FWM). The effect of fiber four-wave mixing (FWM) depends on the number of wavelengths/channels transmitted, fiber chromatic dispersion, separation between two adjacent channel wavelengths, fiber span between two nodes, bandwidth of optical multi/demultiplexers etc.. Significant amount of research works have been carried out during the last few years to estimate the amount of FWM power and the crosstalk induced by FWM effect in multiwavelength optical networks [6,8, 10-15]. Crosstalk effects due to FWM in direct detection optical FSK multiwavelength optical transmission system is already reported [6]. A theoretical model of an optical network incorporating wavelength selective elements, amplifiers, couplers and switches is also reported where IM/DD technique is considered [23] and the network dimensions have been shown to be limited by the optical crosstalk in the switch matrices, the FWM effects and the polarization dependent loss in optical components. Although, the FWM power in a coherent multiwavelength transport network is experimentally reported [10-15], no theoretical analysis is yet reported which accounts for the above mentioned system imperfections on coherent multiwavelength optical transport network.

In this chapter, a novel theoretical analysis is provided for wavelength division multiplexed (WDM) coherent optical

transmission system considering a single network element or a building block for an optical mesh network. The analysis is carried out to evaluate the impact of fiber non-linear effects, viz. chromatic dispersion and fiber four-wave mixing on the overall system performance. Theoretical results based on the analysis is provided in the next chapter.

2.2 System Architecture:

A schematic architecture for the optical core network is shown in Fig. 2.1. The optical nodes are linked in a mesh configuration where transmission in opposite directions in the network is carried over two separate sub-networks. Optical isolators are assumed to eliminate problems caused by optical reflections. An optical path through the network will typically comprise a number of fiber transmission sections interconnected by optical network nodes incorporating optical space switches, optical amplifiers and WDM components. This network forms a high capacity optical transport layer of simple functionality with access to an electronic transport layer of limited bandwidth capable of providing a number of network management functions, drop-insert of new channels, etc.. Each module in the optical network consists of a network node and a length of fiber. If operation of the single network elements is independent of the overall network architecture, this approach allows simple overall network configuration and ease of upgrade and extensions.

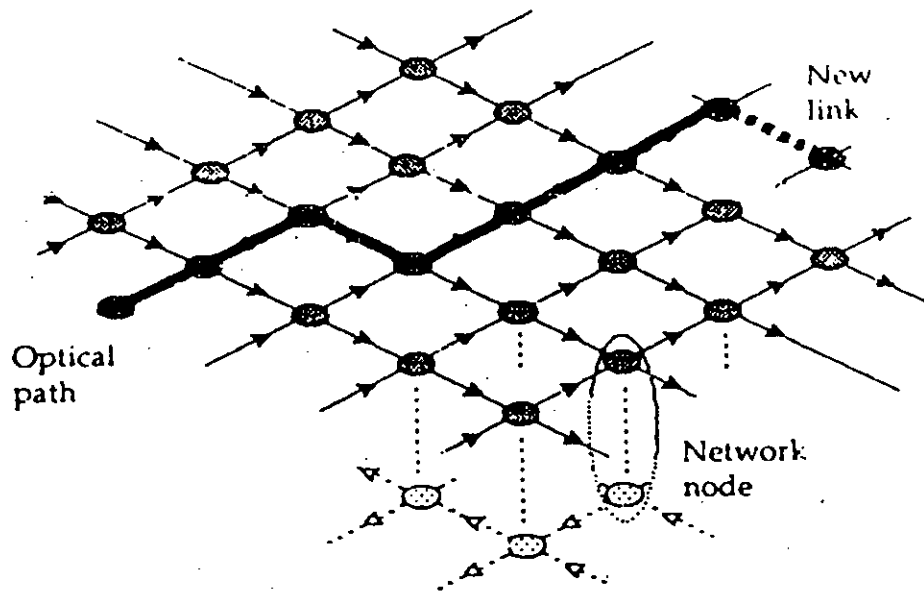


Fig.2.1 Optical mesh network.

In Fig. 2.2 a single network module (building block) is illustrated along with a schematic of an optical path through the network. An optical building block comprises wavelength selective elements for improved capacity and flexibility, amplifiers for signal level restoration, a splitter and a small switch for path protection, an optical crosspoint switch matrix, and a length of fiber for network node interconnection. The signals at the input and at the output of a network building block are to be maintained at the same level.

2.3 Transmitter and Receiver Models:

The transmitter and receiver models considered in the analysis is shown in Fig. 2.3. For each channel we consider CPFSK modulation of the transmitter DFB laser using direct frequency modulation of its driving current as shown in Fig.2.3(a).

In the receiver we consider heterodyne delay-demodulation reception. The model of the optical heterodyne delay-modulation receiver is shown in figure 2.3(b). The light source used by the transmitter is assumed to be a single-mode laser, and the receiver includes a similar laser as a local oscillator (LO). The received optical signal is mixed with the LO signal. The combined optical signal is detected by a PIN photodetector and thus a microwave intermediate frequency (IF) electrical signal is produced. During the conversion process, Gaussian noise is added in three ways, (i) shot noise produced in the process of

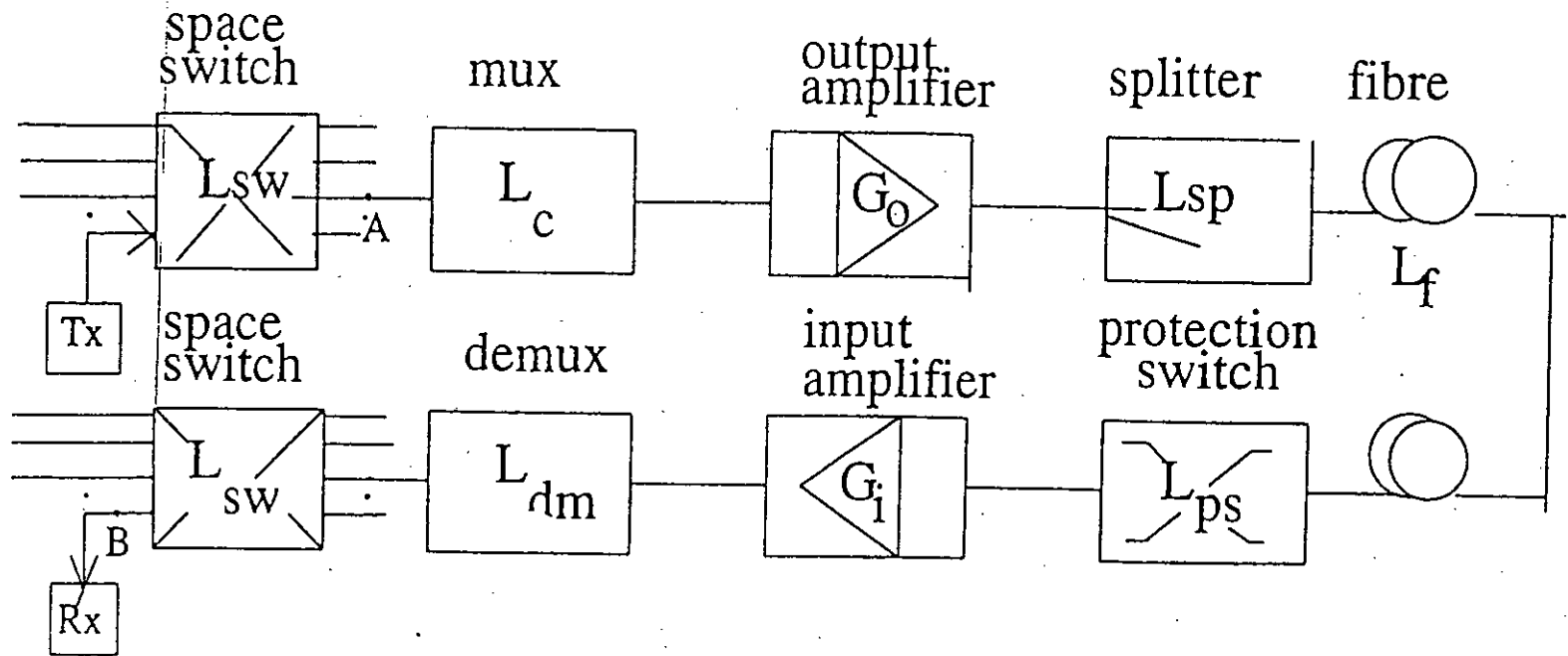


Fig.2.2 Schematic of optical path between two consecutive nodes.

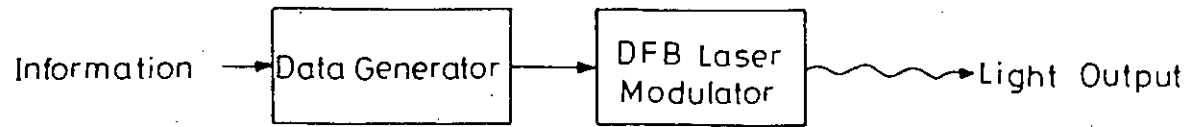


Fig.2.3a Block diagram of an optical transmitter.

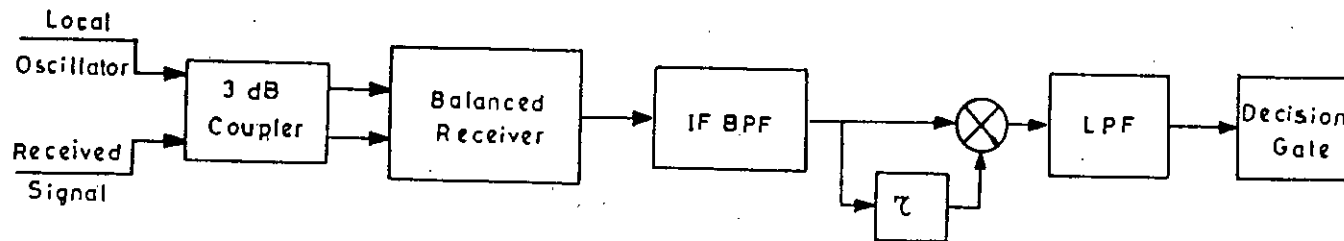


Fig.2.3b Schematic diagram of a typical CPFSK-DD optical heterodyne receiver.

photodetection, (ii) thermal noise introduced by the circuitry following the photodetector, and (iii) beat noise terms arising out from the beating of the signal, local oscillator power, FWM signal and optical amplifier's spontaneous emission (ASE) noise in the photodetection process.

The IF signal at the output of photodetector is filtered by a bandpass IF filter centered at the IF frequency. In the absence of laser phase noise and with ideal LD FM response, the optical IF filter would be a matched filter with integration time equal to bit period. With phase noise present, a shorter integration time and hence, a larger IF bandwidth ($B_{IF} > 1/T$) is required in situation experiencing non-zero IF linewidth and / or nonflat LD FM response.

After IF filtering, demodulation is performed by delay-demodulation technique. The signal and its time-delayed (τ sec. delay) version are multiplied. With certain conditions maintained, the polarity of the output signal, after passing through a low pass filter, contains the bit information. Data decision is made by using the polarity of this output signal.

2.4 Theoretical Analysis of Coherent Optical Multiwavelength Transmission System:

2.4.1 The Optical Signal:

The optical signal at the output of the laser transmitter can be expressed as

$$e_s(t) = \sqrt{2P_s} e^{j[\omega_s t + \phi_s(t) + \theta_{tr}(t)]} \quad (2.1)$$

where P_s is the optical signal power.

ω_s is the angular frequency of the optical carrier

θ_{tr} represents the phase noise of transmitting laser

and ϕ_s represents the angle modulation given by

$$\phi_s = 2\pi f_d \int_{-\infty}^t \sum_{k=-\infty}^{\infty} a_k \cdot P(t-kT) dt \quad (2.2)$$

where $P(t)$ is the phase shape, a_k is the k -th information bit, f_d is the peak frequency deviation and T is the bit period.

At the optical amplifier output, the signal is given by

$$e_o(t) = \sqrt{2GP_s} e^{j[\omega_s t + \phi_s(t) + \theta_{tr}(t)]} + e_{ASE}(t) \quad (2.3)$$

where G is the amplifier gain and

$e_{ASE}(t)$ is the optical amplifier's spontaneous emission signal which is given by [20]

$$e_{ASE}(t) = \sum_{K=-M}^M \sqrt{2N_0\delta\nu} e^{j[\omega_s t + 2\pi k\delta\nu t + \Omega_k]} \quad (2.4)$$

where $N_0 = N_{sp} (G - 1) h\nu$ is the power spectral density of ASE signal, N_{sp} is the spontaneous emission factor, $h\nu$ is the photon energy, $\delta\nu$ is the frequency separation between the discrete components of $e_{ASE}(t)$. Such that M becomes as integer $M = B_0/2\delta\nu$, B_0 is the bandwidth of optical amplifier and Ω_k is the random phase for each component of the spontaneous emission [20].

If the Four-wave mixing (FWM) power generated within the fiber, which falls on the desired signal channel frequency, is represented by P_{pqr} with frequency f_{pqr} , then the FWM signal is given by [8,10,13]

$$e_{FWM}(t) = \sum \sqrt{2P_{pqr}} \exp[j2\pi f_{pqr} t + \theta_{pqr}] \quad (2.5)$$

where, $f_{pqr} = f_p + f_q - f_r$, θ_{pqr} is the random phase of FWM signal and f_p , f_q and f_r represents the carrier frequency of the p-th, q-th, and r-th channel respectively. The expression for P_{pqr} is given in Appendix A.

The total optical field at the output of the fiber is given by

$$\begin{aligned} E(t) &= e_s(t) \otimes h(t) + e_{FWM}(t) + e_{ASE}(t) \\ &= \sqrt{2P_s} \exp[j2\pi f_s t + \phi_s'(t)] + e_{FWM}(t) + e_{ASE}(t) \end{aligned} \quad (2.6)$$

where \otimes denotes convolution, $h(t)$ is the low-pass equivalent

impulse response of the fiber and

$$\phi_s'(t) = \phi_s(t) \otimes h(t)$$

$$h(t) = F^{-1}[H(f)]$$

where F^{-1} denotes inverse Fourier transform and $H(f)$ is the transfer function of the optical fiber span and is given by filter [9]

$$H(f) = e^{-j\alpha f^2} \quad (2.7)$$

where $\alpha = \pi D_c L \lambda^2 / c$, D_c is the fiber chromatic dispersion factor, L is the fiber length, λ is the optical wavelength of the desired channel and c is the velocity of light.

Now $\phi_s'(t)$ can be expressed as [24]

$$\begin{aligned} \phi_s'(t) &= 2\pi f_d \cdot \int_{-\infty}^t \sum_{k=-\infty}^{\infty} a_k P(t-kT) \otimes h(t) dt \\ &= 2\pi f_d \cdot \int_{-\infty}^t \sum_{k=-\infty}^{\infty} a_k p'(t - kT) dt \end{aligned} \quad (2.8)$$

where $p'(t) = p(t) \otimes h(t)$

The Local oscillator (LO) signal, with power P_{LO} and frequency f_{LO} , is given by

$$E_{LO}(t) = \sqrt{2P_{LO}} \exp[j2\pi f_{LO}t + \theta_{LO}] \quad (2.9)$$

Following Appendix B, the IF signal $r(t)$ can be written as

$$r(t) = A \cos[\omega_{IF}t + \phi_s'(t) + \phi_{FWM} + \theta_t(t)] + n(t) \quad (2.10)$$

where R_L is the receiver load resistance, K is the Boltzmann's constant, T is the receiver temperature in $^{\circ}K$ and B is the receiver bandwidth, $\theta_t(t)$ is the composite phase noise of transmitting and LO laser, and $n(t)$ is the total noise and ϕ_{FWM} and A are given by

$$\phi_{FWM} = \tan^{-1} \frac{\sqrt{P_{FWM} P_{LO}} \sin \theta_{PQT}}{\sqrt{P_s P_{LO}} + \sqrt{P_{FWM} P_{LO}} \cos \theta_{PQT}} \quad (2.11)$$

$$A = 2R_d \sqrt{(\sqrt{P_s P_{LO}} + \sqrt{2P_{FWM} P_{LO}} \cos \theta_{PQT})^2 + (\sqrt{2P_{FWM} P_{LO}} \sin \theta_{PQT})^2} \quad (2.12)$$

2.4.2 Output Phase of IF Filter:

The IF signal at the output of P.D. (input to IF filter) is

$$r(t) = A \cos[2\pi f_{IF}t + \phi(t)] + n(t) \quad (2.13)$$

where

$$\phi(t) = \phi_{FWM}(t) + \phi_s'(t) + \theta_t(t)$$

and

$$\phi_s'(t) = \pm 2\pi f_d t + \phi_d(t) \quad (2.14)$$

$$\phi_d(t) = 2\pi f_d \cdot \int_{-\infty}^t \sum_{k \neq 0} a_k p'(t - kT) dt \quad (2.15)$$

where $\phi(t)$ represents the additive phase noise due to fiber chromatic dispersion.

We assume the IF filter to be a bandpass filter centered about f_{IF} with bandwidth $2B$, where B is the bandwidth of the transmitted signal. The above equation is a realistic value for practical values of laser linewidths $BT=2$ is good for a practical choice [5,25].

The output of the IF filter can be written as,

$$\begin{aligned}
 y(t) &= r(t) \otimes q(t) + n_o(t) \\
 &= \int_t^{\infty} q(t) r(t - t') dt' + n_o(t) \\
 &= A(t) \cos[2\pi f_{IF}t + \psi(t)] + n_o(t)
 \end{aligned} \tag{2.16}$$

where $\psi(t)$ is the output phase and $n_o(t)$ is the filtered additive noise with variance σ^2 , $q(t) = F^{-1} [Q(f)]$ is the impulse response of IF filter.

The IF signal-to-noise ratio (IF SNR) can be defined as

$$IF\ SNR = \frac{A^2}{2\sigma^2} \tag{2.17}$$

where σ^2 is the variance of total noise $n(t)$.

The total noise power σ^2 is given by

$$\sigma^2 = P_{shot} + P_{th} + P_{FWM-sp} + P_{LO-sp} + P_{ssp} + P_{LO-FWM} + P_{s-FWM} + P_{sp-sp} \quad (2.18)$$

where P_{FWM-sp} , represents the FWM-spontaneous emission beat noise power, P_{LO-sp} is the local-oscillator-spontaneous emission beat noise power, P_{ssp} is the power of signal-spontaneous emission beat noise, P_{LO-FWM} is the local-oscillator-FWM beat noise power, P_{s-FWM} is the signal-FWM beat noise power and P_{sp-sp} is the spontaneous-spontaneous beat noise power. The expressions for these above noise powers are given in Appendix C.

Defining the normalized equivalent baseband filter impulse response as

$$h_{IF}(t) = \frac{q(t)}{Q(f_{IF})} \cdot e^{-j2\pi f_{IF}t} \quad (2.19)$$

where, $h_{IF}(t)$ is complex if $Q(f)$ is not symmetrical around f_{IF} i.e., if the IF filter is not symmetric.

According to Bedrosian and Rice [24] showed that the output phase process can be written as

$$\psi(t) = \text{Re}[h_{IF}(t) \otimes \phi'(t)] + \sum_{n=2}^{\infty} \frac{1}{n!} I_n[j^n f_n] \quad (2.20)$$

In the above equation (2.20) the first term represents linear filtering of the input phase $\phi'(t)$ and the summation represents various orders of distortion introduced by the filter. Assuming that the linear filtering term dominates, we get the output phase process relative to the carrier phase of the IF filter output, as

$$\begin{aligned}
\psi(t) &= h_{IF}(t) \otimes \phi'(t) \\
&= h_{IF}(t) \otimes \phi(t) + h_{IF}(t) \otimes \theta_c(t) \\
&= h_{IF}(t) \otimes \phi_d(t) + h_{IF}(t) \otimes \phi_{FWM}(t) + h_{IF}(t) \otimes \theta_c(t) \\
&= h_{IF}(t) \otimes 2\pi f_d \int_{-\infty}^t \sum_{k=-\infty}^{\infty} a_k \cdot p'(t - kT) dt \\
&\quad + h_{IF}(t) \otimes \phi_{FWM}(t) + h_{IF}(t) \otimes \theta_c(t) \\
&= 2\pi f_d \cdot \int_{-\infty}^t \sum_{k=-\infty}^{\infty} a_k \cdot g(t - kT) dt + \alpha_{FWM}(t) \\
&\quad + \theta_n(t)
\end{aligned} \tag{2.21}$$

Where \otimes denotes convolution and

$$g(t - kT) = h_{IF}(t) \otimes p'(t - kT) \tag{2.21a}$$

$$\alpha_{FWM}(t) = h_{IF}(t) \otimes \phi_{FWM}(t) \tag{2.21b}$$

$$\theta_n(t) = h_{IF}(t) \otimes \theta_c(t) \tag{2.21c}$$

$$\theta_c(t) = \theta_{tr}(t) + \theta_{LO}(t) \tag{2.21d}$$

Now, the accumulated phase over the demodulation interval with respect to IF carrier phase ($2\pi f_{IF}\tau$)

$$\begin{aligned}
\Delta\psi_\tau &= \psi(t) - \psi(t - \tau) \\
&= 2\pi f_d \cdot \int_{t-\tau}^t \sum_{k=-\infty}^{\infty} a_k \cdot g(t - kT) dt \\
&\quad + \alpha_{FWM}(t) - \alpha_{FWM}(t - \tau) \\
&\quad + \theta_n(t) - \theta_n(t - \tau)
\end{aligned} \tag{2.22}$$

The total accumulated phase over the demodulation interval can be written as in the following way, we have

$$\begin{aligned}
 \Delta\psi_T &= 2\pi f_{IF}\tau + \Delta\psi_\tau \\
 &= 2\pi f_{IF}\tau - 2\pi f_d\tau \\
 &\quad + 2\pi f_d\tau + \Delta\psi_\tau
 \end{aligned}
 \tag{2.23}$$

Hence putting the value of $\Delta\psi_\tau$ from equation (2.22), we have

$$\begin{aligned}
 \Delta\psi_T &= [2\pi f_{IF}\tau - 2\pi f_d\tau] \\
 &\quad + [2\pi f_d\tau + 2\pi \int_{t-\tau}^t f_d \sum_{k=-\infty}^{\infty} a_k \cdot g(t-kT) dt] \\
 &\quad + [\alpha_{FWM}(t) - \alpha_{FWM}(t - \tau)] + [\theta_n(t) - \theta_n(t - \tau)]
 \end{aligned}
 \tag{2.24}$$

The IF center frequency is adjusted such that

$$2\pi f_{IF}\tau = (m + 1/2)\pi, \quad m = 1, 2, \dots \tag{2.25}$$

Then, we get from the equation (2.25)

$$\begin{aligned}
\Delta\Psi_T = & \left[\left(m + \frac{1}{2}\right)\pi - \frac{\pi}{2} \right] \\
& + \left[2\pi f_d \tau + 2\pi \int_{t-\tau}^t f_d \sum_{k=-\infty}^{\infty} a_k \cdot g(t - kT) dt \right] \quad (2.26) \\
& + \left[\alpha_{FWM}(t) - \alpha_{FWM}(t - \tau) \right] \\
& + \left[\theta_n(t) - \theta_n(t - \tau) \right]
\end{aligned}$$

where $2\pi f_d \tau = \pi/2$, when modulation index satisfy the relation $h = T/2\tau$;

In the above equation (2.26).

(i) The first term represents the correct phase difference in an ideal case for desired frequency deviation when the transmitted bit is '1'.

(ii) The second term represents the phase distortion due to the effect of chromatic dispersion.

(iii) The third term represents the phase distortion due to FWM (four-wave mixing) phase noise.

(iv) The fourth or last term represents the phase distortion due to laser phase noise.

It is reported in Ref. [25] that noise correlation will be nonzero in a narrow deviation CPFSK-DD coherent optical receiver, and in particular, when using IF filters with a sharp cut-off and narrow bandwidth (tight-IF frequency), sensitivity penalties in excess of 0.5 dB have been demonstrated [25,26].

Because tight IF filtering will be an important requirement in dense optical WDM/FDM networks, we consider noise correlation at the filter output in presence of laser phase noise.

2.4.3 Data Decision:

Data Decision can be made using the polarity of the output signal $v_0(t)$. The polarity depends on the phase of the signal $v_0(t)$. When '1' is transmitted, the correct phase would be $(m + 1/2)\pi - \pi/2$, $m = 1, 2, \dots$. So, an error will occur if $-\pi < \Delta\psi_{\text{mod } 2\pi} < 0$. Similarly, an error will occur when '0' is transmitted if $0 < \Delta\psi_{\text{mod } 2\pi} < \pi$. That means, error will occur when $0 < |\Delta\psi_{\text{mod } 2\pi}| < \pi$.

Now, rewriting the equation (2.26), the total accumulated phase is

$$\begin{aligned}
 \Delta\psi_T &= \left[\left(m + \frac{1}{2}\right)\pi - \frac{\pi}{2} \right] \\
 &+ \left[2\pi f_d \tau + 2\pi a_o \int_{t-\tau}^t f_d \cdot g(t) dt \right. \\
 &+ \left. 2\pi \int_{t-\tau}^t f_d \sum_{k=-\infty}^{\infty} a_k \cdot g(t-kT) dt \right] \\
 &+ [\alpha_{FWM}(t) - \alpha_{FWM}(t - \tau)] \\
 &+ [\theta_n(t) - \theta_n(t - \tau)] \\
 &= \left(m + \frac{1}{2}\right)\pi + \phi_o + \Delta\phi_d + \Delta\alpha_{FWM} + \Delta\theta_n \\
 &= \psi_o + \Delta\psi
 \end{aligned} \tag{2.27}$$

where Σ' excludes $k = 0$. It is to be noted that the desired phase change over the demodulation period is distributed by the effect of fiber chromatic dispersion, laser phase noise and the phase noise due to FWM power.

At the decision moment t_n , the current waveform at the output of the LPF can be expressed as

$$y_0(t) = \frac{1}{2} \operatorname{Re}[z_1^* z_2] \quad (2.28)$$

where $*$ denotes complex conjugate, $z_1 = y(t_n)$, and $z_2 = -jy(t_n - \tau)$. Furthermore, the in-phase and quadrature components of the narrow-band Gaussian noise process $n_0(t)$ viz. $n_I(t)$, $n_Q(t)$, $n_I(t - \tau)$ and $n_Q(t - \tau)$, become Gaussian random variables with a correlation matrix [25].

$$R_n = \sigma^2 \begin{bmatrix} 1 & 0 & \rho & 0 \\ 0 & 1 & 0 & \rho \\ \rho & 0 & 1 & 0 \\ 0 & \rho & 0 & 1 \end{bmatrix} \quad (2.29)$$

where

$$\begin{aligned} \rho &= \frac{E[n_{I} n_{Id}]}{\sigma^2} \\ &= \frac{E[n_{Q} n_{Qd}]}{\sigma^2} \end{aligned} \quad (2.30)$$

$$K^2 = \frac{1+\rho}{1-\rho} \quad (2.31)$$

is the correlation co-efficient (which is determined using the Wiener-Khintchine relations), $E[.]$ denotes mathematical expectation, and an IF filter with a symmetrical frequency response about ω_{IF} has been assumed. For an ideal rectangular filter bandwidth B Hz, $\rho = \text{Sa}(\pi B \tau_d)$, where $\text{Sa}(x) = \sin(x)/x$. For a Butterworth filter of order n and 3-dB bandwidth B_{3dB} , it can be shown that [25]

$$\rho = \sin\left(\frac{\pi}{2n}\right) \sum_{k=1}^n \exp[-\eta \sin(\chi_k)] x \sin[\chi_k + \eta \cos(\chi_k)] \quad (2.32)$$

where $\eta = \pi B_{3dB} \tau$, $\chi_k = (2k-1) \frac{\pi}{2n}$, and the equivalent

noise bandwidth is related to the 3-dB bandwidth by [23]

$$B_{eq} = B_{3dB} \frac{\pi/2n}{\sin(\pi/2n)} \quad (2.33)$$

For Gaussian IF filter [25]

$$\rho = \exp[-\pi (B_{eq} \tau)^2] \quad (2.34)$$

where $B_{eq} = 1.064 B_{3dB}$.

2.4.4 Probability of Bit Error:

Using equation (2.28), the probability of error (for a decision threshold set to zero), conditioned on the random phase drift $\Delta\Psi_T$ is

$$P(e|\Delta\Psi_T) = Pr [Re[z_1^* z_2] > 0 | \Delta\Psi_T] \quad (2.35)$$

The integral solution to (2.35) is a recognizable problem in classical communication theory and, following [27, pp. 314-329], the average probability of error can be expressed as

$$P(e) = \int_{-\infty}^{\infty} p(\Delta\Psi_T) P(e|\Delta\Psi_T) d\Delta\Psi_T \quad (2.36)$$

$$p(e|\Delta\Psi_T) = \frac{1}{2} [1 - Q(a, b) + Q(b, a)] \quad (2.37)$$

$$\left\{ \begin{matrix} a^2 \\ b^2 \end{matrix} \right\} = \frac{(1+K^2)(a_n^2 + a_{nd}^2) \pm 4a_n a_{nd} K \sin \Delta\Psi_T + 2(1-K^2)a_n a_{nd} \cos \Delta\Psi_T}{8\sigma^2(1+\rho^2)} \quad (2.38)$$

where $p(\Delta\Psi_T)$ is the pdf of the random phase drift $\Delta\Psi_T$, and where $a_n = a(t_n)$, $a_{nd} = a(t_n - \tau_d)$, and $Q(\cdot, \cdot)$ is the Marcum Q-function [27,28]

$$Q(a, b) \triangleq \int_b^{\infty} x \exp\left(-\frac{a^2 + b^2}{2}\right) I_0(ax) dx \quad (2.39)$$

where $I_0(\cdot)$ is the zero-order modified Bessel function, and

$$Q(a, 0) = 1, \quad Q(0, b) = \exp\left(-\frac{b^2}{2}\right) \quad (2.40)$$

The pdf of $\Delta\Psi_T$, $p(\Delta\Psi_T)$ can be obtained from $p(\Delta\Psi)$ with mean value of Ψ_0 where $p(\Delta\Psi)$ is given by

$$p(\Delta\Psi) = p(\Delta\phi_d) \otimes p(\Delta\alpha_{FWM}) \otimes p(\Delta\theta_n) \quad (2.41)$$

where \otimes denotes convolution and $p(\Delta\phi_d)$, $p(\Delta\alpha_{FWM})$ and $p(\Delta\theta_n)$ represents the pdf of $\Delta\phi_d$, $\Delta\alpha_{FWM}$ and $\Delta\theta_n$ respectively. Following the Ref. [29], the pdf of $\Delta\alpha_{FWM}$ can be given by

$$p(\Delta\alpha_{FWM}) = \frac{e^{-u}}{4\pi} \int_0^\pi \alpha \sin\theta [1 + U + U \sin\theta \cos\Delta\alpha_{FWM}] \times e^{u \sin\theta \cos\Delta\alpha_{FWM}}, \quad |\Delta\alpha_{FWM}| \leq \pi \quad (2.42)$$

where

$$U = \frac{P_s}{\sum P_{pqr}} \quad (2.43)$$

The characteristic function $F_{\Delta\phi_d}(j\omega)$ [$F\{p(\Delta\phi_d)\}$] of random variable $\Delta\phi_d$ can be shown to be [30]

$$\begin{aligned} F_{\Delta\phi_d}(j\omega) &= \prod_{i=1}^{\infty} \cos[\omega g_i(t')] \\ &= \sum_{i=1}^{\infty} \frac{(j\omega)^{2i}}{(2i)!} M_{2i} \end{aligned} \quad (2.44)$$

where $g_i(t') = |g(t' - iT)|$ and M_{2i} are the even order moments of the characteristic function of $\Delta\theta_i$ which can be evaluated using the following recursive relation [30]

$$M_{2i} = Y_{2r}(N)$$

$$Y_{2r}(i) = \sum_{j=0}^r \binom{2r}{2j} Y_{2j}(i-1) g_i^{2r-2j} \quad (2.45)$$

where N is the actual number of interfering terms in the summation of equation (2.44).

The pdf $p(\Delta\theta_n)$ has a zero-mean Gaussian distribution with variance $2\pi\Delta\nu\tau$ [24].

Since $\Delta\Psi_T$ is mod 2π , the equation (2.36) is to be written as

$$P(e) = \sum_{-\infty}^{\infty} \int_{-\pi}^{\pi} (P_e | \Delta\Psi_T) P(\Delta\Psi_T - 2n\pi) d\theta \quad (2.46)$$

This is the bit error rate (BER) expression for the coherent optical heterodyne CPFSK system with delay demodulation.

CHAPTER - III

RESULTS AND DISCUSSIONS

Following the theoretical analysis presented in chapter 2, the theoretical performance results for multiwavelength optical transport system is evaluated at a bit rate of 2.5 Gb/s with and without considering the FWM effect for several sets of values of the receiver and system parameters. The parameters used in the theoretical computations are:

Bit rate, $B_r = 2.5$ Gb/s

Fiber attenuation, $\alpha = 0.2$ dB/Km

Fiber chromatic dispersion, $D_c = 1$ ps/nm-Km

Optical wavelength, $\lambda = 1550$ nm

Responsivity factor, $R_d = 0.85$

Local oscillator power, $P_{lo} = 0.001$ w (0 dBm)

Loss of WDM MUX, $L_m = -4.0$ dB

Loss of splitter, $L_s = -3.0$ dB

Loss of fiber protection switch, $L_{ps} = -6.0$ dB

Loss of WDM DMUX, $L_{dm} = -4.0$ dB

Loss of cross-connect switch, $L_{sw} = -10.0$ dB

Gain of optical amplifier in the head-end, $G_1 = 18.0$ dB

Gain of optical amplifier in the fount-end, $G_2 = -G_1 - L_T$ (dB)

Bandwidth of optical filter, $B_{fp} = 4.0B_r$

Bandwidth of IF filter, $B_e = 0.7B_r$

Fiber core diameter, $W = 0.5 \times 11^{-6}$ m

Refractive index of fiber, $n = 1.45$

Nonlinear susceptibility, $\chi = 5 \times 10^{-14}$ m³/watt-sec.

Thermal noise current spectral density, $I_{th} = 10^{-12}$ A/ $\sqrt{\text{Hz}}$

The bit error rate (BER) performance results in absence of FWM effect for coherent CPFSK modulated MWTN with delay-demodulation is shown in Fig.3.1 as a function of the number of nodes M for three values of input transmitter power $P_{in} = -10, -5, 0.0$ dBm when fiber span $L = 20$ Km and number of WDM channels $N = 11$ and optical amplifier's bandwidth $B_o = 15$ GHz. The plots illustrate how the bit error rate varies with the number of nodes. It is found that for a given input power, the error rate increases with increasing value of the number of nodes due to accumulation of optical amplifier's spontaneous emission (ASE) from one node to another. At an specified BER, the allowable number of nodes is more at higher input power. For example, at $BER = 10^{-9}$ the allowable number of nodes is around 30 when $P_{in} = -10$ dBm, when P_{in} is increased to 0 dBm, the number of allowable nodes reaches around 300.

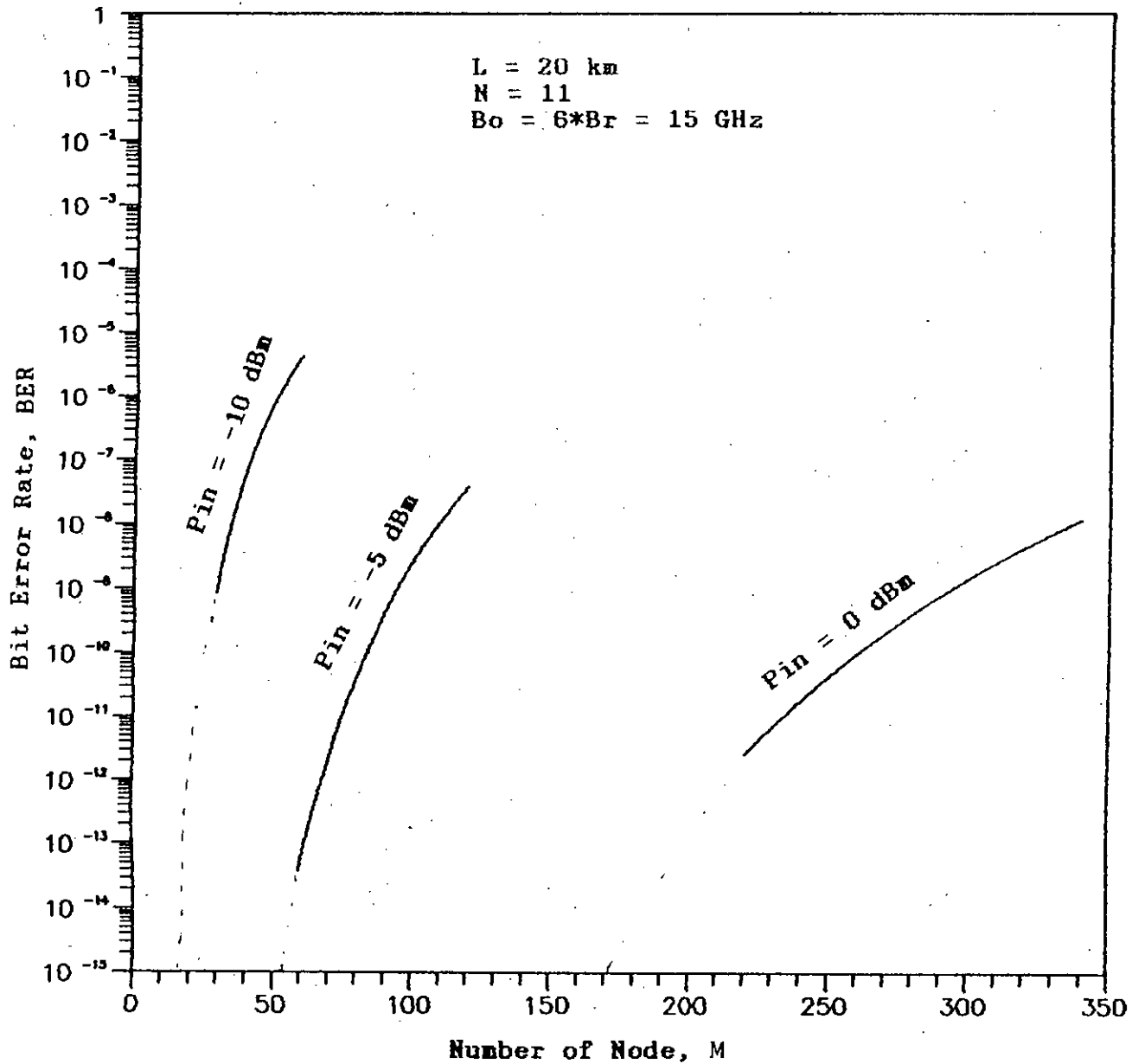


Fig.3.1 Bit error rate (BER) performance of optical multiwavelength transport network (MWTN) at a bit rate of 2.5 Gb/s as a function of the number of nodes M when number of channels $N=11$, fiber span $L=20 \text{ Km}$, optical bandwidth $B_o=6B_r=15 \text{ GHz}$ and $P_{\text{FWM}}=0.0$ for three different values of the optical transmitter power P_{in} (dBm).

When the fiber span is increased to 50 Km, the performance results are depicted in Fig.3.2. Comparing with Fig.3.1 it becomes evident that for the same input power the number of allowable nodes is reduced due to increased fiber span. When L is increased to 100 Km, the number of allowable nodes are further reduced as is evident from Fig.3.3. This is due to increased ASE with increased amplifier gain to meet the additional fiber loss due to increased fiber span.

When the optical amplifier's bandwidth B_o is increased to 10 times B_r i.e., 25 GHz, the performance results are shown in Fig.3.4 for fiber span $L = 100$ Km. Comparison of Fig.3.4 with Fig.3.3 reveals that increased optical bandwidth causes the system performance to be degraded and the allowable number of nodes is considerably reduced at $BER = 10^{-9}$ at a given input power P_{in} (dBm). This is due to increased ASE and several beat noise terms arising out of beating of ASE with signal and local oscillator signals at increased optical bandwidth. The number of node is further reduced as the optical bandwidth is further increased to $B_o = 50$ GHz as depicted in Fig.3.5. For example, $P_{in} = 0$ dBm, the number of allowable nodes at $BER = 10^{-9}$ is around 9 when $B_o = 50$ GHz and it is approximately 17 when $B_o = 25$ GHz.

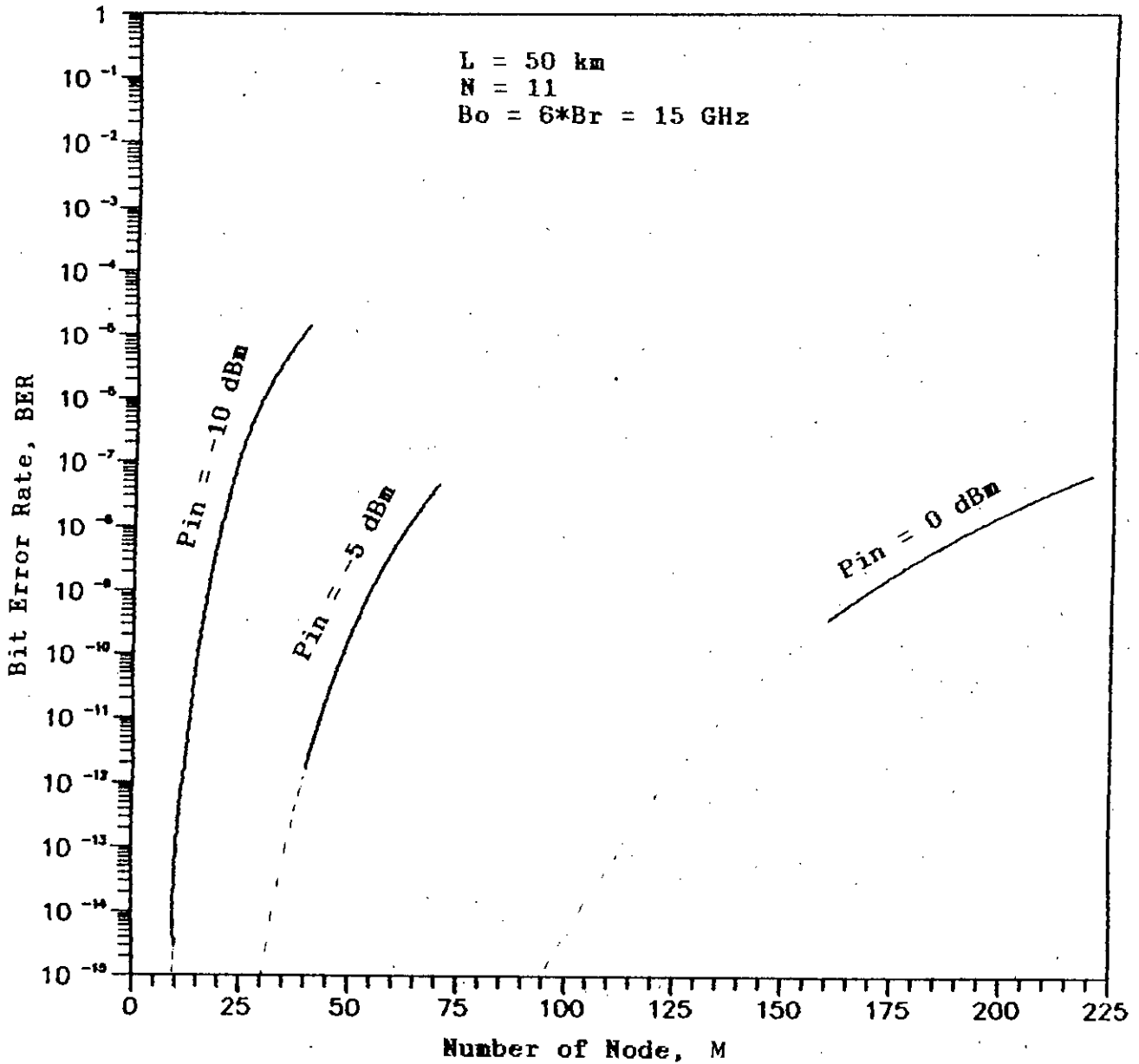


Fig.3.2 Bit error rate (BER) performance of optical MWTN at a bit rate of 2.5 Gb/s as a function of the number of nodes M when number of channels $N=11$, fiber span $L=50$ Km, optical bandwidth $B_o=6B_r=15$ GHz and $P_{\text{PWM}}=0.0$ for three different values of the optical transmitter power P_{in} (dBm).

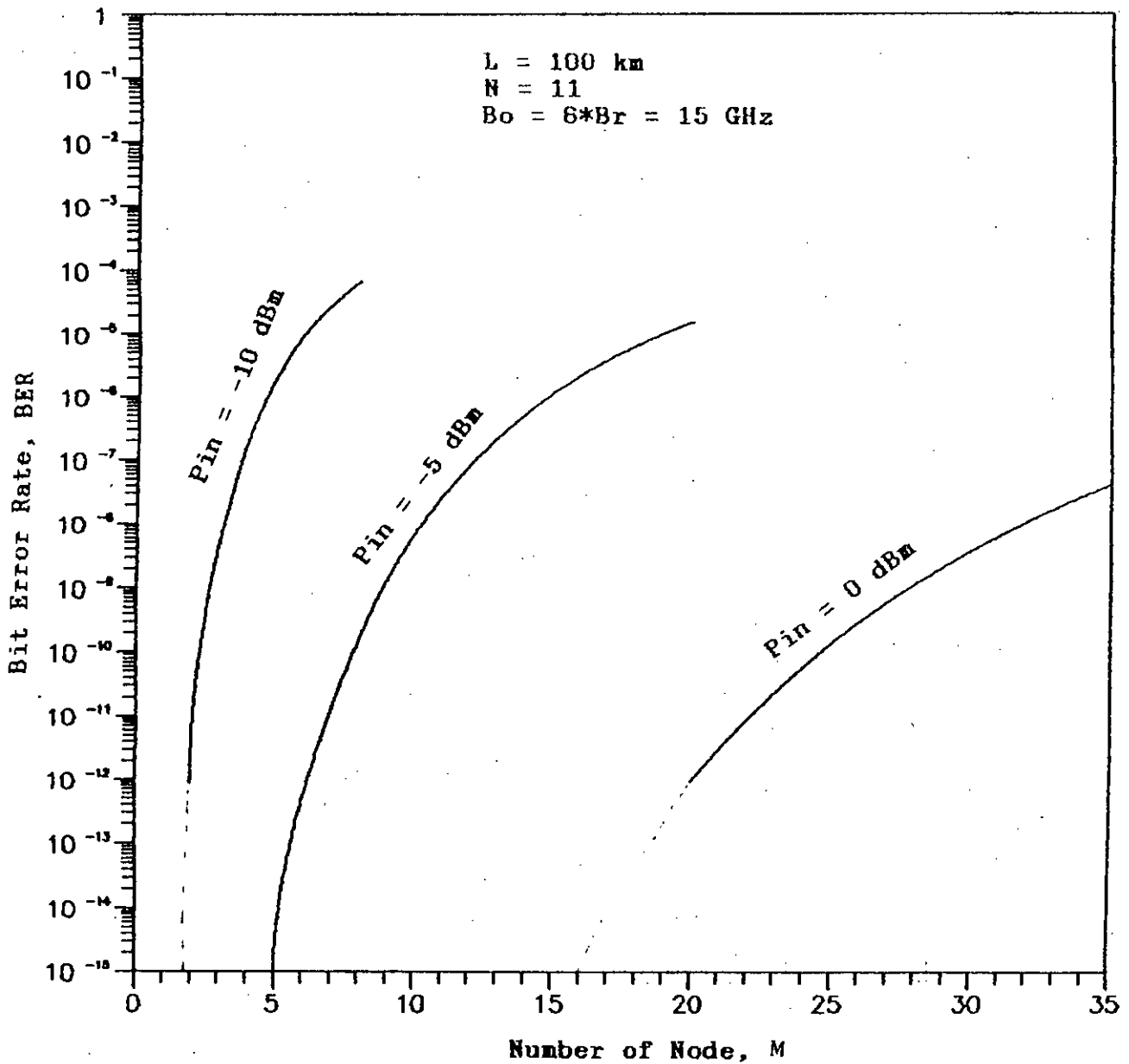


Fig. 3.3 Bit error rate (BER) performance of optical MWTN at a bit rate of 2.5 Gb/s as a function of the number of nodes M when number of channels $N=11$, fiber span $L=100 \text{ Km}$, optical bandwidth $B_o=6B_r=15 \text{ GHz}$ and $P_{\text{FWM}}=0.0$ for three different values of the optical transmitter power P_{in} (dBm).

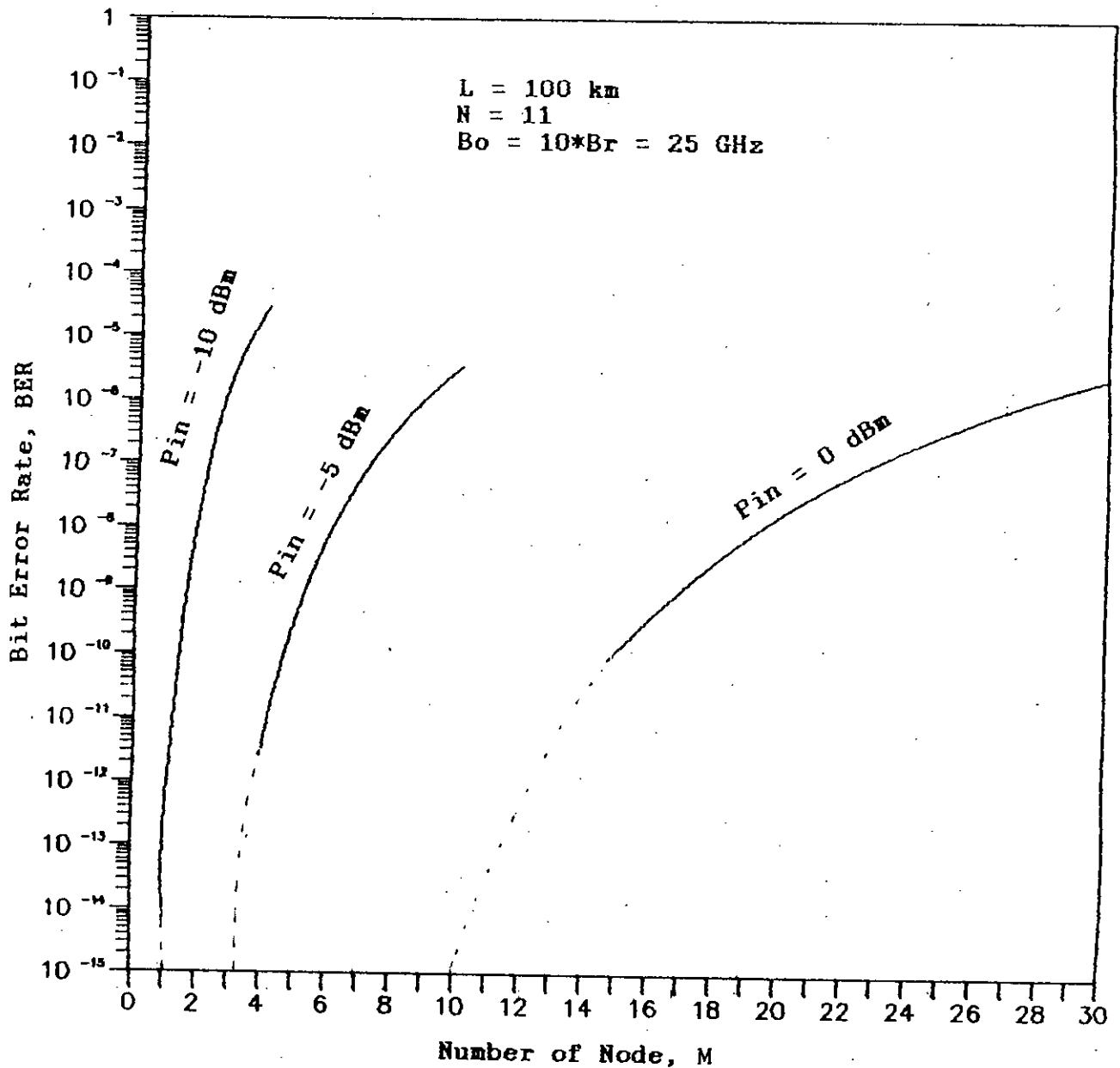


Fig.3.4 Bit error rate (BER) performance of optical MWTN at a bit rate of 2.5 Gb/s as a function of the number of nodes M when number of channels $N=11$, fiber span $L=100 \text{ Km}$, $B_o=10B_r=25 \text{ GHz}$ and $P_{\text{PWM}}=0.0$ for three different values of the optical transmitter power P_{in} (dBm).

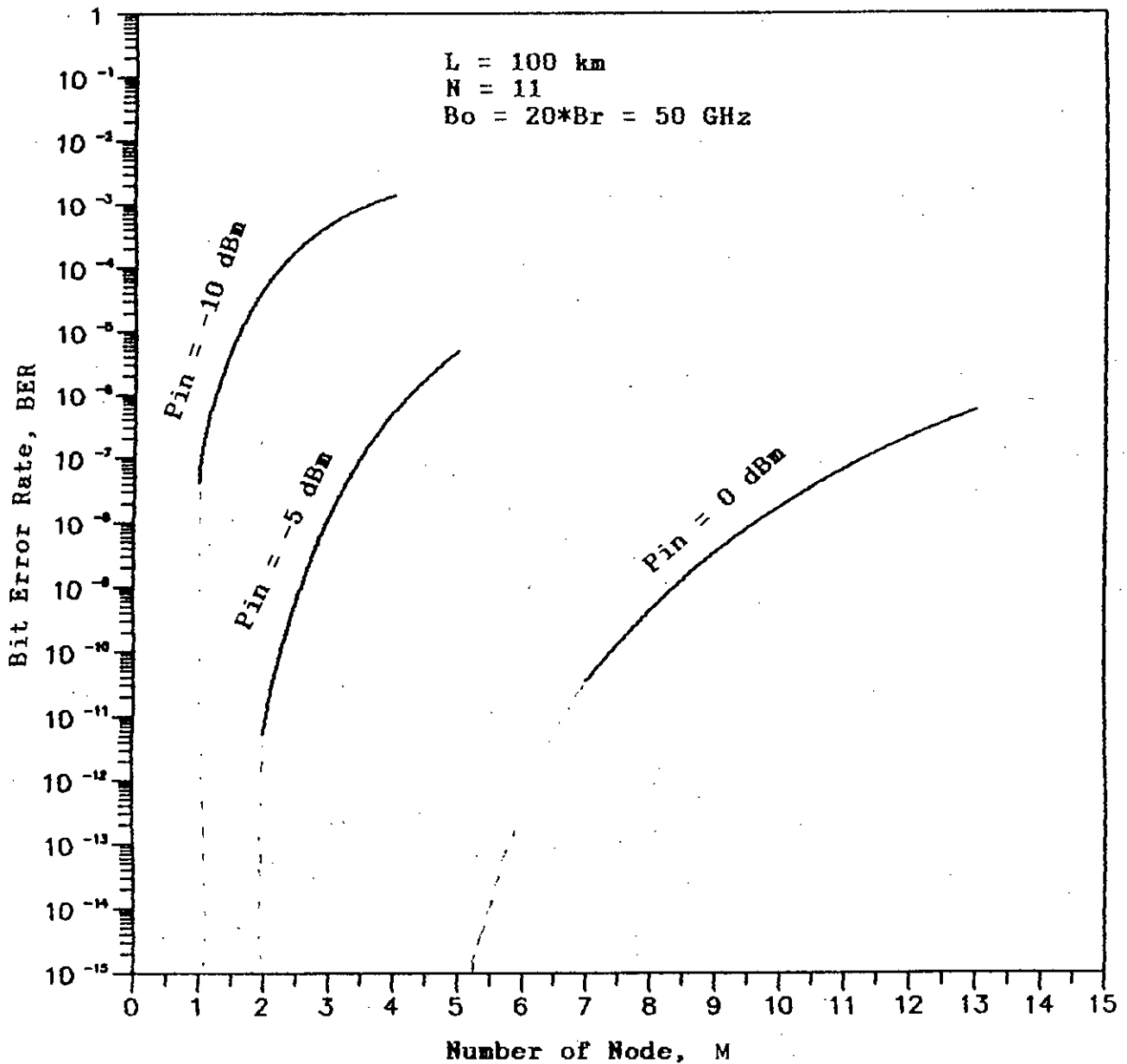


Fig.3.5 Bit error rate (BER) performance of optical MWTN at a bit rate of 2.5 Gb/s as a function of the number of nodes M when number of channels $N=11$, fiber span $L=100 \text{ Km}$, $B_o=20B_r=50 \text{ GHz}$ and $P_{\text{PWM}}=0.0$ for three different values of the optical transmitter power P_{in} (dBm).

The plots of the allowable number of nodes at $BER = 10^{-9}$ versus the transmitter power P_{in} (dBm) is depicted in Fig. 3.6 with fiber span L as a parameter when $B_o = 15$ GHz. It is observed that as the input power increases the allowable number of nodes increases without limit due to increased receiver sensitivity. However, as the node separation or fiber span (L) is increased, the allowable number of nodes becomes drastically reduced. As is evident from the figure it is noticed that the number of allowable nodes is around 100 when $L = 20$ Km whereas it reduces to 10 when L is increased to 100 Km. It is also observed that the product $N.L \leq 2000$ when $P_{in} = -5$ dBm and reaches an upper limit of 6000 when $P_{in} = 0$ dBm.

For optical bandwidth, $B_o = 10Br = 25$ GHz, the variation of number of nodes at $BER = 10^{-9}$ with input power P_{in} (dBm) is shown in Fig.3.7. Comparison of this curve with Fig.3.6 shows that the product NL is considerably less at higher optical bandwidth.

Similar observations are also found when B_o is increased to 50 GHz as shown in Fig.3.8.

The plots of allowable number of nodes at $BER = 10^{-9}$ as a function of optical bandwidth B_o (GHz) is shown in Fig.3.9, Fig.3.10 and Fig.3.11 for $L = 20$ Km, 50 Km and 100 Km

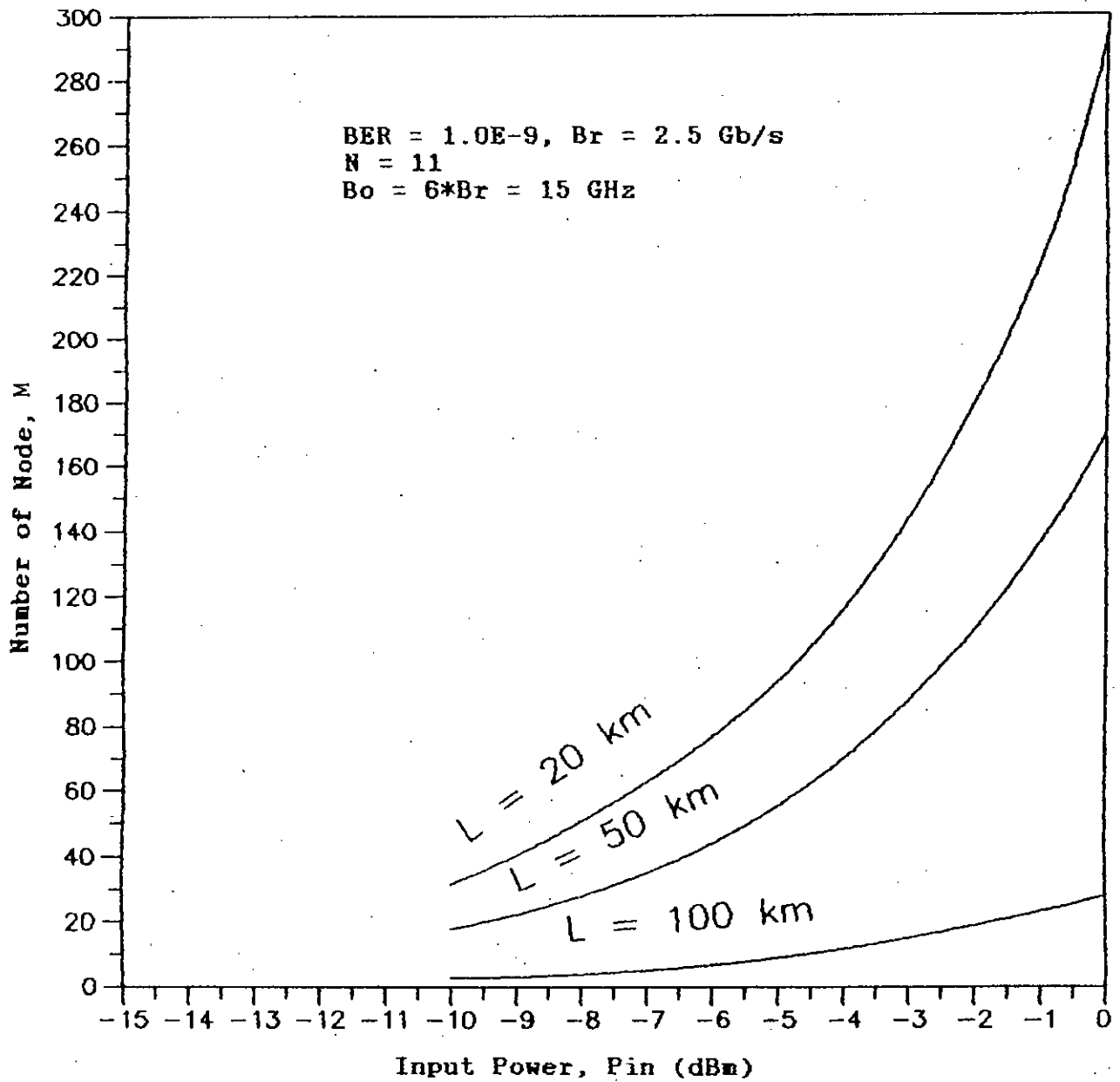


Fig.3.6 Plots of allowable maximum number of nodes M corresponding to BER of 10^{-9} as a function of the input transmitter power P_{in} (dBm) at a bit rate of 2.5 Gb/s and optical bandwidth $B_o=6Br=15$ GHz for three values of the fiber span $L=20$ Km, $L=50$ Km and $L=100$ Km, and $P_{FWM}=0.0$.

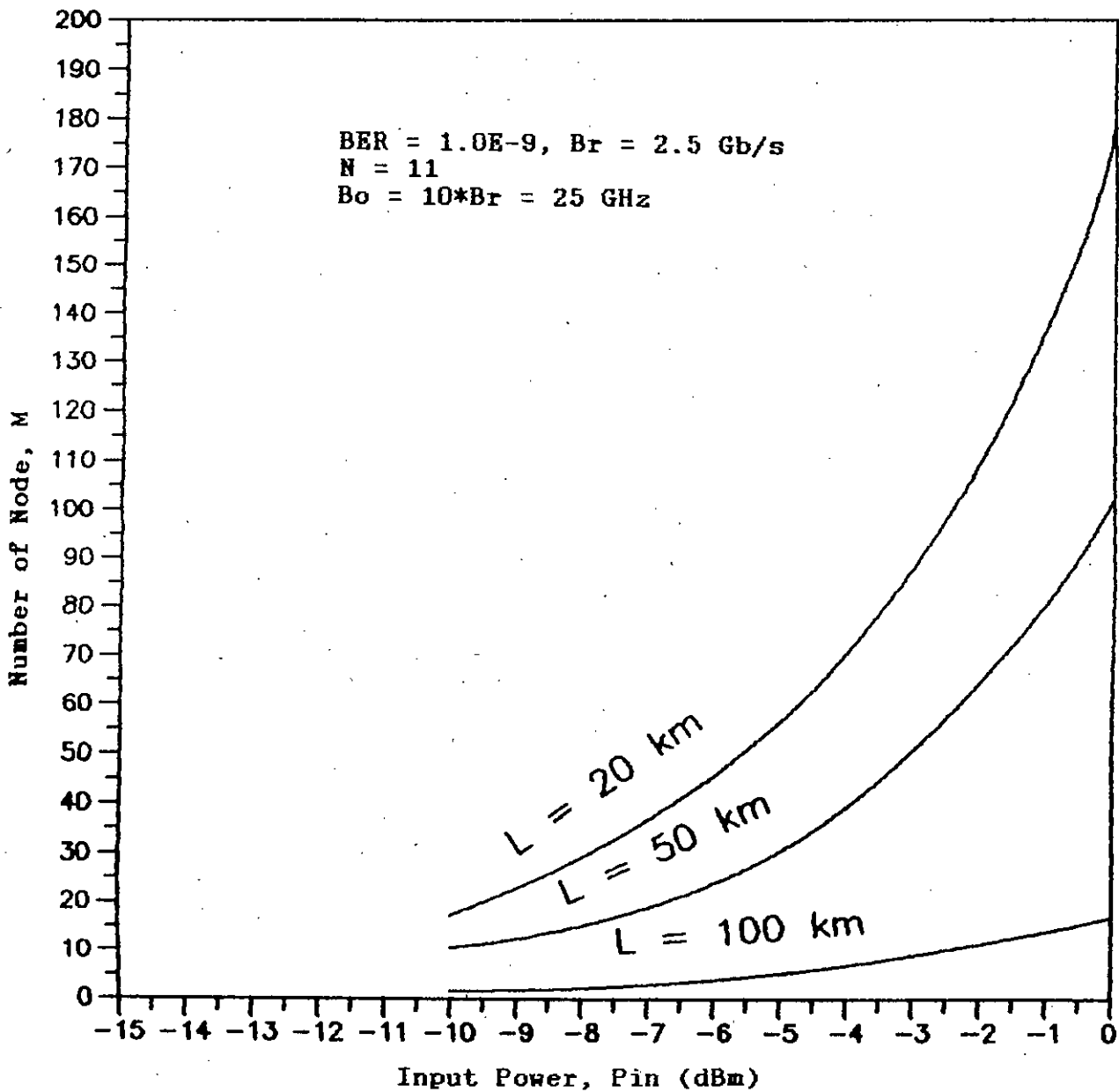


Fig.3.7 Plots of allowable maximum number of nodes M corresponding to BER of 10^{-9} as a function of the input transmitter power P_{in} (dBm) at a bit rate of 2.5 Gb/s and optical bandwidth $B_o=10Br=25$ GHz for three values of the fiber span $L=20$ Km, $L=50$ Km and $L=100$ Km, and $P_{PVM}=0.0$.

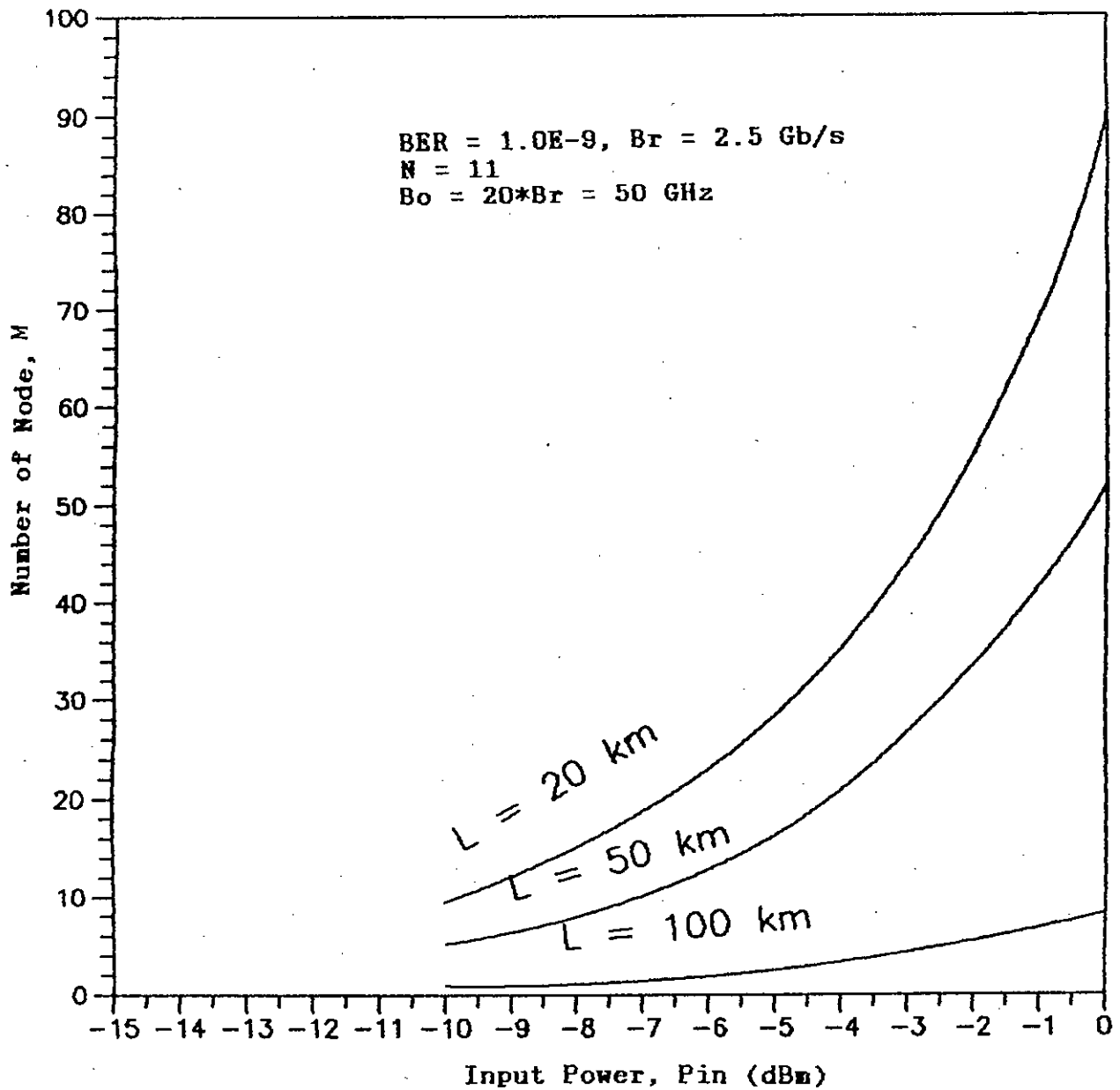


Fig.3.8 Plots of allowable maximum number of nodes M corresponding to BER of 10^{-9} as a function of the input transmitter power P_{in} (dBm) at a bit rate of 2.5 Gb/s and optical bandwidth $B_o=20Br=50$ GHz for three values of the fiber span $L=20$ Km, $L=50$ Km and $L=100$ Km, and $P_{FWM}=0.0$.

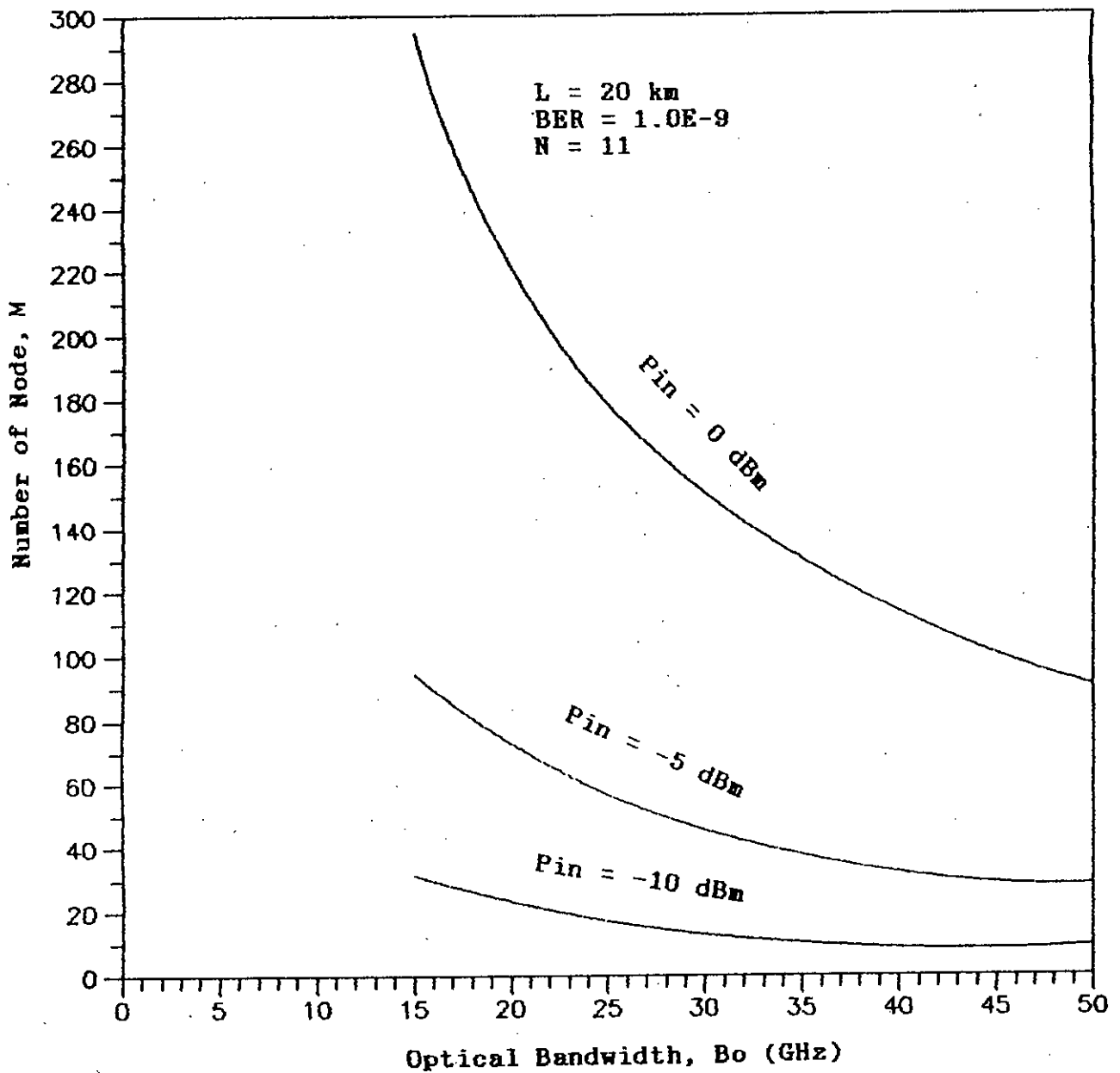


Fig.3.9 Variation of the allowable maximum number of nodes M as a function of optical bandwidth B_o for three values of the transmitter power P_{in} (dBm) at $BER=10^{-9}$, $P_{FWM}=0.0$ and fiber span $L=20 \text{ Km}$.

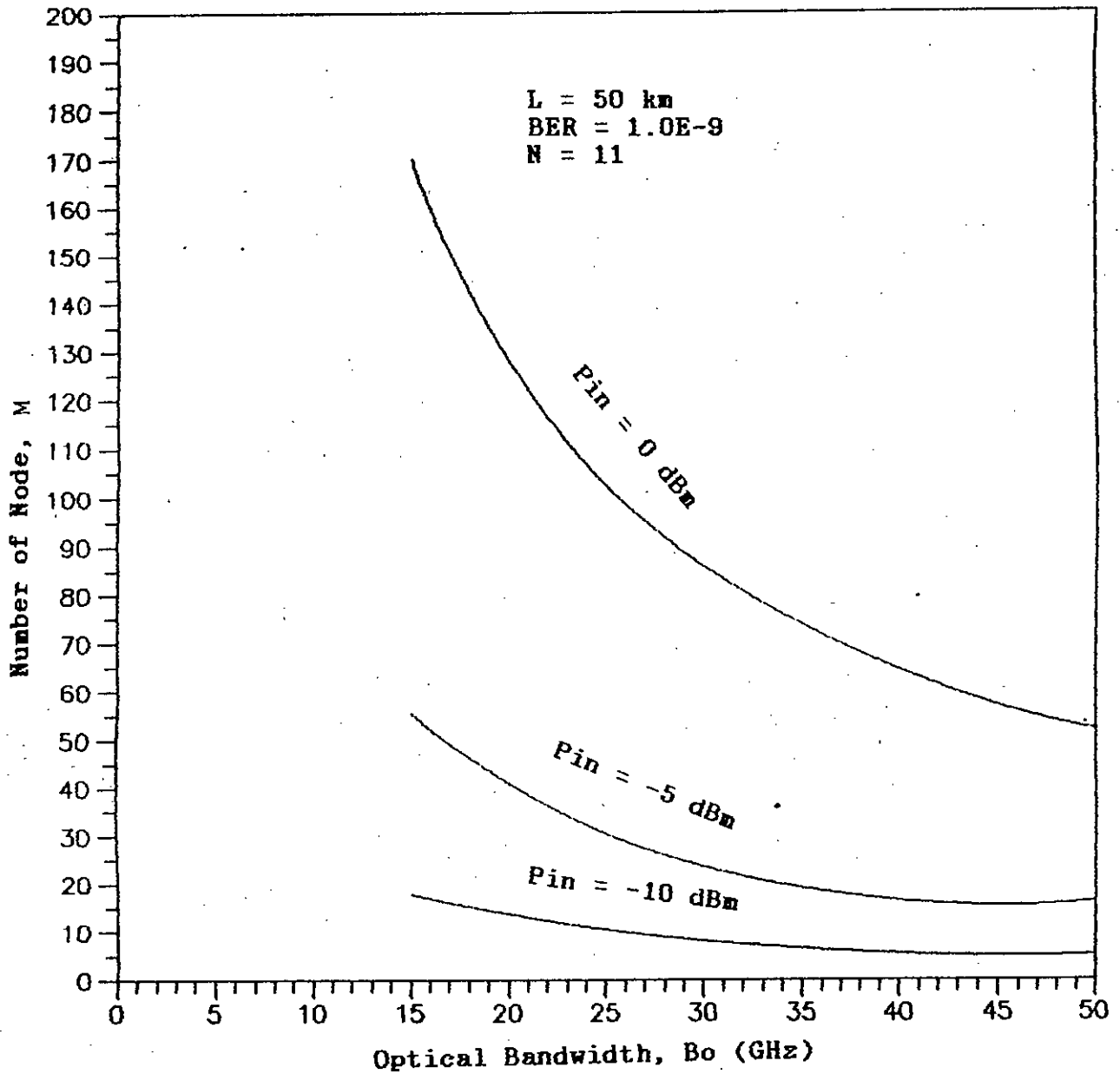


Fig.3.10 Variation of the allowable maximum number of nodes M as a function of optical bandwidth B_o for three values of the transmitter power P_{in} (dBm) at $BER=10^{-9}$, $P_{PWM}=0.0$ and fiber span $L=50 \text{ Km}$.

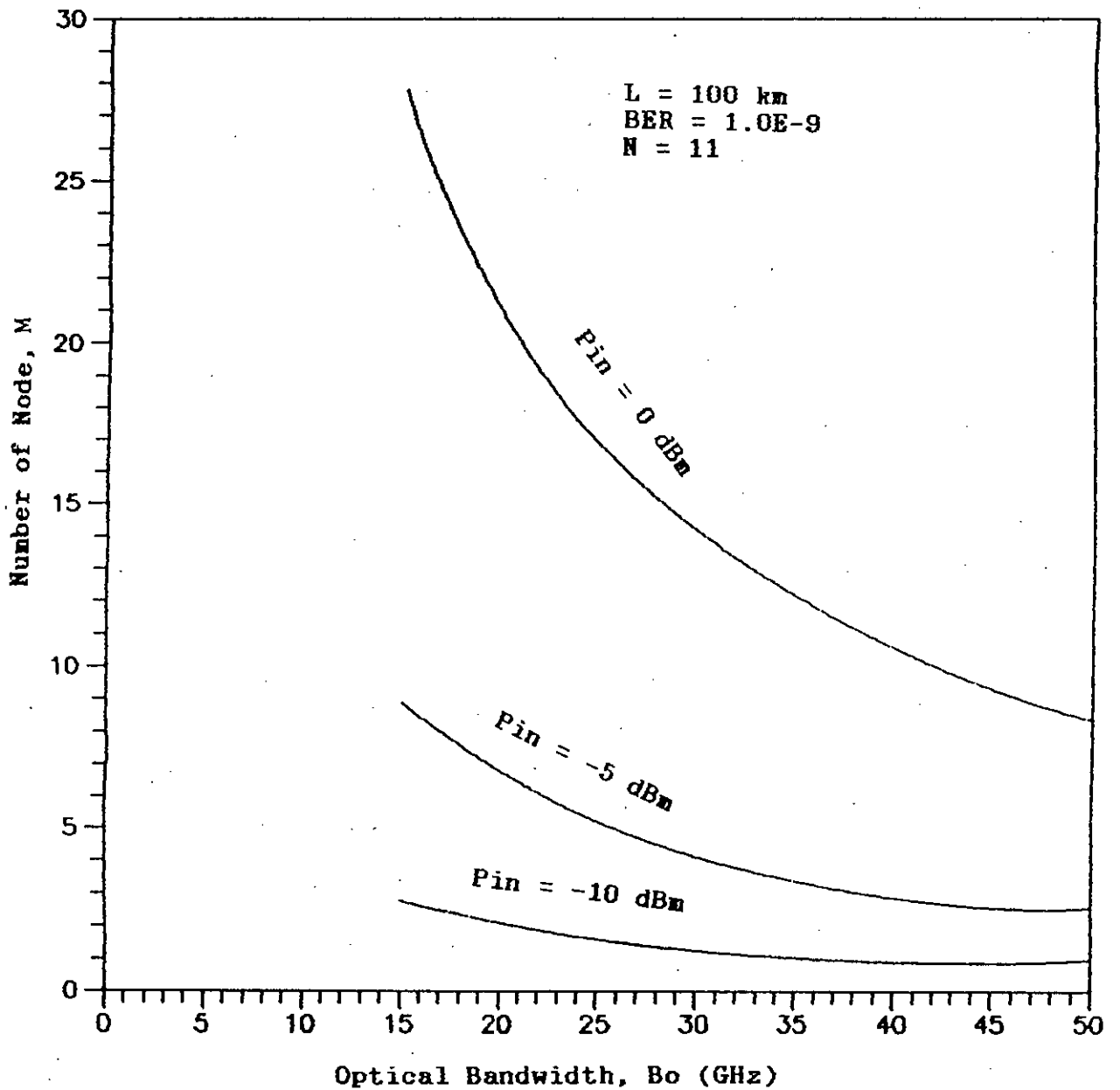


Fig.3.11 Variation of the allowable maximum number of nodes M as a function of optical bandwidth B_o for three values of the transmitter power P_{in} (dBm) at $BER=10^{-9}$, $P_{FWM}=0.0$ and fiber span $L=100 \text{ Km}$.

respectively with $P_{in} = -10, -5, \text{ and } 0 \text{ dBm}$. The figures depict how the number of allowable nodes corresponding to $BER = 10^{-9}$ varies with bandwidth of optical amplifier. However, the number of allowable nodes are higher at higher input power and are less at higher fiber length.

When FWM power is included, the BER performance results as a function of number of nodes M are depicted in Fig.3.12 when fiber span $L = 20 \text{ Km}$, $P_{in} = -5 \text{ dBm}$, $B_o = 15 \text{ GHz}$ for number of WDM channels $N = 11, 51 \text{ and } 101$. The figure depicts the effect of FWM power on the system performance. As the number of channels N is increased at a given input power P_{in} , the BER performance of the system degrades due to increased FWM effect. When the input power is increased to -2.5 dBm , system performance improves in terms of number of nodes at a given BER as becomes evident from Fig.3.13. It is further noticed that at a given BER, the allowable number of nodes differ largely at higher input power P_{in} . This is due to the fact that for a given values of N , effect of FWM is more prominent at higher input optical power per channel. Similar observations are also found at higher input power, i.e., for $P_{in} = -5.0 \text{ and } -2.5 \text{ dBm}$ as shown in Fig.3.14 and Fig.3.15.

The plots of allowable number of nodes M at $BER = 10^{-9}$ as a function of input power P_{in} (dBm) is shown in Fig.3.16 for

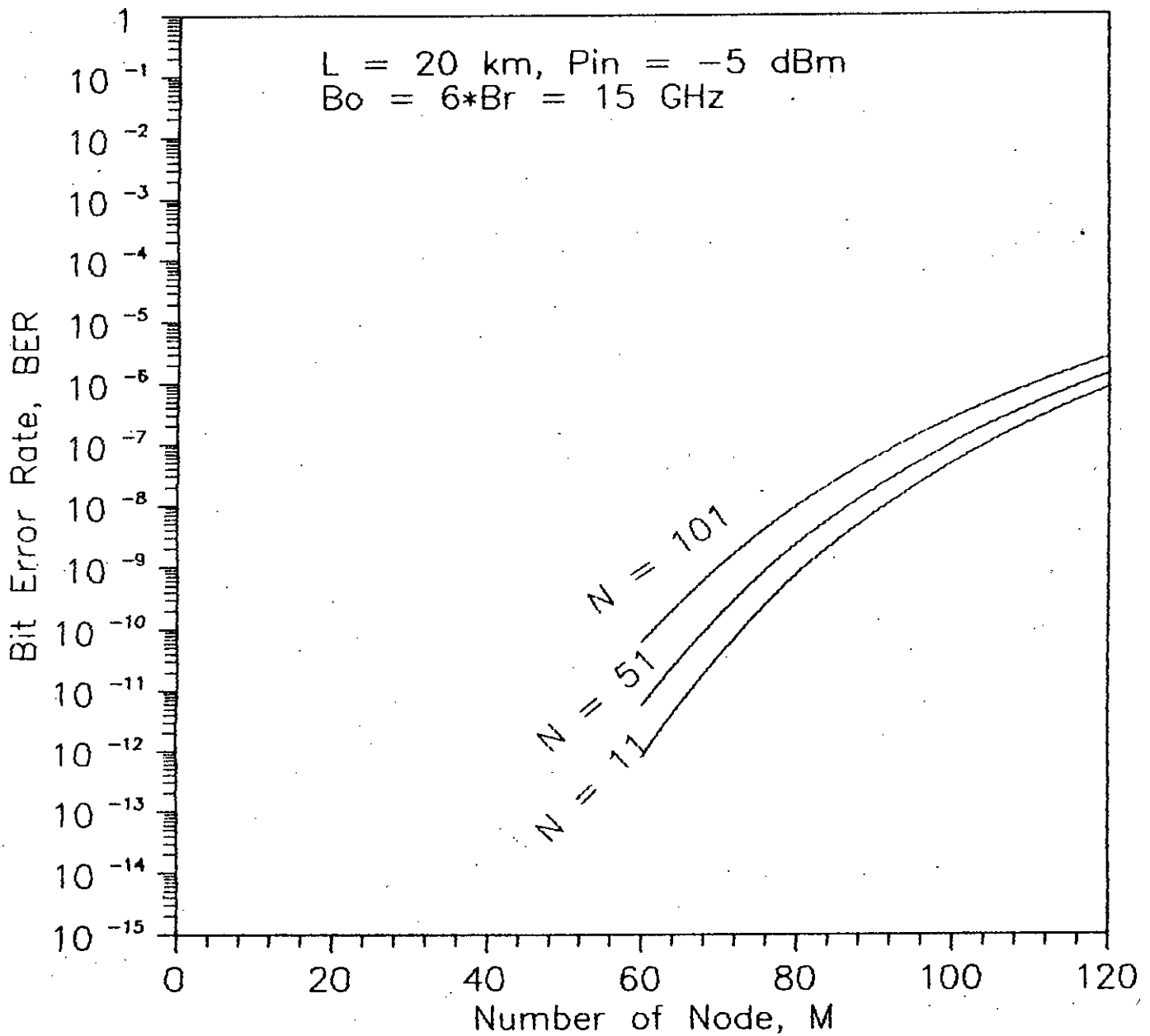


Fig.3.12 Bit error rate (BER) performance of optical MWTN versus number of nodes M , at a bit rate of 2.5 Gb/s for transmitter power $P_{in} = -5 \text{ dBm}$ and number of channels $N=11, 51, 101$ with $L=20 \text{ Km}$ and $B_o=6B_r=15 \text{ GHz}$.

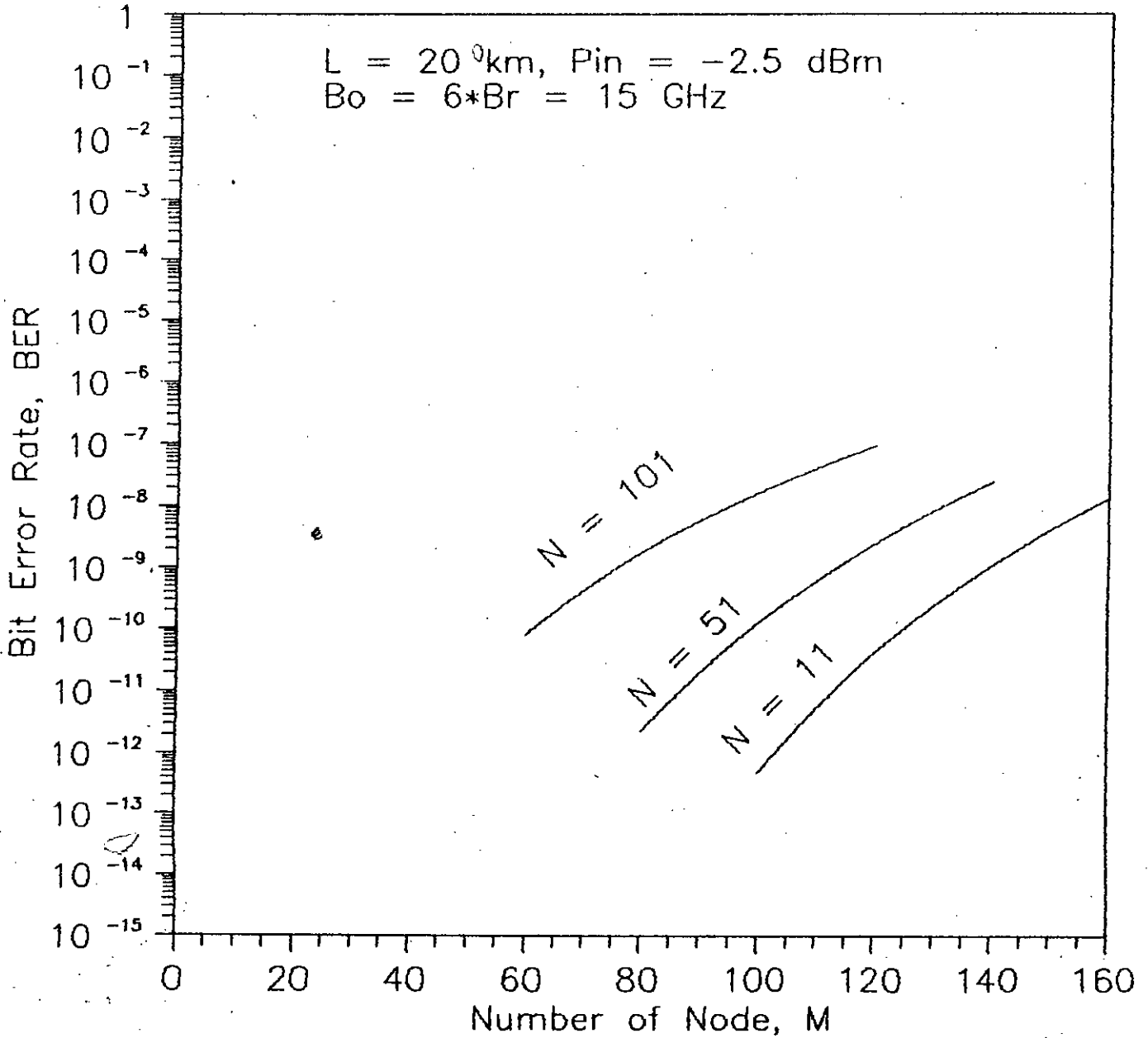


Fig.3.13 Bit error rate (BER) performance of optical MWTN versus number of nodes M, at a bit rate of 2.5 Gb/s for transmitter power $P_{in} = -2.5 \text{ dBm}$ and number of channels $N=11, 51, 101$ with $L=20 \text{ Km}$ and $B_o=6B_r=15 \text{ GHz}$.

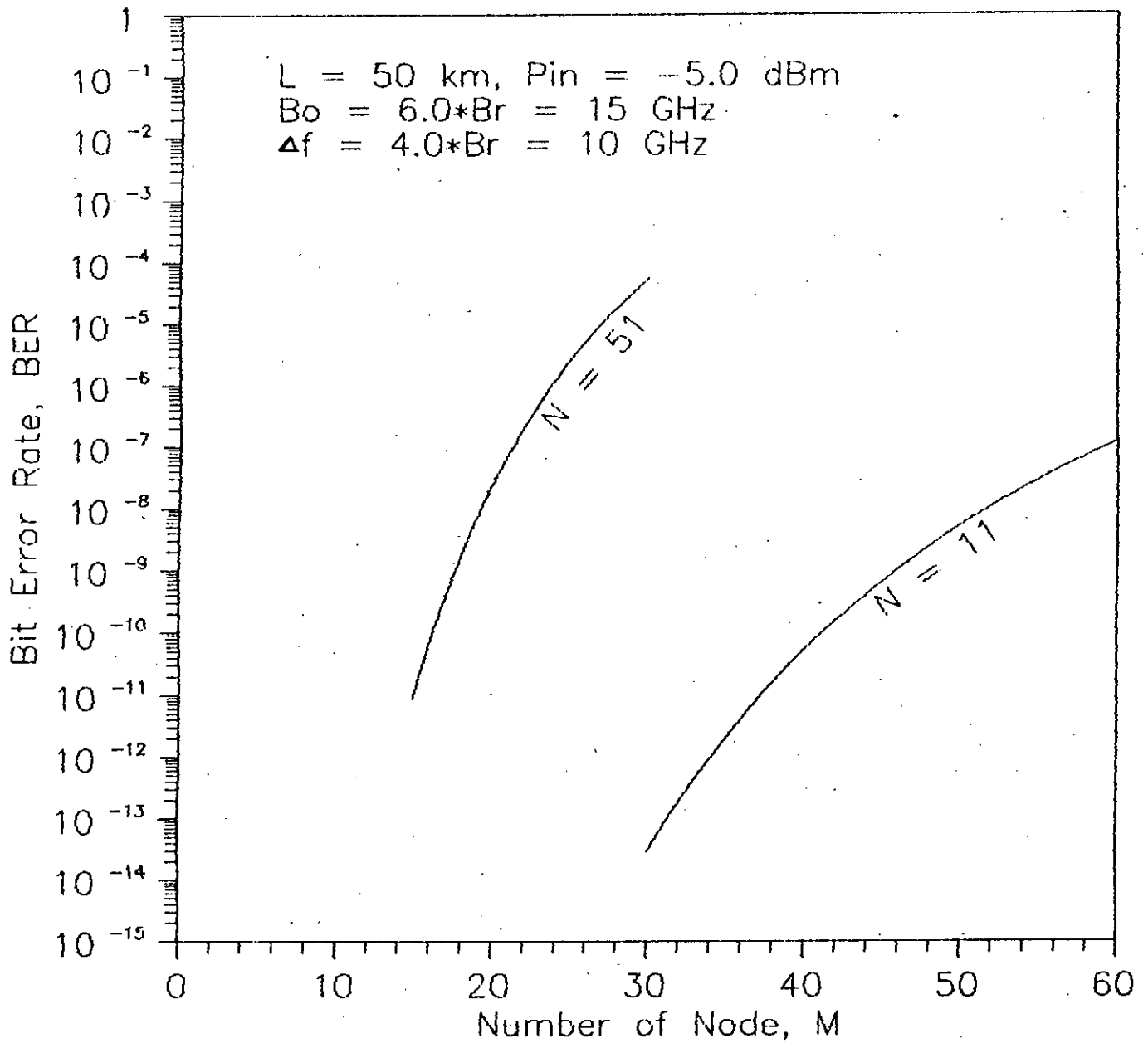


Fig.3.14 Bit error rate (BER) performance of optical MWTN versus number of nodes M , at a bit rate of 2.5 Gb/s for transmitter power $P_{in} = -5 \text{ dBm}$ and number of channels $N=11$ and 51 with $L=50 \text{ Km}$ and $B_o=6B_r=15 \text{ GHz}$.

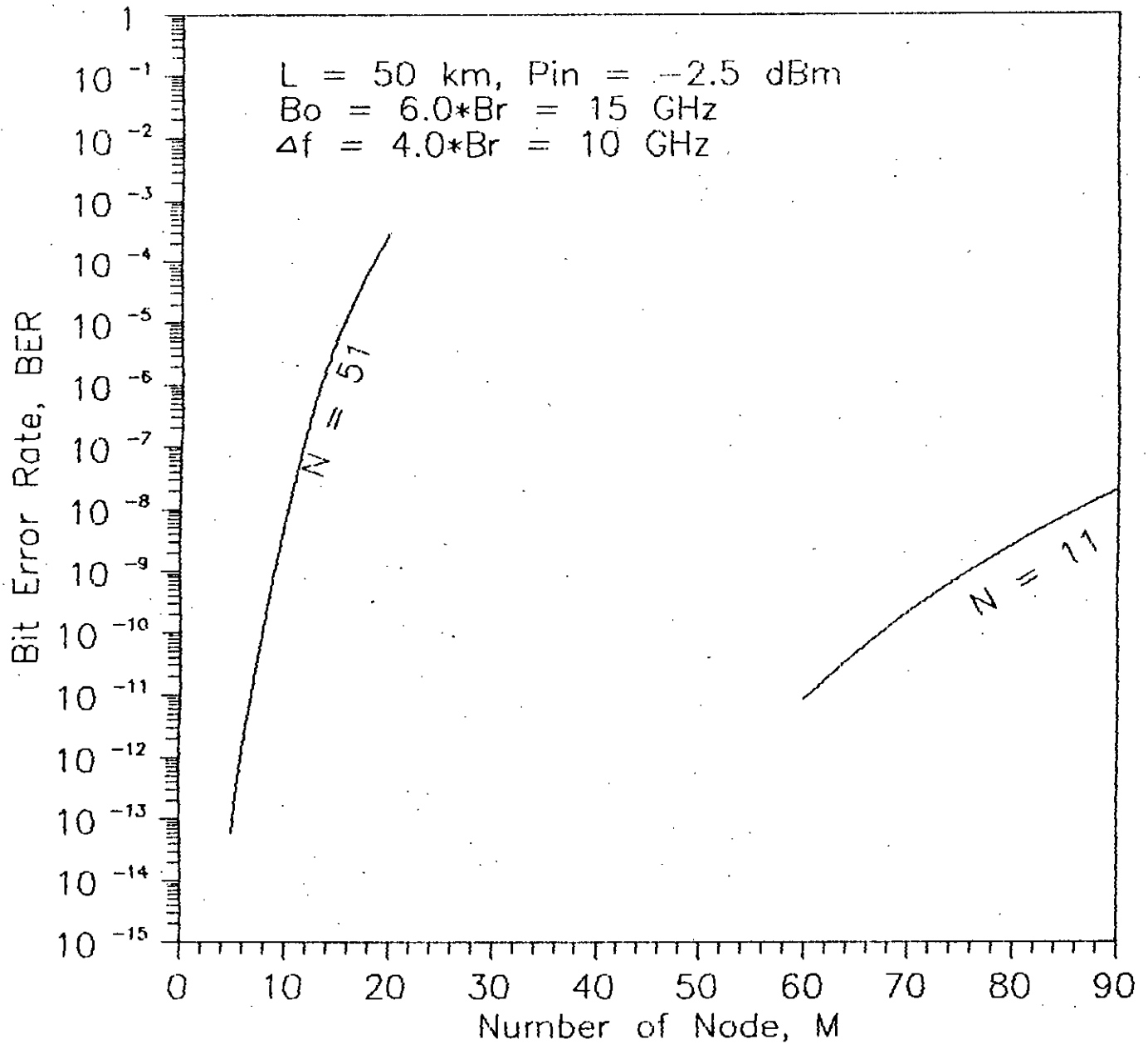


Fig.3.15 Bit error rate (BER) performance of optical MWTN versus number of nodes M , at a bit rate of 2.5 Gb/s for transmitter power $P_{in} = -2.5 \text{ dBm}$ and number of channels $N=11$ and 51 with $L=50 \text{ Km}$ and $B_o=6B_r=15 \text{ GHz}$.

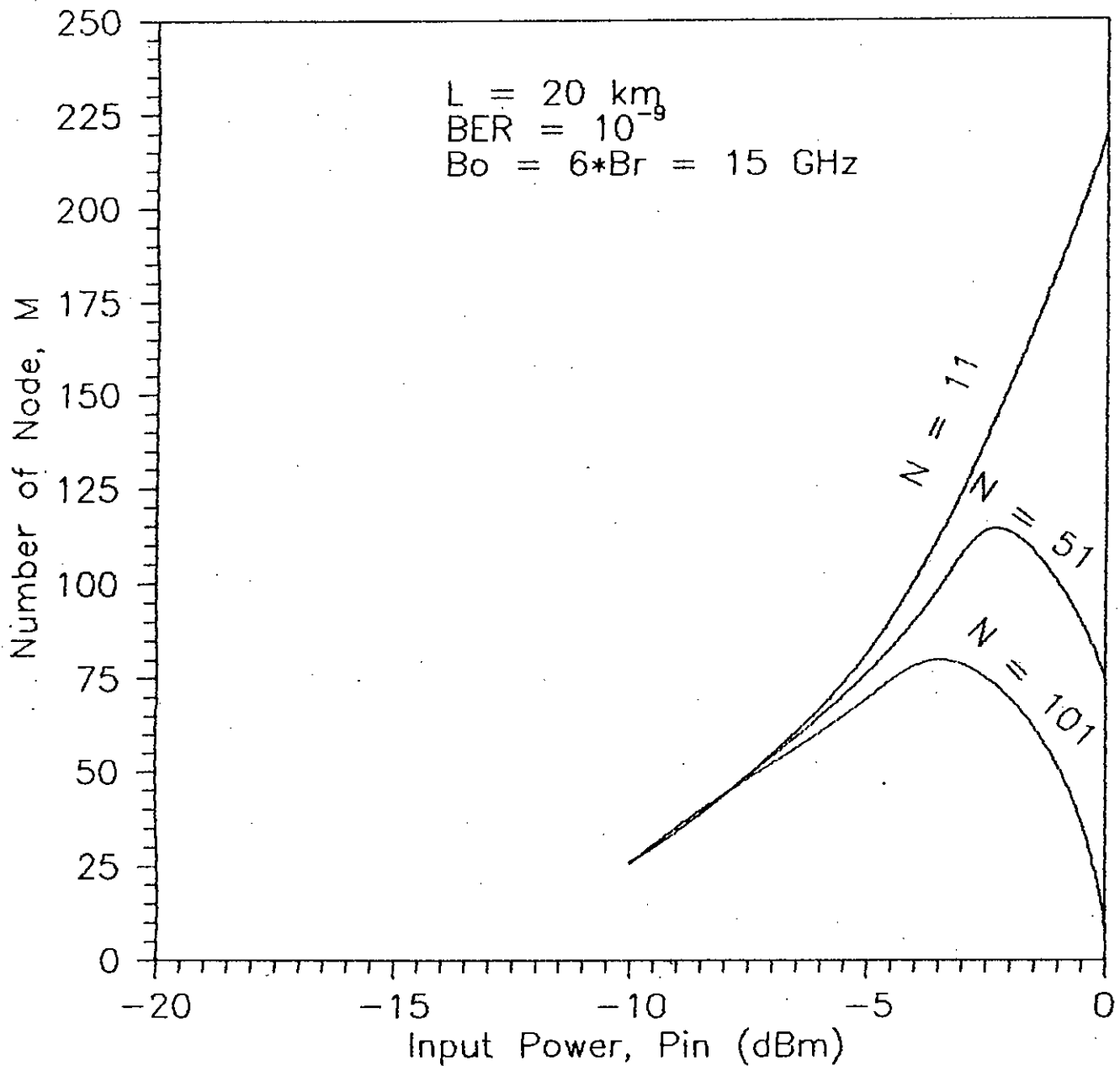


Fig.3.16 Plots of maximum allowable number of nodes M corresponding to BER of 10^{-9} as a function of the input transmitter power P_{in} (dBm) in the presence of four-wave mixing (FWM) effect at a bit rate of 2.5 Gb/s with optical bandwidth $B_o=6B_r=15$ GHz and fiber span $L=20$ Km for number of channels $N=11, 51, 101$ and channel separation $\Delta f=10$ GHz.

three values of the number of channels $N = 11, 51$ and 101 , when $L = 20$ Km, $B_o = 15$ GHz. The plots depict that the number of nodes increases with P_{in} but up to a certain limit where it reaches a maximum value at a given values of P_{in} and then decreases. This is due to the fact that as the input power increases, the receiver sensitivity and hence the allowable number of nodes increases and the receiver performance is limited by ASE and associated beat noise components. At increased P_{in} , the FWM power drastically increases with P_{in}^3 and as a consequence the system performance degrades and the allowable number of nodes is greatly reduced. Thus, there is a maximum value of the allowable number of nodes for a given value of the number of channels N which can be termed as M_{max} . The maximum value of M i.e., M_{max} is further reduced at increased values of the number of channels N . It is also evident that the maximum number of nodes M_{max} occurs corresponding to a maximum allowable input power $P_{in,max}$. The value of $P_{in,max}$ is less when the number of channels is increased.

Similar plots of allowable number of nodes M versus P_{in} (dBm) for higher fiber span e.g., $L = 50$ Km and 100 Km are provided in Fig.3.17 and Fig.3.18. Comparing these curves with Fig.3.16 we found that the maximum allowable node is greatly reduced at higher length of fiber span and the allowable

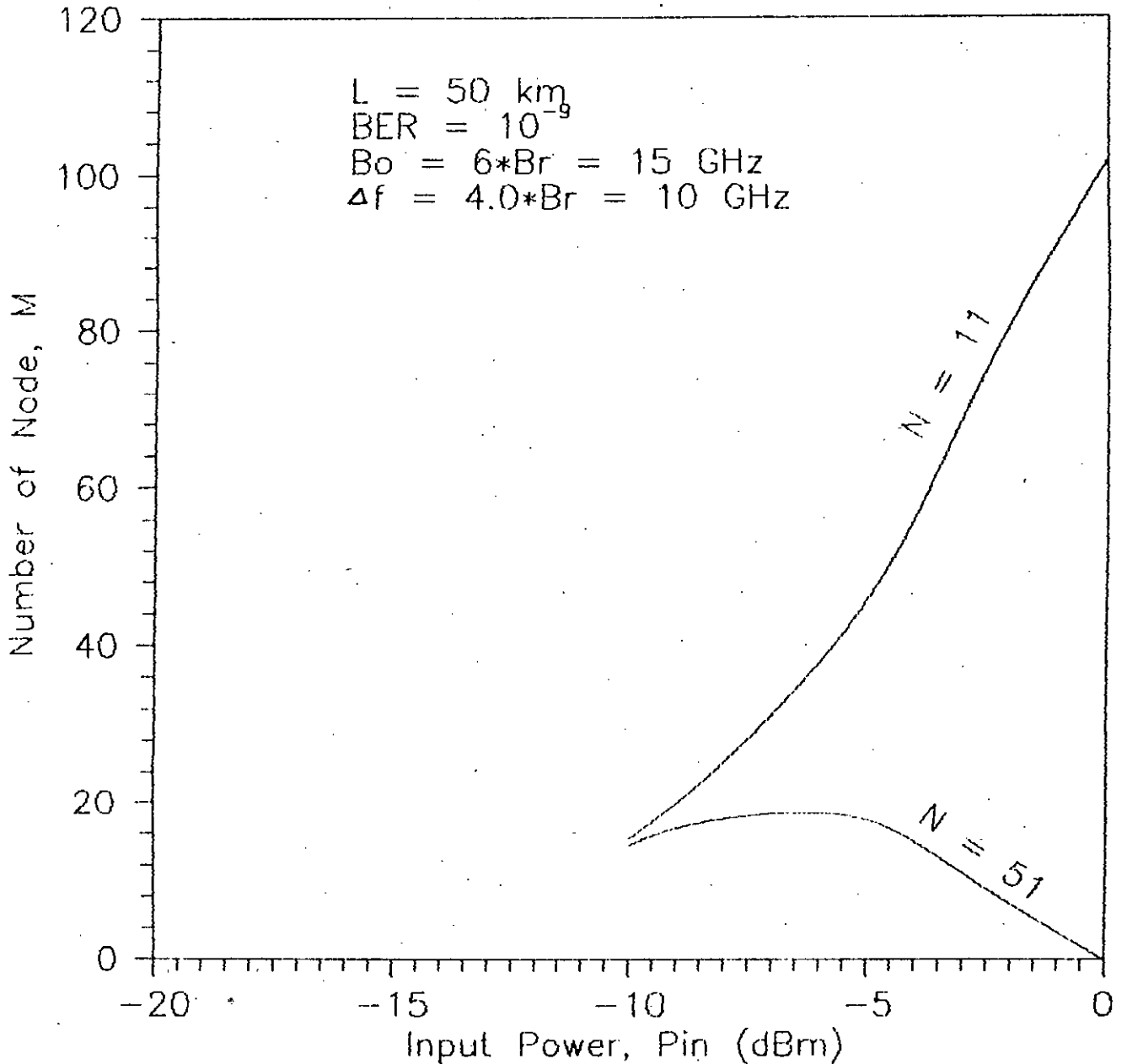


Fig.3.17 Plots of maximum allowable number of nodes M corresponding to BER of 10^{-9} as a function of the input transmitter power P_{in} (dBm) in the presence of four-wave mixing (FWM) effect at a bit rate of 2.5 Gb/ with optical bandwidth $B_o=6B_r=15$ GHz and fiber span $L=50$ Km for number of channels $N=11$ and 51 and channel separation $\Delta f=10$ GHz.

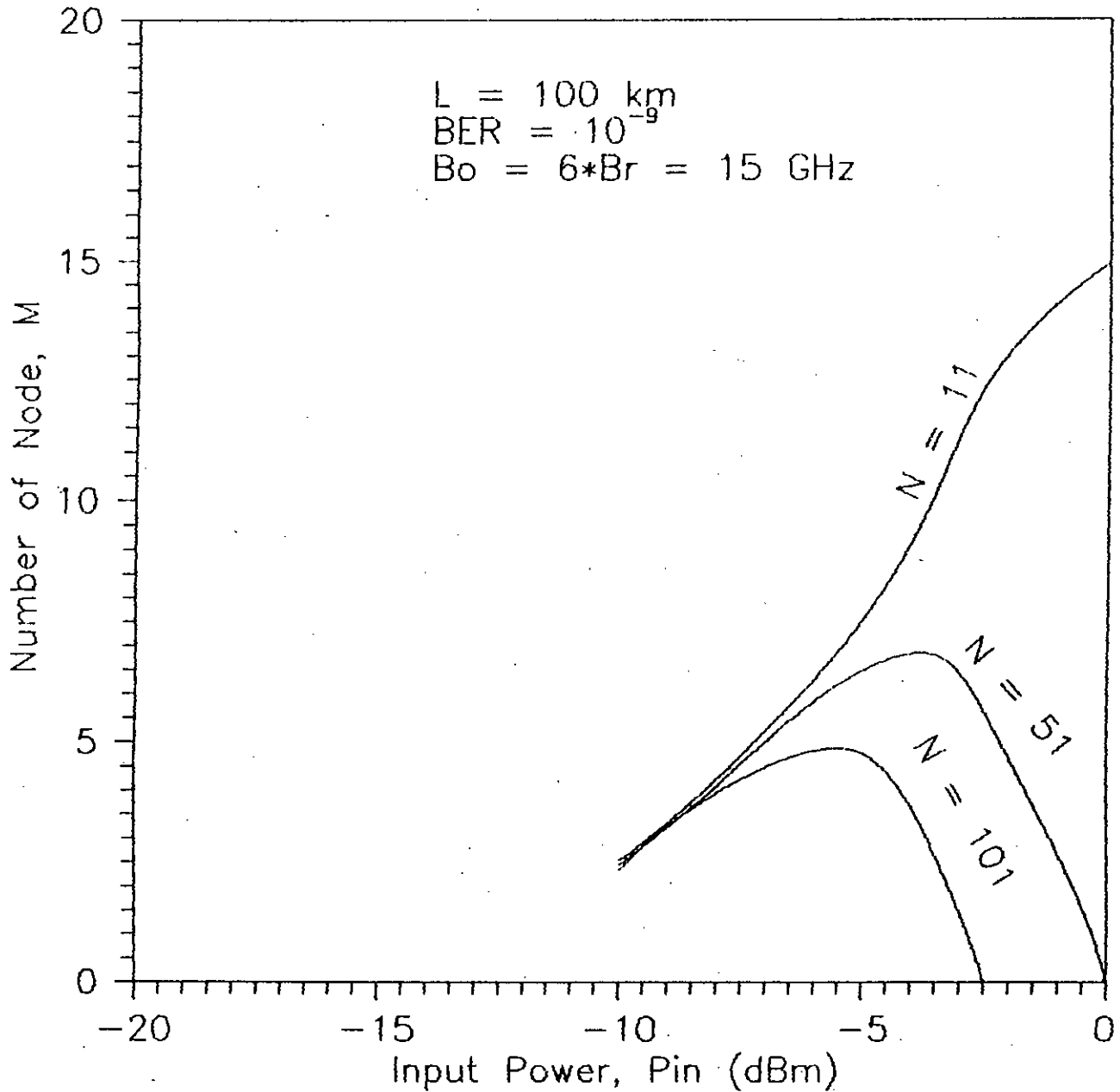


Fig.3.18 Plots of maximum allowable number of nodes M corresponding to BER of 10^{-9} as a function of the input transmitter power P_{in} (dBm) in the presence of four-wave mixing (FWM) effect at a bit rate of 2.5 Gb/s with optical bandwidth $B_o=6B_r=15$ GHz and fiber span $L=100$ Km for number of channels $N=11, 51, 101$ and channel separation $\Delta f=10$ GHz.

maximum transmitter power $P_{in,max}$ is also less.

When the optical bandwidth B_o is increased, the plots of number of nodes M , corresponding to $BER = 10^{-9}$, versus P_{in} (dBm) for a given fiber span ($L = 50$ Km) is illustrated in Fig.3.19 and Fig.3.20 for $B_o = 25$ and 50 GHz respectively. It is noticed that there is a considerable reduction in the number of allowable nodes as B_o is increased from 25 GHz to 50 GHz due to increased ASE, FWM and beat noise components. The reduction is more pronounced at higher values of input power. Further, the maximum values of M i.e., M_{max} is also less at higher optical bandwidth.

Further, the maximum allowable number of nodes is further reduced when the frequency separation Δf between two adjacent channels is increased as depicted in Fig.3.21 with $\Delta f = 50$ GHz, $L = 50$ Km and $B_o = 15$ GHz. Comparison with Fig.3.17 when $\Delta f = 15$ GHz we see that the allowable number of nodes is considerably less at higher Δf .

In Fig.3.22 the allowable number of nodes at $BER = 10^{-9}$ is plotted as a function of the number of channels N when $L = 50$ Km and $B_o = 15$ GHz for several input transmitter power. It is noticed that at a given input power, the number of nodes reduces with increasing values of the number of channels due

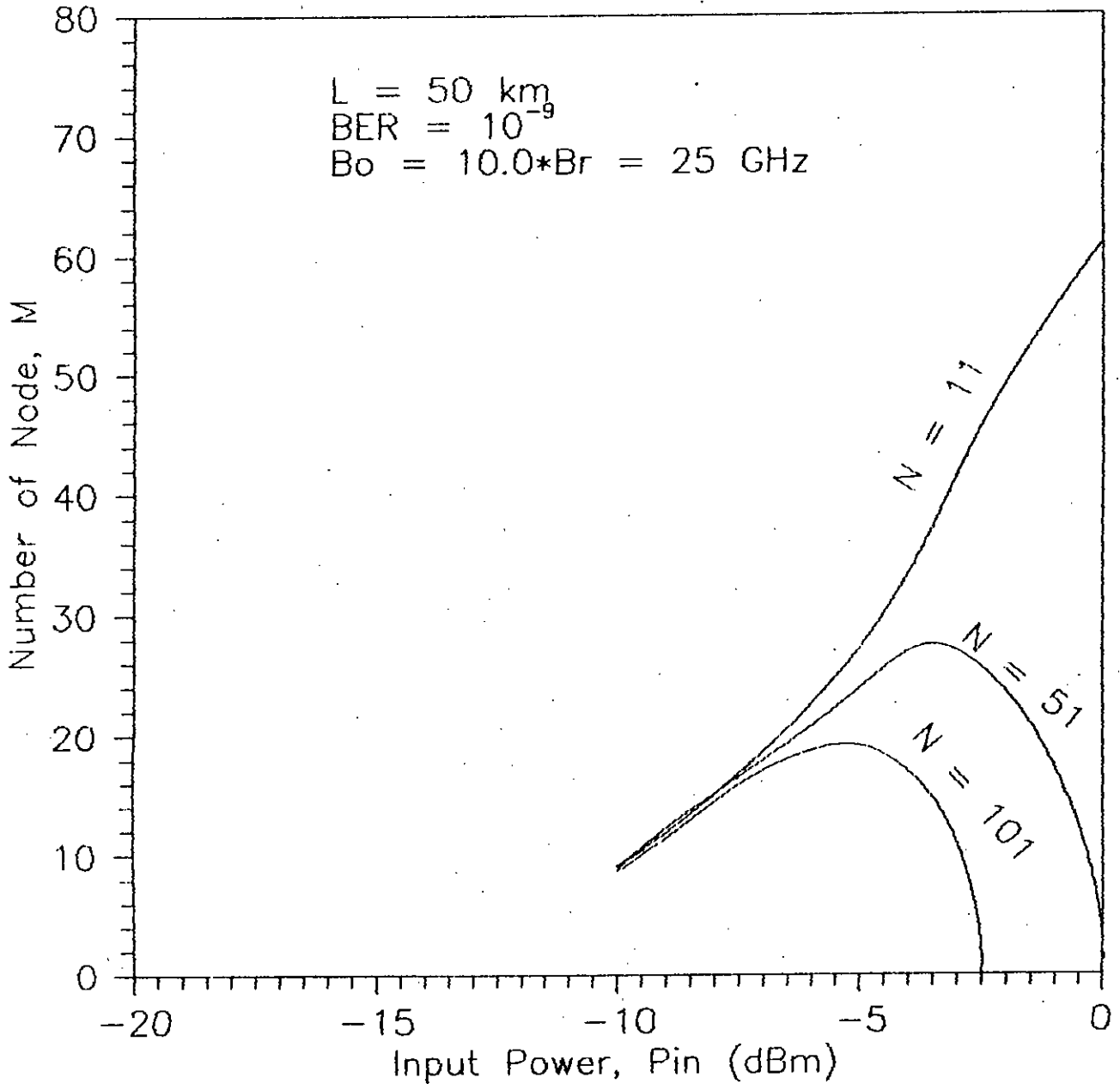


Fig.3.19 Plots of maximum allowable number of nodes M corresponding to BER of 10^{-9} as a function of the input transmitter power P_{in} (dBm) in the presence of four-wave mixing (FWM) effect at a bit rate of 2.5 Gb/s with optical bandwidth $B_o=10B_r=25$ GHz and fiber span $L=50$ Km for number of channels $N=11, 51, 101$ and channel separation $\Delta f=10$ GHz.

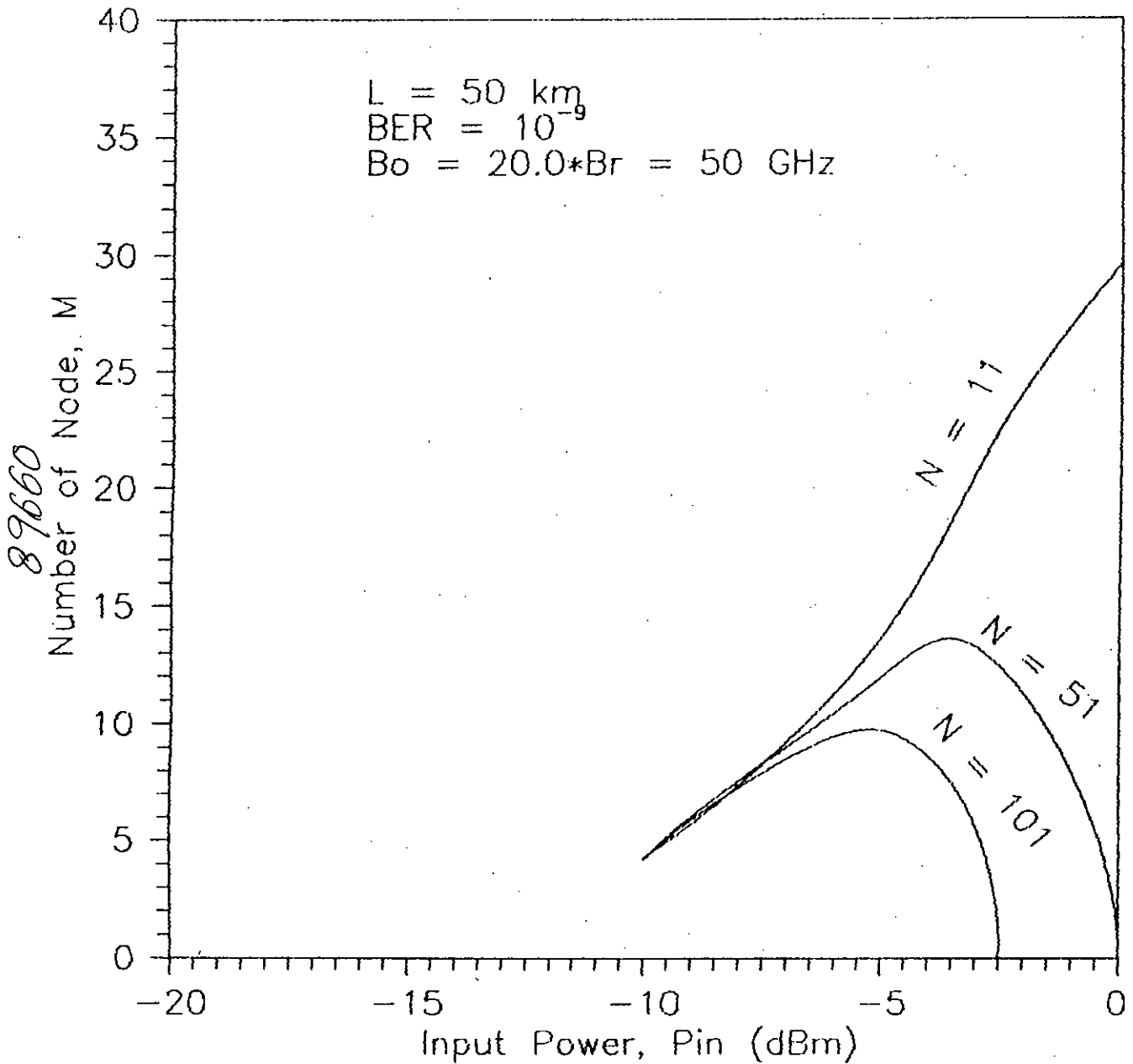


Fig.3.20 Plots of maximum allowable number of nodes M corresponding to BER of 10^{-9} as a function of the input transmitter power P_{in} (dBm) in the presence of four-wave mixing (FWM) effect at a bit rate of 2.5 Gb/s with optical bandwidth $B_o=20B_r=50$ GHz and fiber span $L=50$ Km for number of channels $N=11, 51, 101$ and channel separation $\Delta f=10$ GHz.

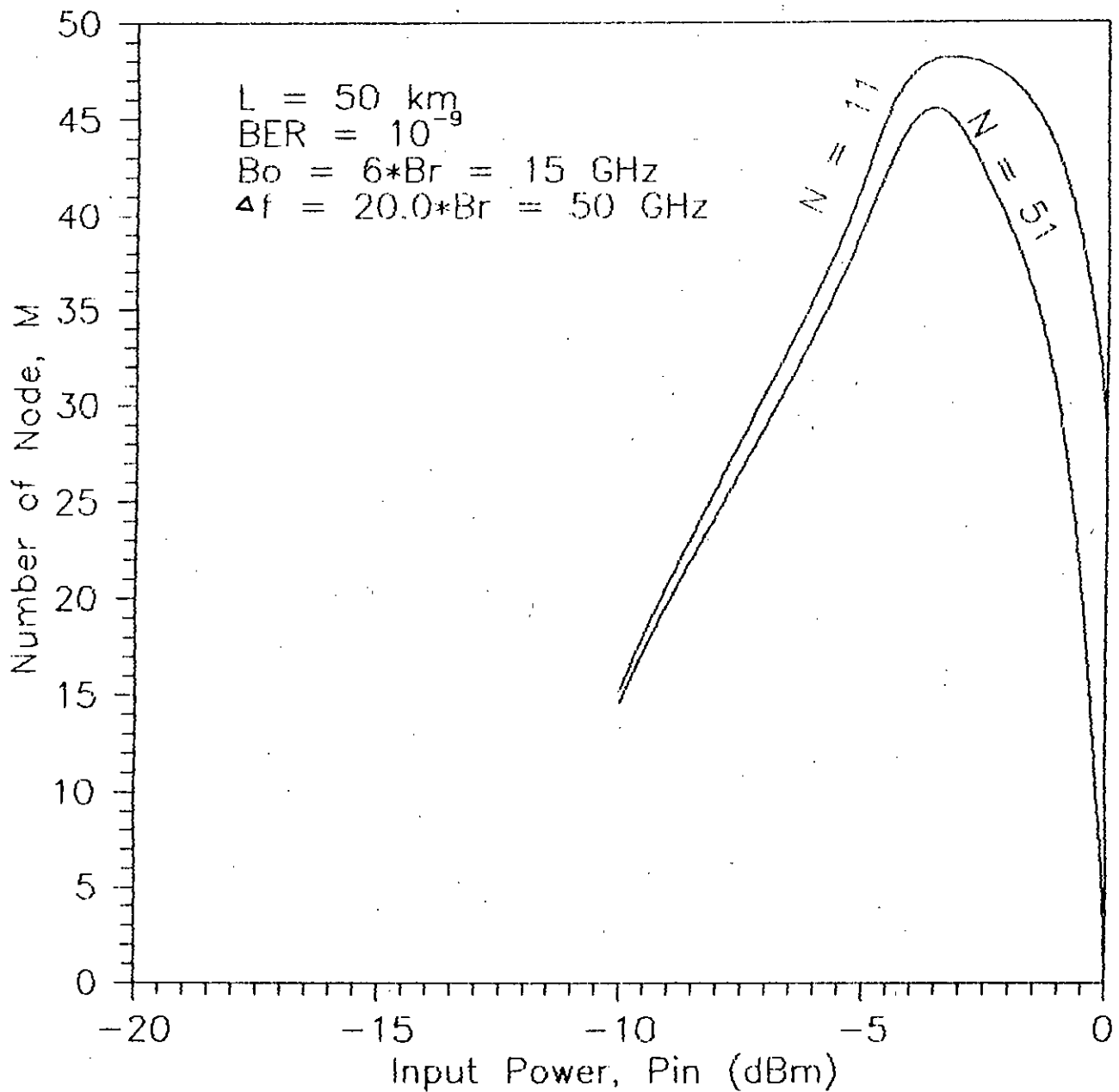


Fig.3.21 Variation of the allowable number of nodes M at $BER=10^{-9}$ versus the transmitter power P_{in} (dBm) in the presence of FWM effect when the number of channels $N=11$ and 51 and channel separation $\Delta f=50$ GHz, $B_o=15$ GHz and fiber span, $L=20$ Km.

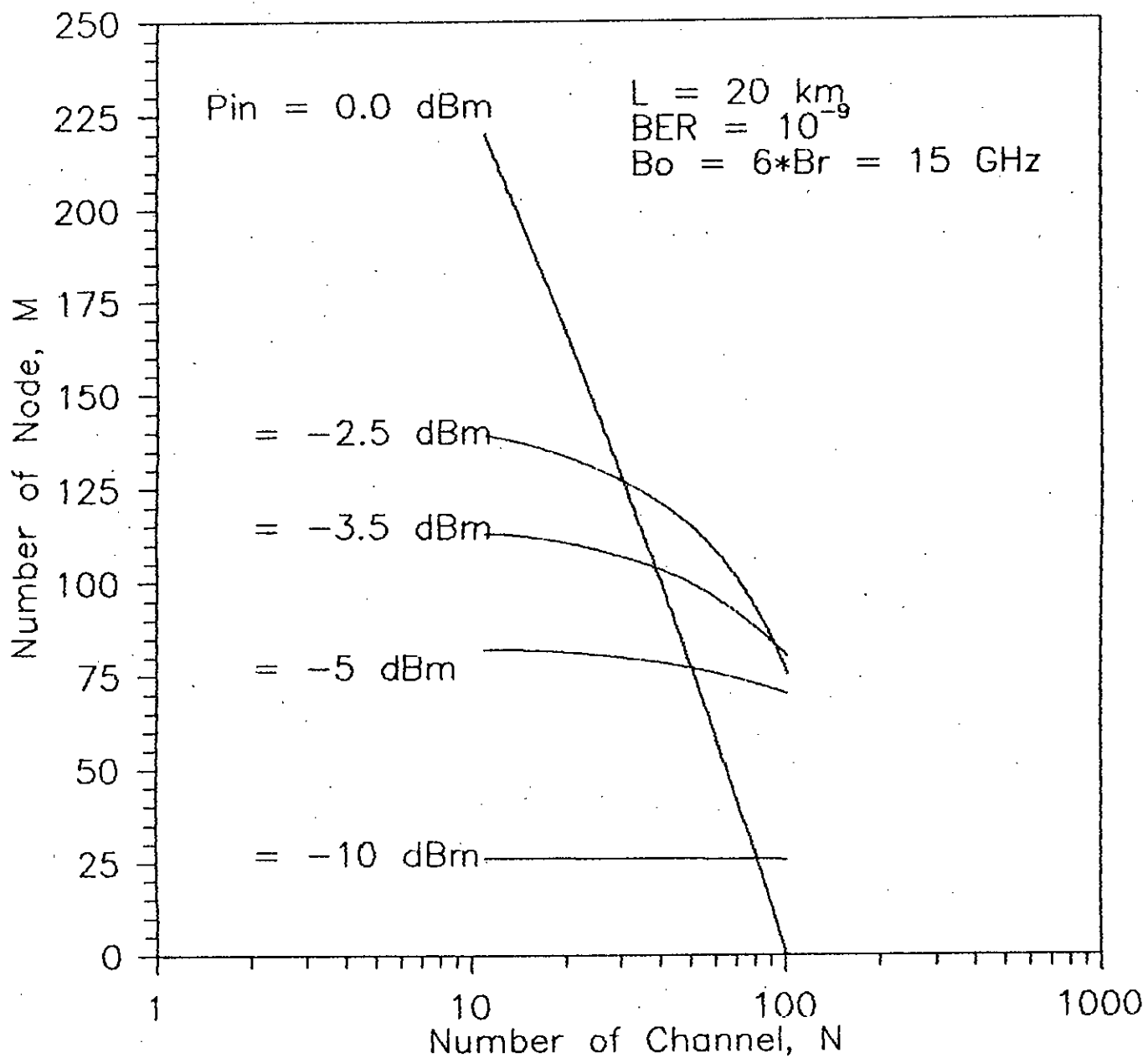


Fig.3.22 Plots of maximum allowable number of nodes M in presence of FWM effect at a bit error rate (BER) of 10^{-9} as a function of the number of WDM channels, N when channel separation is 10 GHz and $L=20 \text{ Km}$ for different values of transmitter power P_{in} (dBm).

to increased FWM effect. The rate at which the number of nodes M decreases depends on input power P_{in} . The reduction is more rapid at higher optical input power and at low value of input power number of nodes M is almost independent of number of channels N . Similar curves of M vs. N for higher span length L and higher optical bandwidth B_o are shown in Fig.3.23 and Fig.3.24 respectively. The figures reveal similar behavior and indicate how the number of allowable nodes is greatly reduced due to increased fiber length and/or increased optical bandwidth.

The maximum achievable number of nodes at $BER = 10^{-9}$ and at a given fiber span L and given value of the number of channels N is plotted against the channel separation Δf (GHz) in Fig.3.25 and Fig.3.26 with input optical power P_{in} as a parameter. These curves illustrate the dependence of FWM effect (and/or maximum allowable number of nodes M_{max}) on the channel separation. It becomes clear that as the channel separation increases, the value of M_{max} increases, attains a maximum value corresponding to a certain value of Δf and then again decreases. The nature of the curve is due to the dependence of FWM phase $\Delta\beta$ on the channel separation Δf .

Fig.3.27 depicts the variation of maximum allowable number of nodes, M_{max} with optical bandwidth B_o for number of channels

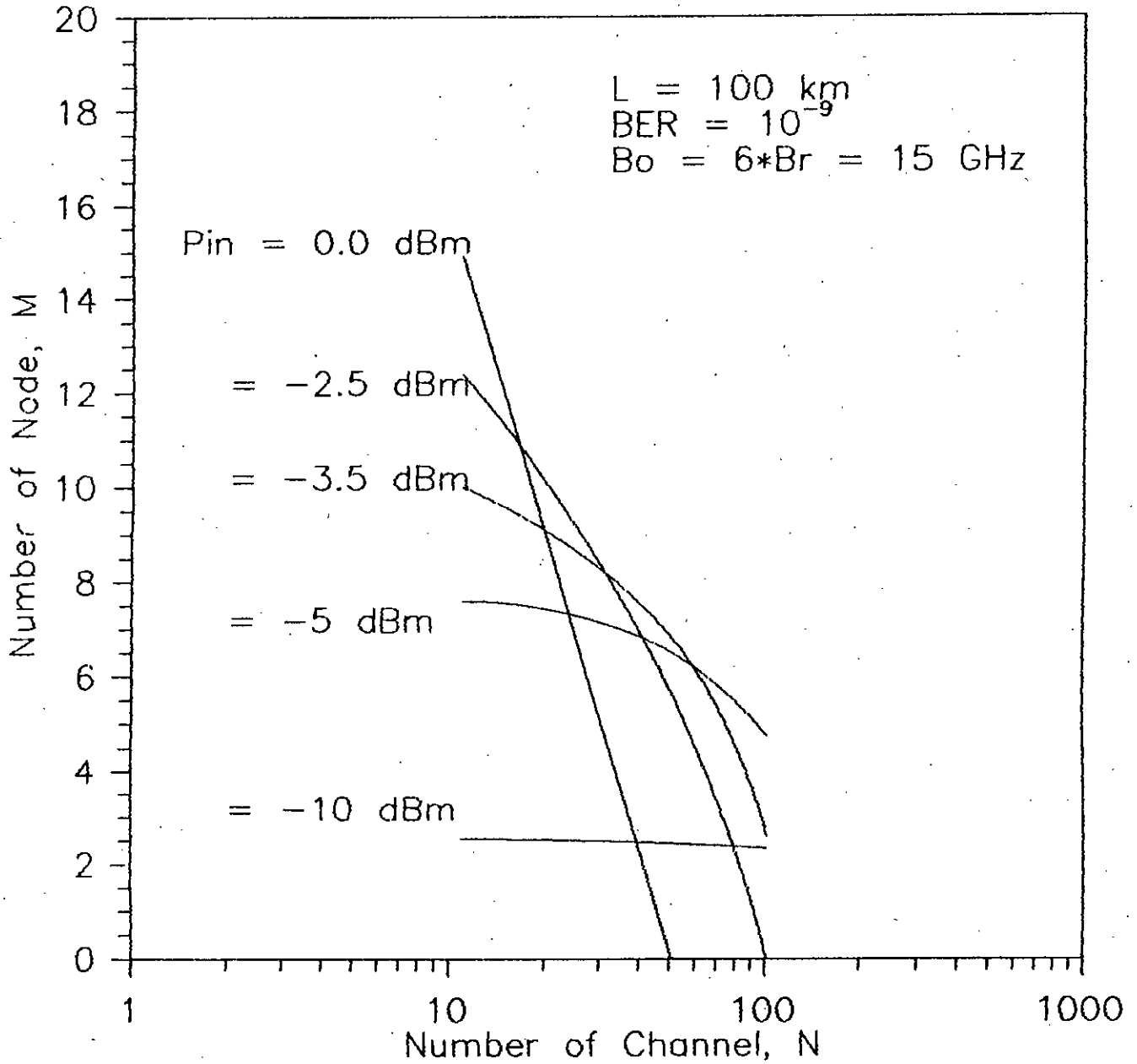


Fig.3.23 Plots of maximum allowable number of nodes M in presence of FWM effect at a bit error rate (BER) of 10^{-9} as a function of the number of WDM channels, N when channel separation is 10 GHz and and $L=100 \text{ Km}$ for different values of transmitter power P_{in} (dBm).

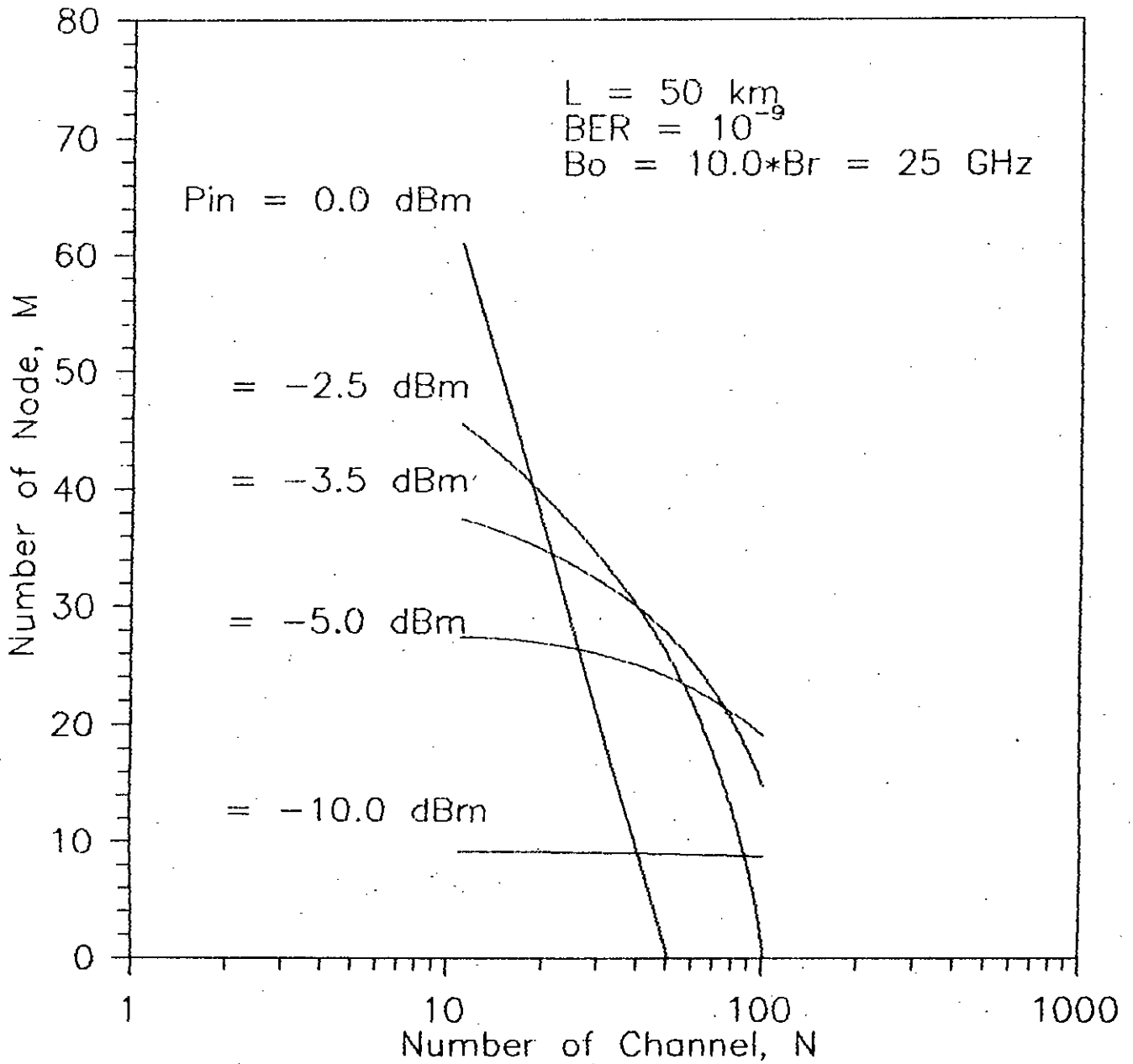


Fig.3.24 Plots of maximum allowable number of nodes M in presence of FWM effect at a bit error rate (BER) of 10^{-9} as a function of the number of WDM channels, N when channel separation is 10 GHz and $L=50 \text{ Km}$ and $B_o=10B_r=25 \text{ GHz}$ for different values of transmitter power P_{in} (dBm).

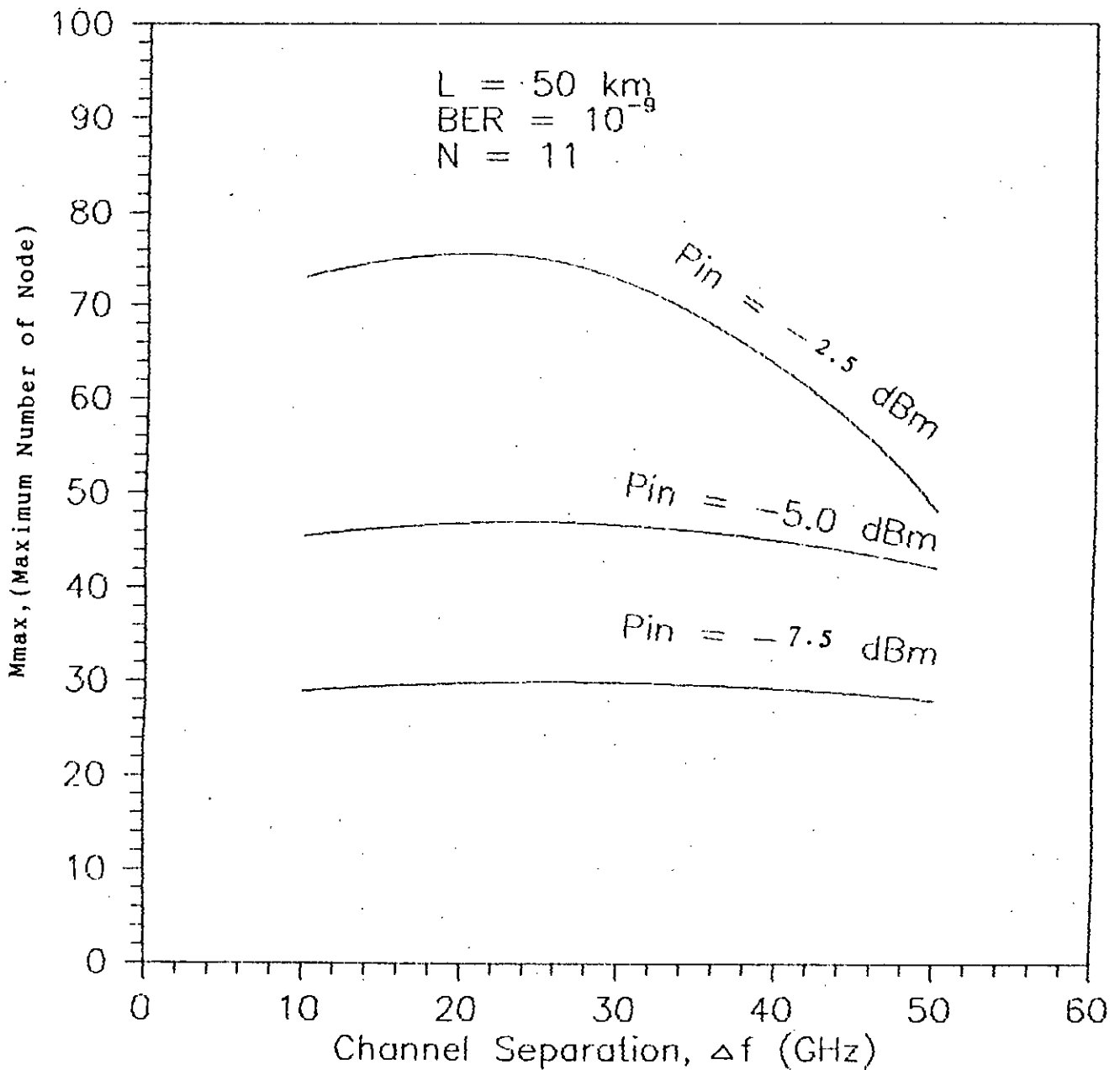


Fig.3.25 Plots of the allowable maximum number of nodes M_{max} at $BER=10^{-9}$ as a function of channel separation Δf in the presence of FWM effect when the number of WDM channels $N=11$ and fiber span $L=50$ Km for $P_{in} = -2.5, -5.0, -7.5 \text{ dBm}$.

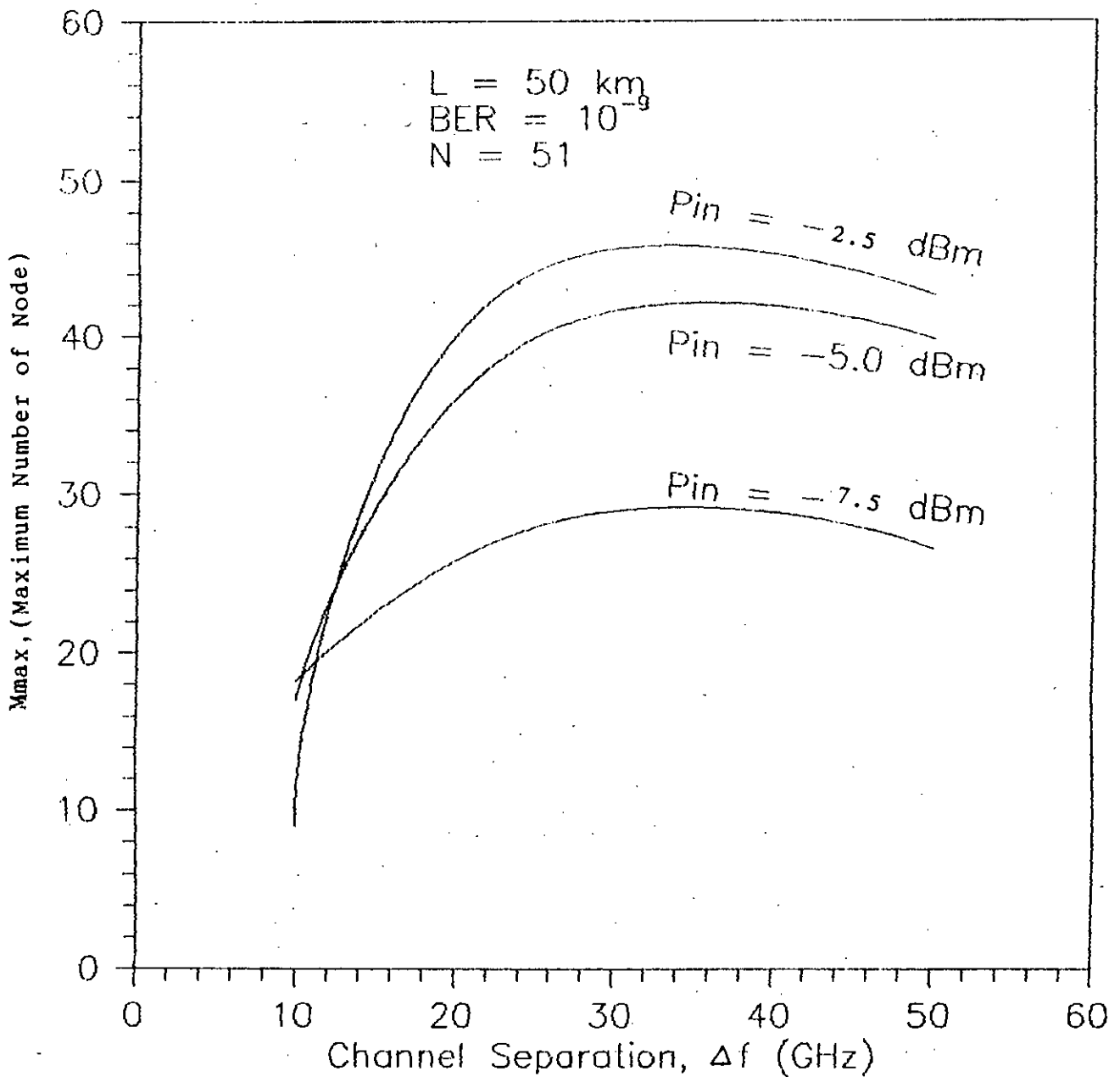


Fig.3.26 Plots of the allowable maximum number of nodes M_{max} at $BER=10^{-9}$ as a function of channel separation Δf in the presence of FWM effect when the number of WDM channels $N=51$ and fiber span $L=50$ Km for $P_{in} = -2.5, -5.0, -7.5$ dBm.

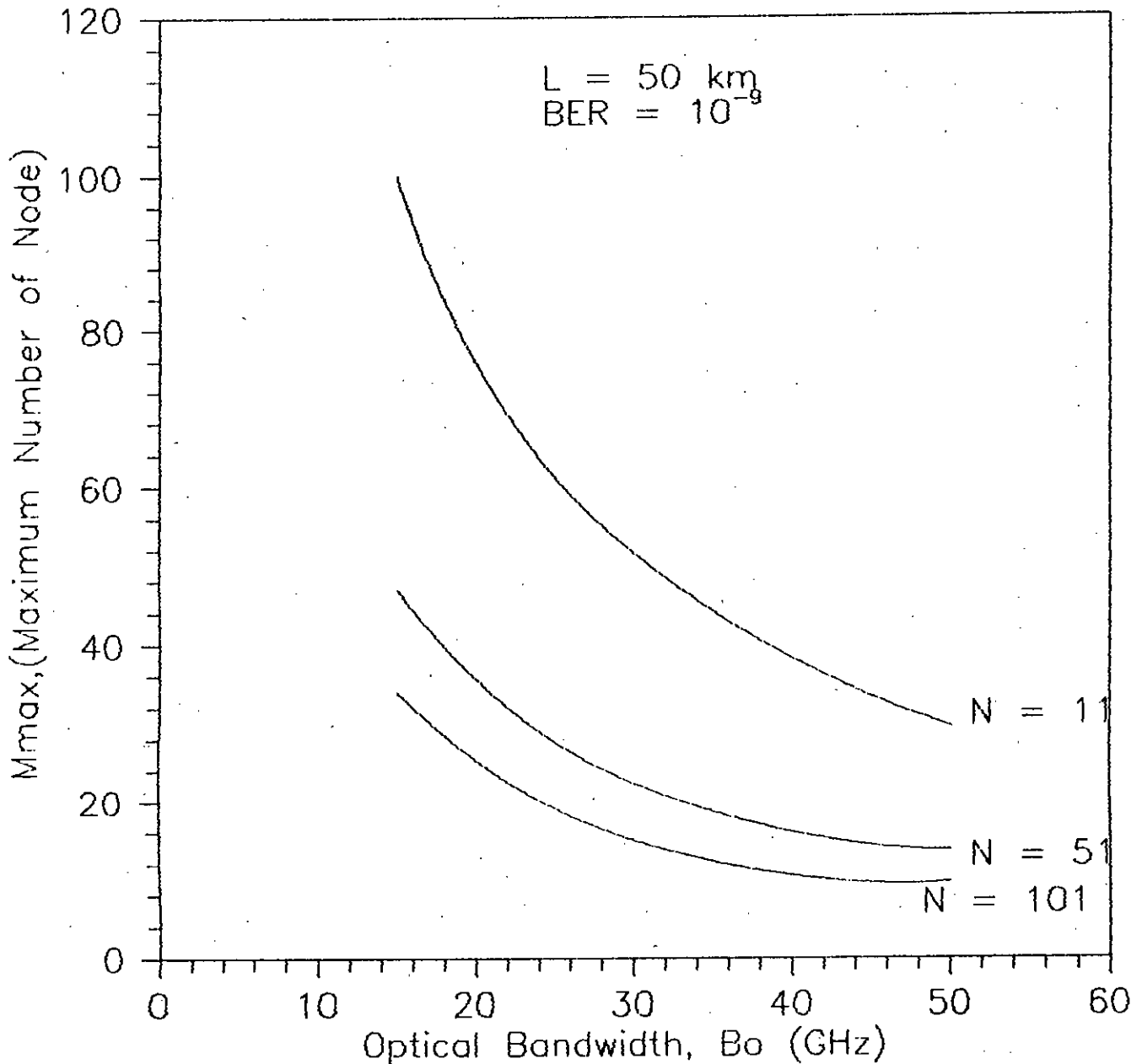


Fig.3.27 Plots of the ultimate maximum number of nodes M_{max} , versus optical bandwidth B_o (GHz) at $\text{BER}=10^{-9}$ in the presence of FWM effect for three different values of the number of WDM channels $N=11, 51, 101$ when fiber span $L=50 \text{ Km}$ and channel separation $\Delta f=25 \text{ GHz}$.

$N = 11, 51$ and 101 . Again it is clearly noticed that M_{\max} decreases exponentially with increased optical bandwidth.

The maximum allowable optical input power, $P_{\text{in,max}}$ corresponding to M_{\max} at $\text{BER} = 10^{-9}$ is plotted against B_o (GHz) in Fig.3.28. It is found that $P_{\text{in,max}}$ is higher at lower values of N and is greatly reduced at higher value of N and is almost independent on B_o which is also evident from Fig.3.29.

In Fig.3.30, the maximum allowable number of nodes is plotted as a function of number of channels N for $B_o = 15, 25$ and 50 GHz and $L = 50$ Km. This figure reveals that M_{\max} is reduced greatly at higher values of N , and higher optical bandwidth. Similar observations are also found in Fig.3.31 where M_{\max} is plotted against N for $L = 20, 50$ and 100 Km.

Fig.3.32 depicts the variation of $P_{\text{in,max}}$ with N for three values of fiber span, $L = 20, 50$ and 100 Km. It reveals that $P_{\text{in,max}}$ decreases exponentially with increasing N at a given value of L .

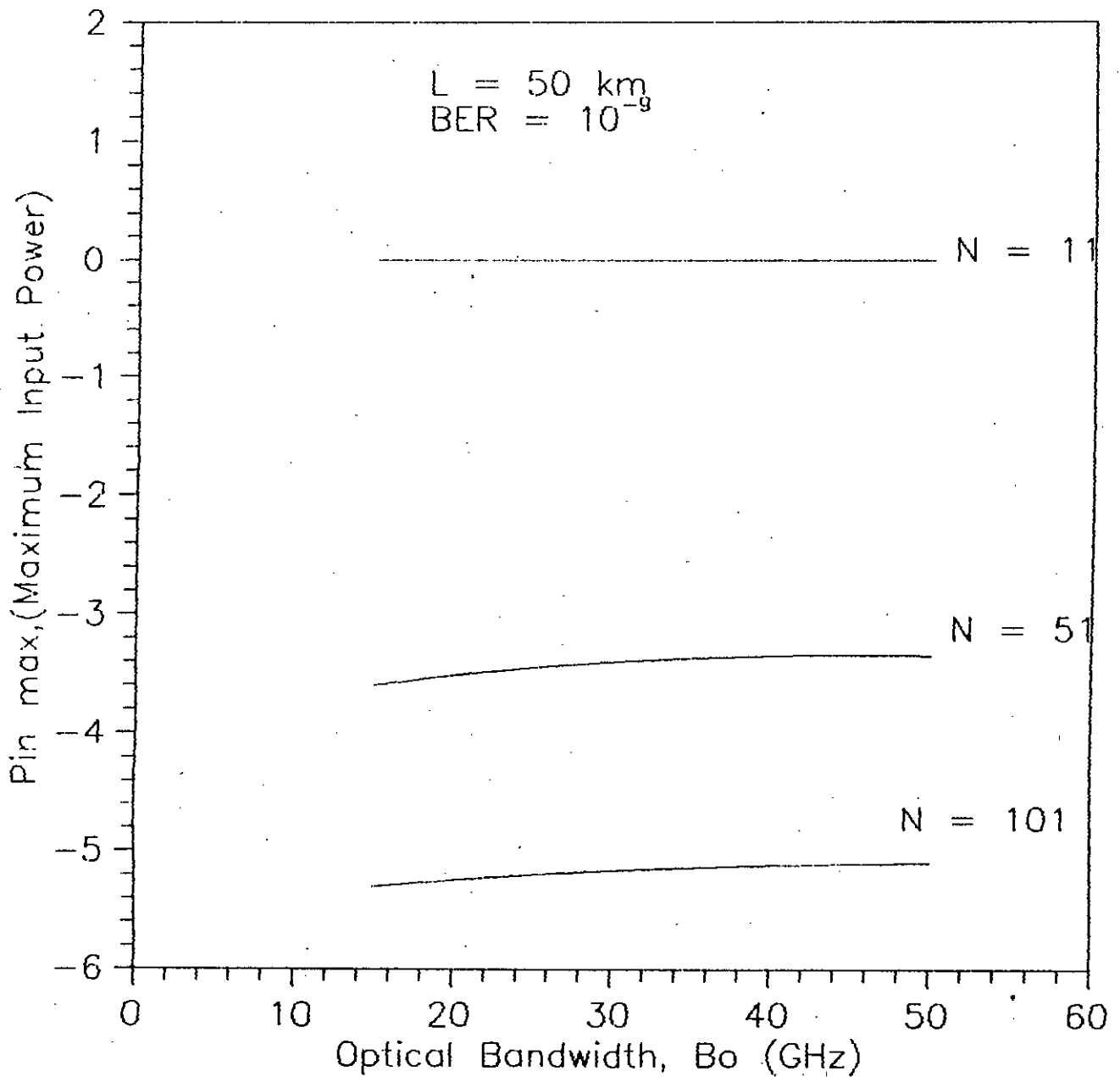


Fig.3.28 Plots of maximum allowable laser transmitter power $P_{in(max)}$ corresponding to the ultimate maximum number of nodes M_{max} at $BER=10^{-9}$ versus optical bandwidth B_o (GHz) in the presence of FWM effect when fiber span $L=50$ Km for the number of WDM channels $N=11, 51, 101$ and channel separation $\Delta f=25$ GHz.

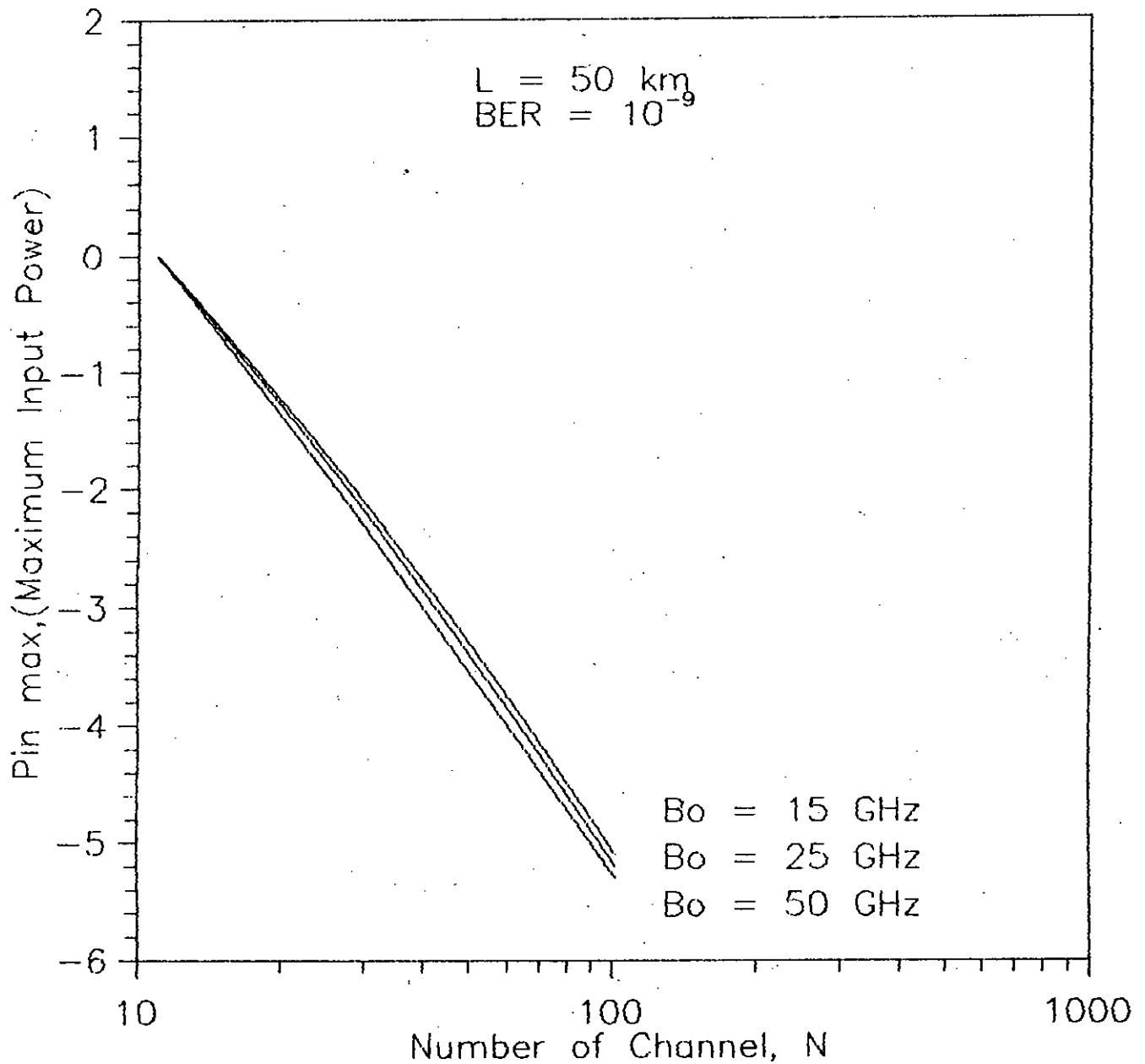


Fig.3.29 Plots of maximum allowable laser transmitter power $P_{in(max)}$ versus number of WDM channels N for three values of optical bandwidth $B_0=15, 25, 50 \text{ GHz}$ at $BER=10^{-9}$ in the presence of FWM effect and fiber span $L=50 \text{ Km}$ and channel separation $\Delta f=25 \text{ GHz}$.

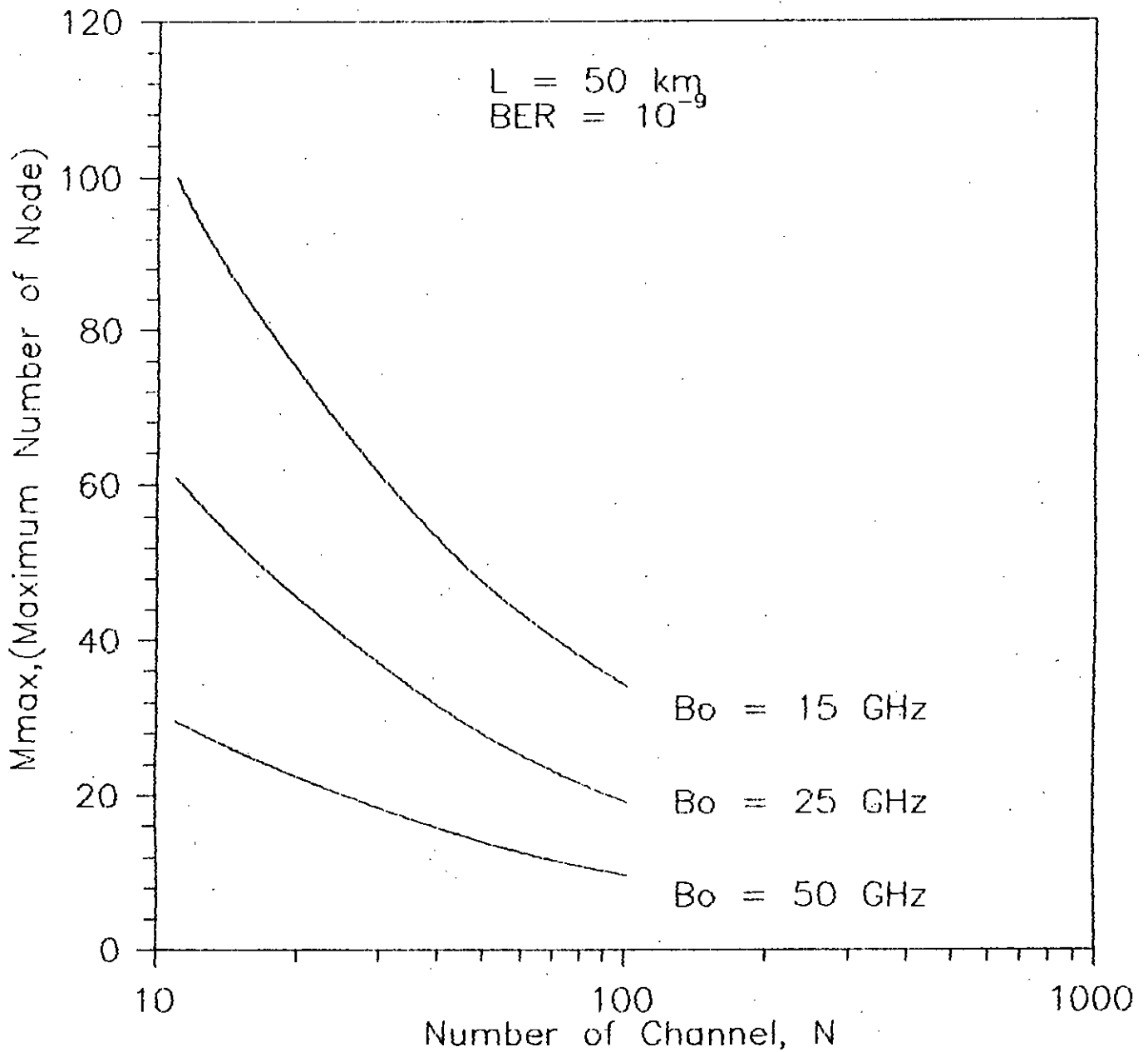


Fig.3.30 Plots of maximum allowable ultimate number of nodes M_{\max} versus number of WDM channels N for three values of optical bandwidth $B_o=15, 25, 50$ GHz at $BER=10^{-9}$ in the presence of FWM effect and fiber span $L=50$ Km and channel separation $\Delta f=25$ GHz.

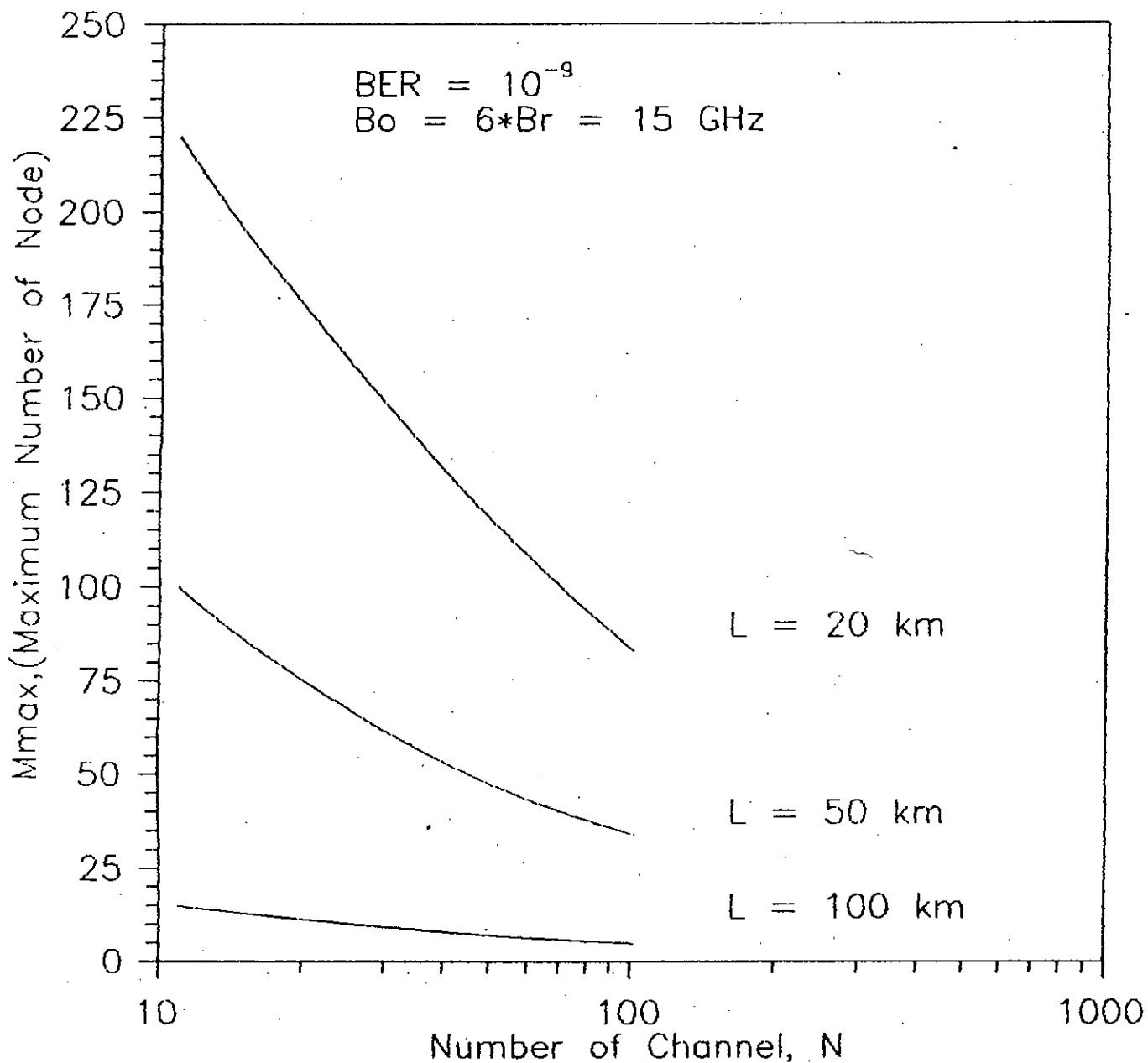


Fig.3.31 Plots of the ultimate maximum number of nodes M_{max} , versus number of WDM channels N at $BER=10^{-9}$ for fiber span $L=20$ Km, 50 Km and 100 Km when optical bandwidth $B_o=15$ GHz and channel separation $\Delta f=25$ GHz.

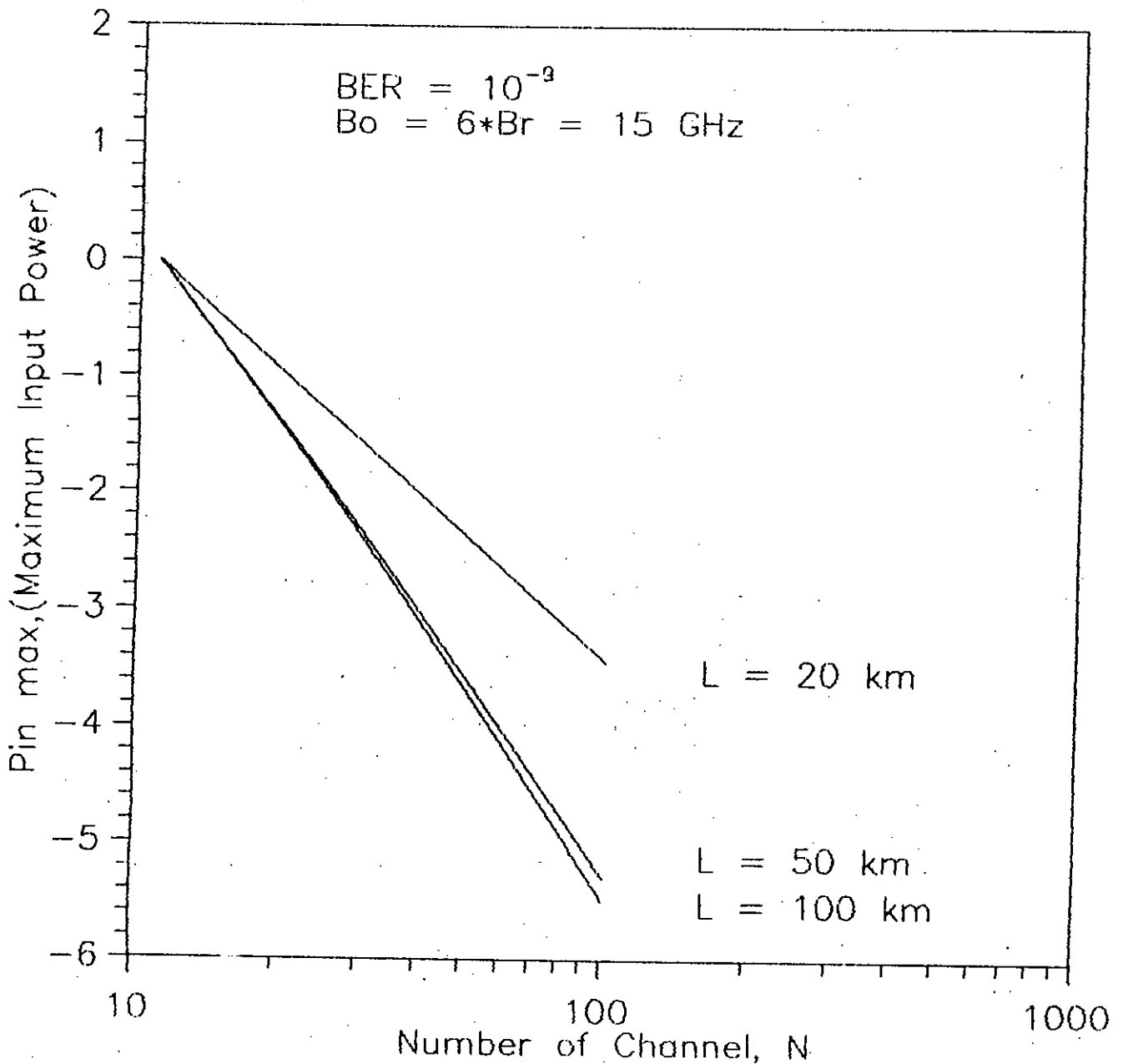


Fig.3.32 Plots of maximum allowable laser transmitter power P_{in} (dBm) corresponding to the ultimate maximum number of nodes M_{max} at $BER=10^{-9}$ versus number of WDM channels N for fiber span $L=20$ Km, 50 Km and 100 Km when optical bandwidth $B_o=15$ GHz and channel separation $\Delta f=25$ GHz.

CHAPTER - IV

CONCLUSIONS AND SUGGESTIONS

4.1 Conclusions:

A detailed theoretical analysis is carried out to evaluate the impact of fiber non-linear effects viz. four-wave mixing (FWM) and chromatic dispersion on the performance of optical multiwavelength transmission system with in-line optical amplifier's and CPFSK heterodyne delay-demodulation reception. Performance results are evaluated at a bit rate of 2.5 Gb/s, considering monomode fiber at an wavelength of 1550 nm for several sets of receiver and system parameters. The results indicate that the bit error rate (BER) increases with increasing value of the number of nodes due to accumulation of optical amplifier's spontaneous emission (ASE) noise for one node to another. At a BER of 10^{-9} , the allowable number of nodes are found to be more at higher input power. However, when the fiber span is larger, the allowable number of nodes is less due to increased ASE with increased amplifier gain to meet additional fiber loss due to increased fiber span.

In the presence of FWM effect the performance of the system is found to be degraded and the number of allowable nodes at $BER = 10^{-9}$ is drastically reduced at a given input transmitter power and fiber span. For example, when the input power $P_{in} = 0$ dBm and $L = 20$ Km, $N = 11$ then the number of allowable node is around 300 whereas it reduces to 220 when the FWM effect is included. The effect of FWM is found to be more pronounced when the number of channels is increased. For example, for $P_{in} = 0$ dBm, the number of allowable nodes at $BER = 10^{-9}$ is around 220 for $N = 11$, $L = 20$ Km whereas it is reduced to 75 and 15 when N is increased to 51 and 101 respectively.

The plots of allowable number of nodes M at $BER = 10^{-9}$ show that the number of nodes increases with P_{in} and attains a maximum value of M_{max} corresponding to a maximum input power $P_{in(max)}$. Further increase in P_{in} causes the number of nodes to decrease. The value of M_{max} depends on the number of channels and fiber span, and decreases with increasing value of the number of channels and fiber span due to increased FWM power and increased ASE and other beat noise components.

Further, it is also observed that the bandwidth of the optical amplifier B_o has a great influence on the maximum achievable number of nodes. At higher optical bandwidth, the

influence of FWM and ASE is higher and as a consequence for a given transmitter power P_{in} , the allowable number of channels and/or number of nodes is significantly less. For example, for $B_o = 15$ GHz and $P_{in} = -3.5$ dBm, the number of nodes at $BER = 10^{-9}$ is around 60 corresponding to $L = 50$ Km and $N = 11$ whereas it reduces to nearly 20 when B_o is increased to 50 GHz. On the other hand, if the number of nodes is kept fixed, the number of channels must be decreased if B_o is increased at a given value of the input power. However, the maximum allowable input power $P_{(inmax)}$ is found to be almost independent of B_o and is significantly less at higher values of N .

It is further noticed that the number of nodes or number of channels can be increased at a given value of P_{in} and fiber span, if the channel separation Δf is increased. It is observed that the number of nodes at a given value of N increases with Δf and attains a maximum value corresponding to an optimum value of the channel separation after which it again decreases. The optimum value of channel separation is slightly less at higher values of input power P_{in} . Also, the required optimum channel separation is slightly higher for increased value of N due to increased FWM effect.

4.2 Suggestions for Future Extension of this Work:

Future works can be carried out to investigate the effect of switch crosstalk in the presence of FWM effect on optically amplified multi-wavelength transport network (MWTN). The packet error probability at a given node can be determined conditioned on a number of bits in a packet. The analysis can be carried out considering a Shuffle-Net or a Manhattan Street Network. An upper bound on the network performance in terms of maximum achievable bit rate and throughput for a given packet error rate can be evaluated.

Future work in this area can also be carried out to include the effect of Raman Scattering, the jitter accumulation due to amplifier's spontaneous emission noise, nonuniform chromatic dispersion along the fiber etc.. A detailed Monte-carlo simulation of the wavelength routed optical network can also be carried out to verify the theoretical results and to determine the optimum system parameters for reliable system performance.

REFERENCES

- [1] T. Okoshi, "Recent advances in coherent optical fiber communication systems", J. Lightwave Tech., vol. LT-5, no. 1, pp. 44-52, 1987.
- [2] T. Kimura, "Coherent optical fiber transmission", J. Lightwave Tech. vol. LT-5, no. 4, pp. 414-428, 1987.
- [3] R. A. Linke, "High capacity coherent lightwave systems", J. Lightwave Tech. vol. 6, no. 11, pp. 1750-1769, November 1988.
- [4] U. Timor, and R. A. Linke, "A comparison of sensitivity degradations for optical homodyne versus direct detection on-off keyed signals", J. Lightwave Tech., vol. 6, no. 11, pp. 1782-1788, November 1988.
- [5] K. Emura, S. Yamazaki, M. Yamaguchi, M. Shikada, and K. Minemura, "An optical FSK heterodyne dual filter detection system for taking advantage of DFB LD applications", J. Lightwave Tech., vol. 8, no. 2, pp. 243-250, February 1990.
- [6] H. Toba, K. Oda and K. Nosu, "Design and performance of FSK-direct detection scheme for optical FDM systems", J. Lightwave Tech., vol. 9, no. 10, pp. 1335-1343, October 1991.
- [7] R. S. Vodhanel, "5 Gbit/s direct optical DPFSK modulation of a 1530-nm DFB laser", IEEE Photon. Tech. Lett., vol. 1, no. 8, pp. 218-220, August 1989.
- [8] M. W. Maeda, W. B. Sessa, W. I. Way, A. Yi-Yan, L. Curtis, and R. I. Laming, "The effect of four-wave mixing in fibers on optical frequency-division multiplexed systems", J. Lightwave Tech., vol. 8, no. 9, pp. 1402-1408, September 1990.
- [9] A. F. Elrefaie, R. E. Wanger, D. A. Atlas, and D. G. Find, "Chromatic dispersion limitations in coherent lightwave systems," J. Lightwave Tech., vol. 6, pp. 704-709, 1988.

- [10] A. R. Chraplyvy, "Limitations on lightwave communications imposed by optical-fiber nonlinearities", J. Lightwave Tech., vol. 8, no. 10, pp. 1548-1557, October 1990.
- [11] E. Lichtman, "Bit rate-distance product limitations due to fiber nonlinearities in multichannel coherent optical communication systems", Electron. Lett., vol. 27, no. 9, pp. 757-759, April 1991.
- [12] E. Iannone, F. S. Locati, F. Matera, M. Romagnoli and M. Settembre, "Performance evaluation of single-channel coherent systems in presence of nonlinear effects", Electron. Lett., vol. 28, no. 7, pp. 645-646, March 1992.
- [13] K. Inoue, "Phase-mismatching characteristic of four-wave mixing in fiber lines with multistage optical amplifiers", Optics Lett., vol. 17, no. 11, pp. 801-803, June, 1992.
- [14] K. Inoue, "Super position technique for fiber four-wave mixing using optical multi-/demultiplexers and a delay line", J. Lightwave Tech., vol. 11, no. 3, pp. 455-461, March 1993.
- [15] K. Inoue and H. Toba, "Fiber four-wave mixing in multi-amplifier systems with nonuniform chromatic dispersion", J. Lightwave Tech., vol. 13, no. 1, pp. 88-93, January 1995.
- [16] K. H. Kim, H. K. Lee, S. Y. Park, and E. -H. Lee, "Calculation of dispersion and nonlinear effect limited maximum TDM and FDM bit rates of transform-limited pulse in single-mode optical fibers", J. Lightwave Tech., vol. 13, no. 8, pp. 1597-1605, August 1995.
- [17] A. Montes and A. M. Rubenchik, "Information rate limit due to stimulated Brillouin scattering for transmission capacity in soliton based optical - fiber communications", Laboratoire de physique de la matiere condense, U.R.A. 190 au C.N.R.S., Universite de Nice-Sophia Antipolis, Parc Valrose, 06034 Nice Cedex, France. pp. 13/1-13/3.

- [18] C-Ching Shih, "Analytical theory of four-wave stimulated brillouin scattering in the saturation regime", IEEE J. Quantum Electron., vol. QE-23, no. 9, pp. 1452-1457, September 1987.
- [19] A. Djupsjobacka and O. Sahlen, "Dispersion compensation by time delay", J. Lightwave Tech., vol. 12, no. 10, pp. 1849-1853, October 1994.
- [20] N. A. Olsson, "Lightwave systems with optical amplifiers", J. Lightwave Tech., vol. 7, no. 7, pp. 1071-1082, July 1989.
- [21] K. Inone, H. Toba, and K. Nosu, "Multichannel amplification utilizing an Er^{3+} -doped fiber amplifier", J. Lightwave Tech., vol. 9, no. 3, pp. 368-373, March 1991.
- [22] G. R. Hill, "A wavelength routing approach to optical communication networks", British Telecom. Technol. J., vol. 6, pp. 42-51, 1988.
- [23] C. Saxtoft, and P. Chidgey, "Error rate degradation due to switch crosstalk in large modular switched optical networks", IEEE Photonics Tech. Lett., vol. 5, no. 7, pp. 828-831, July 1993.
- [24] E. Bedrosian, and S. O. Rice, "Distortion and crosstalk of linearly filtered angle-modulated signals", Proc. IEEE, vol. 56, pp. 2-13, January 1968.
- [25] R. G. McKay, and J. C. Cartledge, "Performance of coherent optical CPFSK-DD with intersymbol interference, noise correlation, and laser phase noise", J. Lightwave Tech., vol. 11, no. 11, pp. 1845-1853, November 1993.
- [26] I. Garrett and G. Jacobsen, "Theory for optical heterodyne narrow-deviation FSK receivers with delay demodulation", J. Lightwave Tech., vol. 6, no. 9, pp. 1415-1423, September 1988.
- [27] M. Schwartz, W. R. Bennett, and S. Stein, "Communication systems and techniques", New York: McGraw-Hill, 1966.

- [28] C. W. Helstrom, "Computing the generalized Marcum Q-function", IEEE Trans. inform. theory, vol. 38, no. 4, pp. 1422-1428, July 1992.
- [29] R. F. Pawula, "On the theory of error rates for narrow-band digital FM", IEE Transaction Commun., vol. 36, no. 4, pp. 509-512, April 1988.
- [30] S. P. Majumder, R. Gongopadyay, M. S. Alam, and G. Parti, "Performance of linecoded heterodyne FSK system with nonuniform laser FM response", J. Lightwave Tech., vol. 13, no. 4, pp. 628-638, April 1995.
- [31] R. Gangopadhyay and S. P. Majumder, "Impact of laser phase noise on optical heterodyne single filter FSK system with optical preamplifier", Electron. Lett., vol. 27, no. 21, pp. 1927-1929, October 1991.

APPENDIX A

The total FWM power can be calculated as follows [8,10,15]:

$$\begin{aligned}
 P_F(l) &= k^2 \cdot P_{in}^3 \exp(-\alpha l) \sum D_c^2 \eta_{pqr} \\
 k^2 &= \frac{1024 \cdot \pi^6 \cdot \chi^2 \cdot L_{eff}}{\eta^4 \cdot \lambda^2 \cdot c^2 \cdot A_{eff}} \\
 \eta_{pqr} &= \left[\frac{\alpha^2}{\alpha^2 + (\Delta\beta)^2} \right] \left[1 + \frac{4 \cdot \exp(-\alpha l) \sin^2(\Delta\beta l/2)}{[1 - \exp(-\alpha l)]^2} \right] \\
 &\quad \times \frac{\sin^2(N\Delta\beta l/2)}{\sin^2(\Delta\beta l/2)} \tag{A.1} \\
 \Delta\beta &= \frac{2\pi D_c \cdot \lambda^2}{c} |(f_p - f_r)| |(f_q - f_r)| \\
 &\equiv \frac{2\pi D_c \cdot \lambda^2}{c} (\Delta f)^2 (p - r) (q - r)
 \end{aligned}$$

f_i ($i = p, q, r$) = optical frequency of the i -th channel.

χ = nonlinear susceptibility of fiber = 6×10^{-14} m³/watt-sec.

A_{eff} = effective core area = $2\pi r^2$, r = modified radius, $r = W/2$

W = modified diameter = 10.7 μ m

α = attenuation of fiber = nepers/Km.

Chromatic dispersion coefficient,

$$D_c = [23 \text{ ps/Km nm}, \lambda = 1300] \text{ DSF}$$

$$[1 \text{ ps/Km nm}, \lambda = 1550] \text{ DSF}$$

$$D_c = [1 \text{ ps/Km nm}, \lambda = 1300] \text{ NDF}$$

$$[17 \text{ ps/Km nm}, \lambda = 1550] \text{ NDF}$$

value of $D = 6$ for $p \neq q \neq r$ fully degenerate

= 3 for $p = q \neq r$ partially degenerate

c = velocity of light = 3×10^8 m/s.

P_{in} = Input transmitter power.

$$L_{eff} = \frac{1 - \exp(-\alpha l)}{\alpha} \quad (\text{A.2})$$

where, l = fiber length (Km),

L_{eff} = effective fiber length (Km).

for $l \gg 1$, $L_{eff} = 1/\alpha$.

Δf = frequency separation between two adjacent channels.

λ = wavelength of the signal channel (i.e. the middle channel).

APPENDIX B

At the output of the photodetector,

$$\begin{aligned}
 r(t) &= R_d \operatorname{Re}[E(t) + E_{LO}(t)]^2 \\
 &= R_d \operatorname{Re}[\sqrt{2P_s} \exp(j2\pi f_s t + \phi'_s t) \\
 &\quad + \sqrt{2P_{PQT}} \exp(j2\pi f_{PQT} t + \theta_{PQT}) \\
 &\quad + \sqrt{2P_{LO}} \exp(j2\pi f_{LO} t + \theta_{LO})]^2
 \end{aligned} \tag{B.1}$$

where R_d represents the responsivity (A/W) of the PIN photodetector.

The expression of $r(t)$ can be simplified as

$$\begin{aligned}
 r(t) &= 2\sqrt{2P_s \cdot 2P_{PQT}} \cos(2\pi f_s t + \phi'_s(t)) \cdot \cos(2\pi f_{PQT} t + \theta_{PQT}) \\
 &\quad + 2\sqrt{2P_s \cdot 2P_{LO}} \cos(2\pi f_s t + \phi'_s(t)) \cdot \cos(2\pi f_{LO} t + \theta_{LO}) \\
 &\quad + 2\sqrt{2P_{LO} \cdot 2P_{PQT}} \cos(2\pi f_{LO} t + \theta_{LO}) \cdot \cos(2\pi f_{PQT} t + \theta_{PQT}) + n'(t)
 \end{aligned} \tag{B.2}$$

where $n'(t)$ is the additive white noise which includes photodetector shot noise and preamplifier thermal noise.

The above equation can be written in the following form:

$$\begin{aligned}
 r(t) &= 2R_d \sqrt{P_s \cdot P_{PQT}} \cos[2\pi (f_s - f_{PQT}) t + \phi'_s(t) + \theta_{PQT}] \\
 &\quad + 2R_d \sqrt{P_s \cdot P_{LO}} \cos[2\pi (f_{LO} - f_s) t + \phi'_s(t) + \theta_{LO}] \\
 &\quad + 2R_d \sqrt{P_{LO} \cdot P_{PQT}} \cos[2\pi (f_{LO} - f_{PQT}) t + \theta_{LO} + \theta_{PQT}] + n'(t)
 \end{aligned} \tag{B.3}$$

Assumed that the $(f_s + f_{pqr})$, $(f_s + f_{LO})$ and $(f_{LO} + f_{pqr})$ are filtered out, then

$$\begin{aligned}
 r(t) &= 2R_{\alpha} \sqrt{P_s \cdot P_{LO}} \cos[2\pi f_{IF} t + \phi'_s(t) + \theta_{LO}] \\
 &+ 2R_{\alpha} \sqrt{P_s \cdot P_{pqr}} \cos[2\pi (f_s - f_{pqr}) t + \phi'_s(t) + \theta_{pqr}] \\
 &+ 2R_{\alpha} \sqrt{P_{LO} \cdot P_{pqr}} \cos[2\pi (f_{LO} - f_{pqr}) t + \theta_{LO} + \theta_{pqr}] + n'(t) \\
 &= i_s(t) + i_{LO-FM}(t) + i_{s-FM}(t) + i_{th}(t) + i_{shot}(t)
 \end{aligned} \tag{B.4}$$

APPENDIX C

The expressions for the different beat-noise terms are as follows [31]

$$P_{FWM-sp} = 4 I_{FWM} \cdot I_{sp} \cdot \frac{B_e}{B_o} \quad (C.1)$$

where B_e = Bandwidth of IF filter,

B_o = Bandwidth of optical amplifier.

$$\begin{aligned} N_{o-LOSP} &= 4 R_d^2 P_{LO} \cdot N_o \\ &= 4 R_d P_{LO} \cdot R_d N_o \\ &= 4 (R_d P_{LO}) \cdot \frac{R_d P_{sp}}{B_o} \\ &= 4 I_{LO} \cdot \frac{I_{sp}}{B_o} \otimes G_{LO-PN}(f) \times 2 \end{aligned} \quad (C.2)$$

where

P_{LO} = Local oscillator power

I_{sp} = Spontaneous emission current

I_{FWM} = Detector current due to FWM power

R_d = Responsivity of photodetector (A/W)

N_o = Power spectral density of spontaneous emission

N_{sp} = Spontaneous emission factor

G = Gain of optical amplifier

h = Plank's constant

ν = Frequency of optical carrier

$$N_o = N_{sp}(G - 1)h\nu \quad (C.2a)$$

$$\begin{aligned} P_{sp} &= N_o \cdot B_o \\ &= N_{sp}(G - 1)h\nu \cdot B_o \end{aligned} \quad (C.2b)$$

$$I_{sp} = R_d \cdot P_{sp} \quad (C.2c)$$

$$I_{LO} = R_d \cdot P_{LO} \quad (C.2d)$$

$$I_s = R_d \cdot P_{in} \quad (C.2e)$$

$$I_{FWM} = R_d \cdot P_{FWM} \quad (C.2f)$$

where

P_{sp} = ASE beat noise power

I_{sp} = Detector current due to P_{sp}

I_{LO} = Detector current due to P_{LO}

I_s = Signal current due to P_{in}

$$\begin{aligned} P_{LOSP} &= N_{o-LOSP} \cdot B_e \\ &= 4I_{LO} \cdot I_{sp} \cdot \frac{B_e}{B_o} \otimes G_{LO-PN}(f) \times 2 \end{aligned} \quad (C.3)$$

where N_{o-LOSP} = PSD of local oscillator-ASE beat noise

$$\begin{aligned}
 N_{o-ssp} &= 4R_d^2 G P_{ln} \cdot N_o \\
 &= 4(R_d G P_{ln}) R_d N_o \\
 &= 4(R_d \cdot G_{Is}) \frac{R_d \cdot P_{sp}}{B_o} \quad (C.4) \\
 &= [4G I_s \cdot \frac{I_{sp}}{B_o}] \otimes G_{FSK-PN}(f) \times 2
 \end{aligned}$$

where N_{o-ssp} = PSD of signal-ASE beat noise, \otimes denotes convolution, $G_{LO-PN}(f) = G_{PN}(f - f_{IF})$ is phase noise corrupted spectrum of LO signal, $G_{FSK-PN}(f)$ is the spectrum of phase noise corrupted FSK signal [27],

$$P_{ssp} = [4I_s \cdot I_{sp} \frac{B_e}{B_o}] \otimes G_{FSK-PN}(f) \times 2 \quad (C.5)$$

$$\begin{aligned}
N_{LO-FWM} &= 4R_d^2 P_{LO} \cdot N_{FWM} \\
&= 4 (R_d P_{LO}) \cdot (R_d N_{FWM}) \\
&= 4 I_{LO} \cdot \frac{R_d \cdot P_{FWM}}{B_o} \\
&= [4 I_{LO} \cdot \frac{I_{FWM}}{B_o}] \otimes G_{LO-PN}(f) \times 2
\end{aligned} \tag{C.6}$$

where N_{LO-FWM} = PSD of LO-FWM beat noise

N_{FWM} = PSD of FWM power

$$\begin{aligned}
P_{LO-FWM} &= N_{LO-FWM} \cdot B_e \\
&= [4 I_{LO} \cdot I_{FWM} \cdot \frac{B_e}{B_o}] \otimes G_{LO-PN}(f) \times 2
\end{aligned} \tag{C.7}$$

$$\begin{aligned}
N_{S-FWM} &= 4R_d^2 G P_{ln} \cdot N_{FWM} \\
&= 4 (R_d P_{ln}) G \cdot (R_d \cdot N_{FWM}) \\
&= 4 G I_s \cdot \frac{R_d P_{FWM}}{B_o} \\
&= [4 G I_s \cdot \frac{I_{FWM}}{B_o}] \otimes G_{FSK-PN}(f) \times 2
\end{aligned} \tag{C.8}$$

where

N_{S-FWM} = PSD of signal-FWM beat noise

$$\begin{aligned} P_{S-FWM} &= N_{S-FWM} \cdot B_e \\ &= \left[4G I_S \cdot I_{FWM} \cdot \frac{B_e}{B_o} \right] \otimes G_{FSK-PN}(f) \times 2 \end{aligned} \quad (C.9)$$

where

P_{S-FWM} = Signal-FWM beat noise power

$$P_{sp-sp} = \left(\frac{I_{sp}}{B_o} \right)^2 [2B_o - B_e] \cdot B_e \quad (C.10)$$

where

P_{sp-sp} = ASE-ASE beat noise power.

APPENDIX D

C***** MAIN PROGRAM FOR BER CALCULATION *****

```
C PROGRAM FOR THESIS (PDF CALCULATION) NF2.FOR

C PROGRAM FOR HET/CPFSK WDM NETWORK NF3.FOR
C INCLUDING THE EFFECTS OF FWM, SWITCH CROSS_TALK, ASE
DOUBLE PRECISION Lm_db,Ls_db,Lps_db,Lf_db,Ldm_db,Lsw_db,L_db
DOUBLE PRECISION Lm,Ls,Lps,Lf,Ldm,Lsw,L,Br,Bo,Delf,Bfp,Be,fin
DOUBLE PRECISION Lambda,c,nu,h,Nsp1,Nsp2,Pin_dbm,Pin,Pf
DOUBLE PRECISION G1_db,G2_db,G1,G2,GT,F0,Pase,Is,Iase,Ifwm
DOUBLE PRECISION kc,Pc,Pspsp,Pssp,Pcsp,Pfwmsp,Pfwm,Ps,Psfwm
DOUBLE PRECISION Pshot,Ith,Pth,Var1,var0,sigma1,sigma0,Rd
DOUBLE PRECISION IO,I1,X_db,X,SX,Pir,Pb,Del,Pb1,D,Arg1,Arg2
DOUBLE PRECISION Pe1,Pe2,BER,e,c1,c2,Pfwm1,Ber1,LT_db
DOUBLE PRECISION La,Dc,Aeff,ZF,alpha,alph_db,pi,Err,sign
DOUBLE PRECISION PST,PE,snr,PY1(1024),PZ1(1024),PEE1(1024)
DOUBLE PRECISION DELY,YY,PHI,qq,SAI,PDELf,DT,DELNEW,TAO
DOUBLE PRECISION VAR,QO,T,Plo,S,BIF,Sigma,U,Z(20),W(20),ILO
DOUBLE PRECISION FC,FIF,PSPN,PLOPN,PLOSP,PLOFWM,HM,S1,S2,SS,Ic
C DOUBLE PRECISION PSDFSK,SFWM,FWMSP,BTSSP,FWMLO,INTEGRAL
Double precision Wlosp,Wssp,Wlofwm,Wfwmsp,Wspsp,Wsfwm,Wcsp

OPEN(20,file='C:\L3N3FO.DAT')
OPEN(40,file='C:\POWER.DAT')
OPEN(40,file='A:\51X1.DAT')
OPEN(30,file='C:\WATFOR\L3N3FO.DAT')
OPEN(10,file='C:\WATFOR\WEIGHT.DAT')
C OPEN(20,file='B:\L3N3FO.DAT')
C OPEN(10,FILE='B:WEIGHT.DAT')

DO 11 I=1,10
READ(10,*)Z(I),W(I)
11 CONTINUE

C FRINC=FT
PI=22.0/7.0
Rd=0.85
C Psp=0.002
Plo=0.001
ILO=Rd*Plo
Lm_db=-4.0
Ls_db=-3.0
Lps_db=-6.0
C Lf_db=-9.0
Ldm_db=-4.0
Lsw_db=-10.0
```

```

L_db=0.0
Alph_dB=0.20

La=50
C La=20

WRITE(20,*)'L=',LA
WRITE(*,*)'L=',LA
WRITE(40,*)'L=',LA
Lf_dB=-alph_dB*La
Alpha=alph_dB/4.34
LT_dB=Lm_dB+Ls_dB+Lps_dB+Lf_dB+Ldm_dB+Lsw_dB
G1_dB=18.0
G2_dB=-G1_dB-LT_dB
C WRITE(*,*)'G2_dB=',G2_dB,' Lf_dB=',Lf_dB
Lm=10.0**(Lm_db/10.)
Ls=10.0**(Ls_db/10.)
Lps=10.0**(Lps_db/10.)
Lf=10.0**(Lf_db/10.)
Ldm=10.0**(Ldm_db/10.)
Lsw=10.0**(Lsw_db/10.)
L=10.0**(L_db/10.)

Br=2.5E9
T=1.0/BR
BO=6.0*Br
Bfp=4.0*Br
BIF=2.0*Br
Be=0.7*Br
DELF = 10*BR
WRITE(20,*)'Br=',Br,' DELF=',DELF
lambda=1550.E-9
c=3.E8
nu=c/lambda
h=6.62E-34
e=1.602E-19

Xc=0.0
C WRITE(20,*)'X_=',X
HM=1.0
DO 1 ID = 1,1
DEVN=BR*HM/2.0
TAO=T/(2.0*HM)
WRITE(20,*)'Mod Index=',HM ,DEVN
DT = 0.00
DO 2 I = 1,1
WRITE(20,*)'Line width=',DT

```

```

DELNEW=DT*BR
C WRITE(*,*)'DELNEW=',DELNEW

N=51
C N=101

WRITE(20,*)'NO OF CHANNELS =',N
WRITE(30,*)'NO OF CHANNELS =',N
ITN=10
Pin_dBm=0.0
DO 3 IT=1,ITN
WRITE(*,*)'Pin_dBm=',Pin_dBm
WRITE(40,*)'Pin_dBm=',Pin_dBm
Pin=1E-3*10.0**(Pin_dBm/10.)
G1=10.0**(G1_dB/10.)
G2=10.0**(G2_dB/10.)
Pf=Pin*Lsw*Lm*G1
Dc=1.0E-12*1.E-3*1.E9
WF=0.5*11.0E-6
Aeff=2.0*pi*(WF**2)
an=1.45
ZF=5.0E-14

Node=40
Inc=20
DO 4 J=1,4
Node=Node+Inc
Nsp1=1.5*Node
Nsp2=1.5*Node

M=Node
CALL FWM(Pfwm,La,Lambda,Pf,Dc,an,Aeff,ZF,alpha,N,M,Delf)
C Pfwm=0.0
C WRITE(*,*)'Pfwm=',Pfwm
Pfwm=Pfwm*G2*Lps*Ls*Ldm*Lsw
Ifwm=Rd*Pfwm

GT=Lm*Ls*Lf*Lps*Ldm*Lsw*G1*G2
FO=2.0*Nsp1*(1.0-1./G1)/Lm
FO=FO+2.0*Nsp2*(1.0-1.0/G2)/(Lm*G1*Ls*Lf*Lps)
PASE=GT*h*nu*Bo*FO
Ps=Pin*GT*L*Lsw
Is=Rd*Ps
IASE=Rd*PASE*L
C WRITE(*,*)'Pase=',Pase,'Iase=',Iase
Fin=(2.0*Delf/Bfp)**2
Kc=1.0/(1.0+fin)

```

Pc=2.0*kc*GT*Pin*L*Lsw
Ic=Rd*Pc

c write(*,*)'Iase=',Iase,' Is=',Is
c write(*,*)'Ilo=',Ilo,' Ifwm=',Ifwm
c write(*,*)'Ic=',Ic

C****

Wfwmsp=4.0*Ifwm*Iase*Be/Bo
Wlosp=8.0*Ilo*Iase*Be/Bo
Wssp=8.0*Is*Iase*Be/Bo
Wcsp=8.0*Ic*Iase*Be/Bo
Wlofwm=8.0*Ilo*Ifwm*Be/Bo
Wsfwm=8.0*Is*Ifwm*Be/Bo
Wspsp=(2.0*Bo-Be)*Be*((Iase/Bo)**2)

c write(*,*)'Wfwmsp=',Wfwmsp,' Wlosp=',Wlosp
c write(*,*)'Wssp=',Wssp,' Wlofwm=',Wlofwm
c write(*,*)'Wsfwm=',Wsfwm,' Wspsp=',Wspsp

C***

C CALL SPCTRM(NU,T,FC,FIF,DELFT,DT,BO,BE,WSSP,PSPN,WLOSP)
FIF=0.0
CALL SPCTRM(NU,T,HM,FC,FIF,DELFT,DT,BO,BE,PSSP,PSPN,PLOPN,PLOSP
+,PFWMS,PSFWM,PLOFWM,PFWM)

PLOSP=PLOSP*T
Pssp=Pssp*(T**2.)
Pfwmsp=Pfwmsp*(T**2)
Psfwm=Psfwm*(T**3)
Plofwm=Plofwm*(T**2)

C WRITE(40,*)'Plosp=',Plosp,' PLOPN=',PLOPN
c write(*,*)'Pssp=',Pssp
c WRITE(*,*)'Plosp=',Plosp,' Pfwmsp=',Pfwmsp
c WRITE(*,*)'Psfwm=',Psfwm,' PLOfwm=',PLOfwm
C WRITE(40,*)'PFWM=',PFWM,' PLOPN=',PLOPN

Plosp=Plosp*Wlosp
Pssp=Pssp*Wssp
Pfwmsp=Pfwmsp*Wfwmsp
Psfwm=Psfwm*Wsfwm
Plofwm=Plofwm*Wlofwm
Pspsp=1.0*Wspsp
Pcsp=1.0*Wcsp

c write(*,*)'Pssp=',Pssp,' Pspsp=',Pspsp
c WRITE(*,*)'Plosp=',Plosp,' Pfwmsp=',Pfwmsp
c WRITE(*,*)'Psfwm=',Psfwm,' PLOfwm=',PLOfwm

```

c    WRITE(*,*)'Pc=',Pc,' Kc=',Kc
c    write(*,*)'Plofwm=',plofwm
ccc  Pspsp=Bo*Be*((Rd*FO*GT*h*nu*L)**2)
C    Pssp=2.0*FO*h*nu*Pin*Lsw*Be*((Rd*GT*L)**2)
ccc  Pssp=2.0*FO*h*nu*Pin*Lsw*Be*((Rd*GT*L)**2)*Pssp*(T**2)
ccc  Pcsp=2.0*FO*h*nu*GT*Pc*L*Be*(Rd**2)
ccc  Pfwmsp=2.0*(Rd**2)*Pfw*FO*h*nu*GT*Be*(L**2)
c    Pfwmsp=2.0*(Rd**2)*FO*h*nu*GT*Be*(L**2)*Pfwmsp*(T**3)
ccc  Ps_dbm=10.0*Dlog10(Ps*1.E3)
ccc  Psfwm=4.0*(Rd**2)*Ps*(Pfw*GT*L)
c    Psfwm=4.0*(Rd**2)*Ps*(Psfwm*GT*L)*(T**4)
Pshot=2.0*e*Rd*Be*(Pin*Lsw+2.0*kc*Pin*Lsw+Pfw+h*nu*Bo*FO)*GT*L
C    PLOFWM=0.0

c    Pfw=Pfw*G2*Lps*Ls*Ldm*Lsw
ccc  WLOFWM=2*Rd**2*(Pfw*G2*Lps*Ls*Ldm*Lsw)*Plo/Bo
ccc  WRITE(*,*)'WLOFWM=',WLOFWM
ccc  PLOFWM=WLOFWM*PLOFWM
c    PLOFWM=WLOFWM
C    PLOSP=0.0
ccc  WLOSP=2*Rd**2*Plo*Pase/Bo
C    WRITE(*,*)'WLOSP=',WLOSP,'PLOSP=',PLOSP
ccc  WRITE(*,*)'PLOFWM=',PLOFWM,' PLOSP=',PLOSP
ccc  PLOSP=WLOSP*PLOSP
C    Ith=10 pA/sqrt(Hz) at 2.5 Gb/s
C    Ith=4 pA/sqrt(Hz) at 10 Gb/s

IF(Br .eq. 2.5E9) ITh=10.0E-12
IF(Br .eq. 10.E9) Ith=4.0E-12
SX=Rd*Ps*(Xc**2)
PTh=(ITh**2)*Be
var1=Pshot+Pth+Pssp+Pcsp+Pspsp+Pfwmsp+Psfwm+Plofwm+Plosp

C    WRITE(40,*)'Pshot=',Pshot,' Pth=',Pth
C    WRITE(40,*)'Pssp=',Pssp,' Pcsp=',Pcsp
C    WRITE(40,*)'Pspsp=',Pspsp,' Pfwmsp=',Pfwmsp
C    WRITE(40,*)'Psfwm=',Psfwm,' Plofwm=',Plofwm
C    WRITE(40,*)'Plosp=',Plosp,' VAR1=',VAR1

c    WRITE(*,*)'Pshot=',Pshot,' Pth=',Pth
c    WRITE(*,*)'Pssp=',Pssp,' Pcsp=',Pcsp
c    WRITE(*,*)'Pspsp=',Pspsp,' Pfwmsp=',Pfwmsp
c    WRITE(*,*)'Psfwm=',Psfwm,' Plofwm=',Plofwm
c    WRITE(*,*)'Plosp=',Plosp,' VAR1=',VAR1

Sigma=Sqrt(var1)

```



```

Pst = 2.0*(Ps+Pfw) + PASE
var0=0.5*(2.0*PI*DELNEW*TAO)*(rd*ps)**2
C WRITE(*,*)'PI=',PI,' DELNEW=',DELNEW
C WRITE(*,*)'TAO=',TAO,' Rd=',Rd
C WRITE(*,*)'Ps=',Ps

VAR = (VAR1+VAR0)
C WRITE(*,*)'var=',var,' var1=',var1
C WRITE(*,*)'var0=',var0
Sigma0=dsqrt(var)

S1=SQRT(Ps*Plo)
S2=SQRT(Pfw*Plo)
S=2.0*Rd*(S1+S2)
SS=S*S
C WRITE(*,*)'S1=',S1,' S2=',S2
C WRITE(*,*)'S=',S,' SS=',SS
C WRITE(40,*)'S1=',S1,' S2=',S2
C WRITE(40,*)'S=',S,' SS=',SS

C U = ro =snr.
U = PS/(Pfw+Pase)
C U = SS/(2.0*VAR1)
WRITE(*,*)'U=',U
WRITE(40,*)'U=',U
IO =2.0*RD*PST*GT
C S=1.0E-5

C R=No. of Cross-points in each node
IR=0
Nd=2** (IR/2)
CALL BITERR(Delnew,TAO,S,BIF,Sigma,U,BER,Z,W)
IF( BER .GE. 1.E-15 ) THEN
WRITE(30,*)Node,sngl(LOG10(BER))
BER1 = DLOG10(BER*1.E9)
WRITE(20,*)Node,sngl(BER1)
WRITE(*,*)'Node=',Node,' Ber=',Ber
WRITE(40,*)'Node=',Node,' Ber=',Ber
END IF
C IF(BER .GT. 1.E-5 ) GO TO 3
4 CONTINUE
Pin_dbm=Pin_dbm+5.0
3 CONTINUE
DT = DT +0.005
2 CONTINUE
HM = HM + 1.0
1 CONTINUE

```

STOP
END

C***** SUBROUTINE 1 *****

SUBROUTINE BITERR(Delnew,TAO,S,BIF,Sigma,U,BER,Z,W)
DOUBLE PRECISION Delnew,TAO,S,BIF,Sigma,U,BER,Z(20),W(20)

CALL SIMPX(Delnew,TAO,S,BIF,Sigma,U,BER,Z,W)

C WRITE(*,*)'BER=',BER

C PAUSE

RETURN

END

C***** SUBROUTINE 2 *****

SUBROUTINE PERI(I,IR,Pir)
DOUBLE PRECISION FactI,FactIR,Factimr,Pir

CALL Fact1(I,FactI)

CALL Fact1(IR,FactIR)

IMR=IR-I

CALL Fact1(Imr,Factimr)

C WRITE(*,*)'I=',I,'IR=',IR,'IMR=',IMR

Pir=FactIR*(2.**(-IR))/(FactI*Factimr)

C WRITE(*,*)'Facti=',facti,'factir=',factir,'factimr=',factimr

C WRITE(*,*)'Pir=',Pir

RETURN

END

C***** SUBROUTINE 3 *****

SUBROUTINE Fact1(Ind,Fact1a)
DOUBLE PRECISION Fact1a

Fact1a=1.0

IF(Ind .eq. 0) go to 2

DO 1 J=Ind,1,-1

Fact1a=Fact1a*Float(J)

C WRITE(*,*)'J=',J,'FacJ=',Fact1a

1 CONTINUE

RETURN

2 Fact1a=1.0

RETURN

END

C ***** SUBROUTINE 4 *****

```

SUBROUTINE SIMPX(Delnew,Tao,S,BIF,Sigma,U,SY,Z,W)

DOUBLE PRECISION Delnew,Tao,S,BIF,Sigma,U,Z(20),W(20)
DOUBLE PRECISION S11Y,SY,FUNHY,FUNC,FNINC
DOUBLE PRECISION SUMKY,FUND,FUNFTY,FUNYK
DOUBLE PRECISION FUN1HY,FUN1C,FUN1D,F1FSTY,FUN1YK
DOUBLE PRECISION FUN2HY,FUN2C,FUN2D,F2FSTY,FUN2YK
DOUBLE PRECISION C,D,DC,DELY,HY,FRSTY,YK,Y(1024)

PI = 3.141592654D0
C=0.0
D =PI/2.0
DELY = 0.000001
IMAXY =9
S11Y=0.0
SY=0.0
DC=D-C
IF(DC) 20,19,20
19  IERY1=1
    RETURN
20  IF(DELY) 22,22,23
22  IERY1=2
    RETURN
23  IF(IMAXY-1) 24,24,25
24  IERY1=3
    RETURN
25  HY=DC/2.0+C
    NHALFY=1
    CALL PDF1(HY,U,FUN1HY)
    CALL GAUSSIAN(HY,FUN2HY,Delnew,Tao,S,BIF,Sigma,Z,W)
    FUNHY=FUN1HY*FUN2HY

C   WRITE(*,*)'HY=',HY,'FUN1HY=',FUN1HY,'f2hy=',fun2hy

    SUMKY=FUNHY*DC*2.0/3.00
    CALL PDF1(C,U,FUN1C)
    CALL GAUSSIAN(C,FUN2C,Delnew,Tao,S,BIF,Sigma,Z,W)
    FUNC=FUN1C*FUN2C

C   WRITE(*,*)'FUNC=',FUNC

    CALL PDF1(D,U,FUN1D)
    CALL GAUSSIAN(D,FUN2D,Delnew,Tao,S,BIF,Sigma,Z,W)
    FUND=FUN1D*FUN2D

C   WRITE(*,*)'FUND=',FUND

```

```

SY=SUMKY+(FUNC+FUND)*DC/(6.00)
DO 28 IY=2,IMAXY
S11Y=SY
SY=(SY-(SUMKY/2.))/2.0
NHALFY=NHALFY*2
ANHLFY=NHALFY
FRSTY=C+(DC/ANHLFY)/2.0

CALL PDF1(FRSTY,U,F1FSTY)
CALL GAUSSIAN(FRSTY,F2FSTY,Delnew,Tao,S,BIF,Sigma,Z,W)
FUNFTY=F1FSTY*F2FSTY

C WRITE(*,*)'FUNFTY=',FUNFTY

SUMKY=FUNFTY
YK=FRSTY
KLASTY=NHALFY-1
FENCY=DC/ANHLFY
DO 26 KY=1,KLASTY
YK=YK+FENCY

CALL PDF1(YK,U,FUN1YK)
CALL GAUSSIAN(YK,FUN2YK,Delnew,Tao,S,BIF,Sigma,Z,W)
FUNYK=FUN1YK*FUN2YK
C WRITE(*,*)'F1YK=',FUN1YK,' F2YK=',FUN2YK
C WRITE(*,*)'FUNYK=',FUNYK

SUMKY=SUMKY+FUNYK
26 CONTINUE
SUMKY=SUMKY*2.0*DC/(3.*ANHLFY)
SY=SY+SUMKY

C WRITE(*,*)'SY=',SY,'S11Y=',S11Y

27 IF(ABS(SY-S11Y)-ABS(DELY*SY))29,28,28

28 CONTINUE
SY=(SY)*2.0
IERY1=4
GO TO 30

29 IERY1=0
C SY=DABS(SY)*2.0
SY=(SY)*2.0
C IF(SY .LE. 1.E-30) SY =0.0
30 NOY=2*NHALFY
C WRITE(*,*) 'SY = ',SY

```

RETURN
END

C***** SUBROUTINE 5 *****

```
      SUBROUTINE FWM(Pfwm,La,Lambda,Pf,Dc,an,Aeff,Z,alpha,N,M,Delf)
      DOUBLE PRECISION Pfwm,La,Leff,Aeff,pi,Z,Dc,c,alpha,Delf,A3,CN5
      DOUBLE PRECISION A1,A2,lambda,sum,CN1,CN2,CN3,CN4,Eta_ijk,Pf
      DOUBLE PRECISION D

      Leff=(1.0-exp(-alpha*La))/alpha
      PI=22.0/7.0
      C=3.0E8
C     WRITE(*,*)'Pfbre=',Pf,' Leff=',Leff
      A1=1024.0*(pi**6)*((Z*Leff)**2)
      A3=(an**4)*(lambda*c*Aeff)**2
      CK=A1/A3
C     WRITE(*,*)'CK=',CK
      A2=(Pf**3)*(exp(-alpha*La))
C     WRITE(*,*)'A1=',A1,' A2=',A2,' A3=',A3
      SUM=0.0
      Fm=c/lambda
      NH=(N-1)/2
      Fmax=Fm+Delf*NH
      Fmin=Fm-Delf*NH
C     WRITE(*,*)'Fmin=',Fmin,' Fm=',Fm,' Fmax=',Fmax
      term=0
      DO 2 J=0,N
      Fj=Fm+Delf*(J-NH)

C     WRITE(*,*)'Fj=',Fj
      DO 3 K=0,N
      IF(J .EQ. K) go to 3

C     WRITE(*,*)'J=',J,' K=',K
      Fk=Fm+Delf*(K-NH)
      Fi=Fm-Fj+Fk
      IF(Fi .lt. Fmin) go to 3
      IF(Fi .gt. Fmax) go to 3

      Delf_ik=Abs(Fi-Fk)
      Delf_jk=Abs(Fj-Fk)
C     WRITE(*,*)'Delf_ik=',Delf_ik,' Delf_jk=',Delf_jk
      Delbeta=2.0*Pi*Dc*(lambda**2.)*Delf_ik*Delf_jk/c
C     WRITE(*,*)'alpha=',alpha,' Delbeta=',Delbeta
      Phi=Delbeta*La*1.E3/2.0
      Theta=Sin(Phi)
```

```

C      WRITE(*,*)'Phi=',Phi,' Theta=',Theta

      CN1=(alpha**2)/((alpha*1.E-3)**2+Delbeta**2)
      CN2=4.*exp(-alpha*La)*(Theta**2)
      CN3=(1.0-exp(-alpha*La))**2
      CN5=1.0+CN2/CN3
C      WRITE(*,*)'alph=',alph
C      WRITE(*,*)'CN1=',CN1,' CN5=',CN5
      IF(theta .eq. 0.0) then
      CN4=1.0
      Else
      CN4=(sin(Phi*M)/sin(Phi))**2
      Endif
      Eta_ijk=CN1*CN5*CN4
C      WRITE(*,*)'CN4=',CN4
      IF(Fi .ne. Fk) Then
        IF(Fi .ne. Fj) Then
          D=6.0
          C=3.0/8.0
        Else
          D=3.0
          C=1.0/4.0
        EndIF
      Else
        IF(Fi .ne. Fj) Then
          D=3.0
          C=1.0/4.0
        Else
          D=0.0
          C=1.0/4.0
        EndIF
      EndIF
      term=term+1
      Sum=Sum+(D**2.0)*Eta_ijk
C      WRITE(*,*)'sum=',sum
      3  CONTINUE
      2  CONTINUE
C      WRITE(*,*)'sum=',sum,'term=',term
      Pfwm=A1*A2*sum/A3
C      WRITE(*,*)'Pfwm=',Pfwm
      RETURN
      END

```

C***** SUBROUTINE 6 *****

```

SUBROUTINE PDF1(PHI,U,PDELFI)
DOUBLE PRECISION PI,H,X1,C,D,U,DELY,SY,PHI,PDELFI

```

C DOUBLE PRECISION

```
PI = 3.141592654
C = 0.0
D = PI
DELY = 0.001
IMAXY =9
CALL SMP(C,D,DELY,IMAXY,SY,PHI,U)
PDELF = SY
RETURN
END
```

C***** SUBROUTINE 7 *****

```
SUBROUTINE SMP(C,D,DELY,IMAXY,SY,PHI,U)
DOUBLE PRECISION S11Y,SY,FUN1HY,FUN2HY,FUNHY,FUN1C,FUN2C,FUNC
DOUBLE PRECISION SUMKY,FUN1D,FUN2D,FUND,F1FSTY,F2FSTY,FUNFTY
DOUBLE PRECISION FUN1YK,FUN2YK,FUNYK,DCNR,V,U,PHI
DOUBLE PRECISION C,D,DC,DELY,HY,FRSTY,YK,Y(1024)

S11Y=0.0
SY=0.0
DC=D-C
IF(DC) 20,19,20
19 IERY1=1
RETURN
20 IF(DELY) 22,22,23
22 IERY1=2
RETURN
23 IF(IMAXY-1) 24,24,25
24 IERY1=3
RETURN
25 HY=DC/2.0+C
NHALFY=1
CALL PDF(HY,FUN1HY,PHI,U)
FUNHY=FUN1HY
SUMKY=FUNHY*DC*2.0/3.0
CALL PDF(C,FUN1C,PHI,U)
FUNC=FUN1C
CALL PDF(D,FUN1D,PHI,U)
FUND=FUN1D
SY=SUMKY+(FUNC+FUND)*DC/(6.00)
DO 28 IY=2,IMAXY
S11Y=SY
SY=(SY-(SUMKY/2.))/2.0
NHALFY=NHALFY*2
ANHLFY=NHALFY
```

```

FRSTY=C+(DC/ANHLFY)/2.0
CALL PDF(FRSTY,F1FSTY,PHI,U)
FUNFTY=F1FSTY
SUMKY=FUNFTY
YK=FRSTY
KLASTY=NHALFY-1
FINCY=DC/ANHLFY
DO 26 KY=1,KLASTY
YK=YK+FINCY
CALL PDF(YK,FUN1YK,PHI,U)
FUNYK=FUN1YK
SUMKY=SUMKY+FUNYK
26 CONTINUE
SUMKY=SUMKY*2.0*DC/(3.*ANHLFY)
SY=SY+SUMKY
27 IF(ABS(SY-S11Y)-ABS(DELY*SY))29,28,28
28 CONTINUE
SY=SY*2.0
IERY1=4
GO TO 30
29 IERY1=0
SY=SY*2.0
30 NOY=2*NHALFY
RETURN
END

```

C***** SUBROUTINE 8 *****

```

SUBROUTINE PDF(DELFF,PFDELFF,PHI,U)
DOUBLE PRECISION PFDELFF,PI,C2,C1
DOUBLE PRECISION DELFF,U,PHI,X1

PI=3.141592654D0
X1 = EXP(-U)/(4.0*PI)
C1=EXP(-(U*(SIN(DELFF))*(COS(PHI))))
C2=1+U+ U*(SIN(DELFF))*(COS(PHI))
PFDELFF=X1*C1*C2*(SIN(DELFF))
C WRITE(*,*)'DELFF=',DELFF,'PROB=',PFDELFF
RETURN
END

```

C***** SUBROUTINE 9 *****

```

SUBROUTINE ERFC(ZZ,YY)
DOUBLE PRECISION ZZ,YY,P1,P2,Q1,Q2,ERROR,A1,A2,A3,A4,A5,PI,ZABS
DOUBLE PRECISION ERFZZ,XX

```



```

PI=3.141592654D0
ZABS=ABS(ZZ)
IF(ZZ .eq. 0.0) then
SIGN=1.0
ELSE
SIGN=ZZ/ZABS
ENDIF
A1=0.254829592
A2=-0.284496736
A3=1.421413741
A4=-1.453152027
A5=1.061405429
C ERROR=1.5E-7
P1=0.3275911
P2=1.0/(1.0+P1*ZABS)
XX=Zabs**2.0
IF(XX .GT. 700.) Then
Q1=0.DO
ELSE
Q1=DEXP(-1.DO*XX)
ENDIF
Q2=A1*P2+A2*(P2**2.)+A3*(P2**3.)+A4*(P2**4.)+A5*(P2**5.)
ERFZZ=(1.0D0-Q1*Q2)*SIGN
YY=1.0D0-ERFZZ
C IF(YY .GT. 1.) WRITE(*,*)'Q1=',Q1,'XX=',XX
C YY=ERFZZ
RETURN
END

```

C***** SUBROUTINE 10 *****

```

SUBROUTINE GAUSSIAN (DPHI,PEDPHI,Delnew,Tao,S,BIF,Sigma,Z,W)
DOUBLE PRECISION Delnew,Tao,S,PEDPHI,DPHI,PI,BIF,Sigma
DOUBLE PRECISION PE_DTH,D_THETA,Z(20),W(20)

PI=22.0/7.0
N=10
C DO 1 I=1,N
C READ(10,*) Z(I),W(I)
C WRITE(50,*) Z(I), W(I)
C 1 CONTINUE

SUM=0.0
DO 2 I=1,N
D_Theta=Z(I)*SQRT(4.0*PI*Delnew*Tao)

```

```

CALL PROB(PE_DTh,BIF,D_Theta,Tao,Delnew,S,DPHI,Sigma)
SUM=SUM+PE_DTH*W(I)
2 CONTINUE

```

```

PEDPHI=SUM*2.0/(SQRT(PI))
RETURN
END

```

C***** SUBROUTINE 11 *****

```

SUBROUTINE PROB (PE_DTh,BIF,D_Theta,Tao,Delnew,
+S,DPHI,Sigma)

```

```

DOUBLE PRECISION SUM,QAB,QBA,SIGMA,A,B,S,Row,PI,BIF,D_THETA
DOUBLE PRECISION N1,N2,N3,D,PEO,PE1,PE_DTh,DPHI,TAO,DELNEW
DOUBLE PRECISION A1,B1

```

```

PI=22.0/7.0
Beq=1.064*BIF
Row=EXP(-PI*(Beq*Tao)**2)
K=(1.0+Row)/(1.0-Row)
AK=Float(K)

```

```

Beta=1.0
Gaman=Beta*PI/2.0+D_Theta+DPHI

```

```

An1=S
And=S
N1=(1.0+K)*(An1**2+And**2)
N2=4.0*An1*And*SQRT(AK)*SIN(Gaman)
N3=2.0*(1.0-K)*An1*And*COS(Gaman)
D=8.0*(Sigma**2)*(1.0+Row)

```

```

C write(*,*)'s=',s,'k=',k,'sigma=',sigma,'gama=',gaman

```

```

A=SQRT((N1+N2+N3)/D)
A1=A/SQRT(2.0)
B=SQRT((N1-N2+N3)/D)
B1=B/SQRT(2.0)

```

```

C write(*,*)'A=',A,' B=',B

```

```

C write(*,*)'A1=',A1,' B1=',B1

```

```

C CALL QFUN(A,B,QAB,QBA)

```

```

PE1=0.5*(1.0-QAB+QBA)
PEO=0.5*(1.0-QBA+QAB)
PE_DTh=PE1+PEO

```

```

C WRITE(*,*)'PEO=',PEO,' PE1=',PE1

```

```

C AB=(A-B)/SQRT(2)

```

```

C CALL erfc((a-b)/SQRT(2.0),pe_dth)

```

```

C      CALL erfc(a1-b1,pe_dth)
C      write(*,*)'pe_dth=',pe_dth
C      PAUSE
      RETURN
      END

```

C***** SUBROUTINE 12 *****

```

      SUBROUTINE QFUN(A,B,QAB,QBA)
      DOUBLE PRECISION A,B,QAB,QBA,X1,X2,Ep,P,C1,C2,D,BI
      C1=A/B
      C2=B/A
      D=A*B
      P=(A**2+B**2)/2.0
C      WRITE(*,*)'P=',P
      Ep=EXP(-P)
C      WRITE(*,*)'Ep=',Ep

      N=30
      SUM1=0.0
      SUM2=0.0
      DO 10 I=0,N
      AI=FLOAT(I)
      CALL Bessel(D,AI,BI)
C      WRITE(*,*)'AB=',D,'BI=',BI,' I=',I
      X1=C1**I
      X2=C2**I
      SUM1=SUM1+X1*BI
      SUM2=SUM2+X2*BI
10    CONTINUE
      QAB=EP*SUM1
      QBA=EP*SUM2

      WRITE(*,*)'QAB=',QAB,' QBA=',QBA
      RETURN
      END

```

C***** SUBROUTINE 13 *****

```

      SUBROUTINE BESSEL(XA,AN,BI)
      DOUBLE PRECISION X,XA,BI,XX,Term,FN,Tol,Fk,EX,PI
      DOUBLE PRECISION factn,bbi,abi,X1

C      READ(*,*) XA,AN
      X=XA
      N=AN
C      WRITE(*,*)'an=',an,' N=',N,' X=',X

```

```

IER=0
BI=1.0
WRITE(*,*) 'Value of N and X in Bessel=',N,X
IF(N-0) 150,15,10
10 IF(X-0.) 160,20,20
15 IF(X-0.) 160,17,20
17 RETURN
20 Tol=1.E-30
IF(X-300.) 40,40,30
30 FN=Float(N)
IF(X-FN) 40,40,110
40 XX=X/2.0

IF(N .LT. 32) then
    FACTN=1.
ELSE
    FACTN=1.E0
ENDIF

IF(N-1) 70,70,50
50 DO 60 I=2,N
    FI=Float(I)
    FACTN=FACTN*FI
C WRITE(*,*) 'Factn=',Factn, 'I=',I
60 CONTINUE

70 Term=(XX**N)
TERM=TERM/FACTN
WRITE(*,*) 'Term=',Term, 'XX=',XX, 'N=',N
IF(N .LT. 32) then
    TERM=TERM*1.E-30
ELSE
    TERM=TERM*1.E-30
ENDIF

BI=TERM
XX=XX*XX
DO 90 k=1,100
ABI=BI*TOL
C WRITE(*,*) 'abi=',abi, ' Term=',Term
IF(ABS(TERM)-ABS(BI*TOL)) 100,100,80
80 FK=Float(K)*Float(N+K)
TERM=TERM*(XX/FK)
C write(*,*) 'bil=',bi, ' term=',term
90 BI=BI+TERM*1.E30

100 RETURN

```

```

110  FN=4.*(N**2)
      XX=1./(8.*X)
      Term=1.E0
      BI=1.0
      DO 130 k=1,50
      bbi=BI*Tol
C     WRITE(*,*)'BI=',BI,'XX=',XX
C     WRITE(*,*)'bbi=',bbi,' Term=',Term
      IF(ABS(TERM)-ABS(TOL*BI)) 140,120,120
120  FK=Float(((2*K)-1)**2)
      FLTK=Float(K)
C     WRITE(*,*)'FK=',FK,' FN=',FN
      TERM=TERM*XX*(FK-FN)/FLTK
      WRITE(*,*)'BIG=',BI,' Term=', Term
130  BI=BI+TERM
C     WRITE(*,*)'BIG=',BIG,'TERM=',TERM
140  PI=Dble(22.0/7.0)
      X1=X/50.0
      write(*,*)'X1=',X1,' X=',X,'Big=',Bi
      EX=DEXP(X1)
      write(*,*)'Ex=',Ex
      DX=exp(50.0)
      write(*,*)'Dx=',Dx
      BI=BI*DX
      write(*,*)'bi=',bi
      BI=(BI*EX)/(DSQRT(2.*pi*x))
C     WRITE(*,*)'BI=',BI,'k=',k
      Go To 200
150  IER=1
      Go To 200
160  IER=2
200  RETURN
      END

```

C***** SUBROUTINE 14 *****

```

SUBROUTINE BESELM(XA,BFx)
DOUBLE PRECISION X,BFx,cf0,cf1,cf2,cf3,cf4,cf5,cf6,cf7,cf8
DOUBLE PRECISION Err,T,XA

X=XA
T=X/3.75D0
IF(X-3.75D0) 10,10,20
10  cf0=1.D0
     cf1=3.5156229D0*(T*T)
     cf2=1.2067492D0*(T**6.)
     cf3=0.2659732D0*(T**8.)

```

```

cf4=0.0360768D0*(T**10.)
cf5=0.0045813D0*(T**12.)
Err=1.60D-7
BFx=cf0+cf1+cf2+cf3+cf4+cf5+err
C WRITE(*,*)'an=0, X=',X,' BFx=',BFx
RETURN
20 cf0=0.39894228D0
cf1=0.01328592D0/T
cf2=0.00225319D0/(T**2.0)
cf3=-0.00157565D0/(T**3.0)
cf4=0.00916281D0/(T**4.0)
cf5=-0.02057706D0/(T**5.0)
cf6=0.02635537D0/(T**6.0)
cf7=-0.01647633D0/(T**7.0)
cf8=0.00392377D0/(T**8.0)
err=1.9D-7
BFx=cf0+cf1+cf2+cf3+cf4+cf5+cf6+cf7+cf8+Err
BFx=BFx*Dexp(x)/(Dsqrt(x))
C WRITE(*,*)'an=0, X=',X,' BFx=',BFx
RETURN
END

```

C***** SUBROUTINE 15 *****

*

***** MAIN SUBROUTINE *****

*

```

SUBROUTINE SPCTRM(NU,T,HM,FC,FIF,DELF,DT,BO,BE,PSSP,PSPN,PLOPN,
+PLOSP,PFWMSP,PSFWM,PLOFWM,PFWM)

```

```

DOUBLE PRECISION T,FC,DELF,DT,DELNEW,DELTA,BO,BE,F,TS,BET
DOUBLE PRECISION FS,FT,PSSP,PSPN,PLOPN,PLOSP,GPN,BOT,AFT,NU
DOUBLE PRECISION PFWMSP,PSFWM,PLOFWM,PFWM,HM,C1,D1,C2,D2,FRINC
DOUBLE PRECISION XO(1024),YO(1024),X(1024),Y(1024),FIF,FI
DOUBLE PRECISION X1(1024),Y1(1024),FIF1,PSD,H,SFSK
DOUBLE PRECISION X2(1024),Y2(1024),X3(1024),Y3(1024)
DOUBLE PRECISION X4(1024),Y4(1024)

```

```

BOT=BO*T

```

```

BET=BE*T

```

C M1=6

```

M1=6

```

```

M2=3

```

```

M=M1+M2+1

```

```

NB=2**M1

```

```

NSB=2**M2

```

```

N=2**M

```

```

NH=N/2

```

```

NQ=N/4

```

```

F=(BO/2.0)/NQ
TS=1.0/(N*F)
C TS=T/NSB
C FS=1.0/TS
C F=FS/N
DELNEW=DT/T
DELTA=2.0*DELF
FT=F*T
FRING=FT
C1=0.0
C2=0.0
D1=BOT/2.0
C D2=FIF-BOT/2.0
D2=BOT/2.0
C WRITE(*,*)'FT=',FT,'T=',T,'BOT=',BOT
NN=BOT/FT
DO 1 I=1,NQ+1
FI=FT*(I-1)
C WRITE(*,*)'Fi=',Fi
CALL PSDFSK(HM,SFSK,FI,T)
X1(I)=SFSK
Y1(I)=0.0
1 CONTINUE
C WRITE(*,*)'FT=',FT,'BOT=',BOT,'NN=',NN
C Pause
DO 10 I=1,NQ+1
FT=F*T*I

IF(FT .LE. BOT/2.0) THEN
XO(I)=1.0
YO(I)=0.0
X4(I)=1.0
Y4(I)=0.0
ELSE
XO(I)=0.0
YO(I)=0.0
X4(I)=0.0
Y4(I)=0.0
ENDIF
C WRITE(*,*)I,'XO=',XO(I)
IF(DT .NE. 0.0) THEN
C FIF=0.0
FIF1=0.0
CALL PSDPN(DELNEW,FT,FIF1,T,GPN)
X3(I)=GPN
ELSE
X3(I)=0.0

```

```

ENDIF
Y3(I)=0.0
10 CONTINUE

CALL TRANSF(X0,Y0,NSB,TS,M,T)
CALL TRANSF(X1,Y1,NSB,TS,M,T)
CALL TRANSF(X3,Y3,NSB,TS,M,T)
CALL TRANSF(X4,Y4,NSB,TS,M,T)
IF(DT .EQ. 0.0) GO TO 11
CALL SPN(X1,Y1,X3,Y3,PSPN,DT,N,M,F)
CALL LOPN(X4,Y4,X3,Y3,PLOPN,DT,N,M,F)
GO TO 12
11 PSPN=0.0
12 CALL PSDFWM(X1,Y1,X2,Y2,PFWM,N,M,NSB,F,T)
C CALL FWM(Pfwm,La,Lambda,Pf,De,an,Aeff,Z,alpha,N,M,Delf)

CALL BTSSP(X1,Y1,X0,Y0,C1,D1,FRINC,PSSP,N,M,F)
C WRITE(*,*)'PSSP=',PSSP
CALL BTLOSP(X0,Y0,X4,Y4,C2,D2,FRINC,PLOSP,N,M,F)
CALL BTSFWM(X1,Y1,X2,Y2,C1,D1,FRINC,PSFWM,N,M,F)
C WRITE(*,*)'PSFWM=',PSFWM
CALL BTFWMSP(X0,Y0,X2,Y2,C1,D1,FRINC,PFWMS,N,M,F)
CALL BTLOFWM(X2,Y2,X4,Y4,C2,D2,FRINC,PLOFWM,N,M,F)

PSSP=PSSP*BE/BO
PSPN=PSPN*BE/BO
C PLOSP=PLOSP*BE/BO
C WRITE(*,*)'PSSP=',PSSP,'PSPN=',PSPN
RETURN
END

```

C***** SUBROUTINNE 16 *****

```

SUBROUTINE SPN(X1,Y1,X3,Y3,PSPN,DT,N,M,F)
DOUBLE PRECISION X1(1024),Y1(1024),X3(1024),Y3(1024),PSPN
DOUBLE PRECISION X(1024),Y(1024),F,DT
DOUBLE PRECISION C1,D1,FRINC

IF(DT .EQ. 0.0) GO TO 12
DO 10 I = 1,N
AA = X1(I)*X3(I)-Y1(I)*Y3(I)
BB = X1(I)*Y3(I)+Y1(I)*X3(I)
X1(I) = AA
Y1(I) = BB
10 CONTINUE
12 DO 11 I=1,N
X(I) = X1(I)

```



```

      Y(I) = -Y1(I)
11  CONTINUE
      CALL BEAT(X,Y,C1,D1,FRINC,PSPN,N,M,F)
      RETURN
      END

```

C***** SUBROUTINE 17 *****

```

      SUBROUTINE LOPN(X4,Y4,X3,Y3,PLOPN,DT,N,M,F)
      DOUBLE PRECISION X4(1024),Y4(1024),X3(1024),Y3(1024),PLOPN
      DOUBLE PRECISION X(1024),Y(1024),F,DT
      DOUBLE PRECISION C1,D1,FRINC

      IF(DT .EQ. 0.0) GO TO 12
      DO 10 I = 1,N
      AA = X4(I)*X3(I)-Y4(I)*Y3(I)
      BB = X4(I)*Y3(I)+Y4(I)*X3(I)
      X4(I) = AA
      Y4(I) = BB
10  CONTINUE
12  DO 11 I=1,N
      X(I) = X4(I)
      Y(I) = -Y4(I)
11  CONTINUE
      CALL BEAT(X,Y,C1,D1,FRINC,PLOPN,N,M,F)
      RETURN
      END

```

C***** SUBROUTINE 18 *****

```

      SUBROUTINE PSDFWM(X1,Y1,X2,Y2,PFWM,N,M,NSB,F,T)
      DOUBLE PRECISION X1(1024),X2(1024),F,TS,T,FRINC
      DOUBLE PRECISION Y1(1024),Y2(1024),PFWM,C2,D2,PWR

      Br=2.5E9
      BO=6.0*Br
      TS=T/NSB
      NQ=N/4
      DO 1 I=1,NQ+1
      X2(I)=X1(I)
      Y2(I)=Y1(I)
1  CONTINUE
      CALL TRANSF(X2,Y2,NSB,TS,M,T)
C  TRANSF(X,Y,NSB,TS,M,T)

      DO 2 I=1,N
C  WRITE(*,*)'X2=',X2(I), 'Y2=',Y2(I)

```

```

X2(I)=X2(I)*1.E-20
Y2(I)=Y2(I)*1.E-20
AA=X2(I)**3-3*X2(I)*Y2(I)**2
BB=3*(X2(I)**2)*Y2(I)-Y2(I)**3
X2(I)=AA
Y2(I)=BB
2 CONTINUE
CALL DFT(X2,Y2,N,M)
C2=0.0
D2=BO*T
FRINC=F*T
CALL INTGRN(C2,D2,X2,FRINC,PWR)
C WRITE(*,*)'PFWM=',PFWM
C WRITE(40,*)'PFWM=',PFWM
RETURN
END

```

C***** SUBROUTINE 19 *****

```

SUBROUTINE BTSSP(X1,Y1,XO,YO,C1,D1,FRINC,PSSP,N,M,F)
DOUBLE PRECISION X1(1024),Y1(1024),XO(1024),YO(1024)
DOUBLE PRECISION X(1024),Y(1024),C1,D1,FRINC,PSSP,F

DO 1 I =1, N
AA = X1(I)*XO(I)-Y1(I)*YO(I)
BB = X1(I)*YO(I)+XO(I)*Y1(I)
X(I)=AA
Y(I)=-BB
1 CONTINUE
CALL BEAT(X,Y,C1,D1,FRINC,PSSP,N,M,F)
RETURN
END

```

C***** SUBROUTINE 20 *****

```

SUBROUTINE BTLOSP(XO,YO,X3,Y3,C2,D2,FRINC,PLOSP,N,M,F)
DOUBLE PRECISION XO(1024),YO(1024),X3(1024),Y3(1024)
DOUBLE PRECISION X(1024),Y(1024),C2,D2,FRINC,PLOSP,F

DO 1 I =1, N
AA = XO(I)*X3(I)-YO(I)*Y3(I)
BB = XO(I)*Y3(I)+YO(I)*X3(I)
X(I)=AA
Y(I)=-BB
C WRITE(*,*)'X=',X(I),' Y=',Y(I)
1 CONTINUE
CALL BEAT(X,Y,C2,D2,FRINC,PLOSP,N,M,F)

```

RETURN
END

C***** SUBROUTINE 21 *****

```
SUBROUTINE BEAT(X,Y,C,D,FRINC,PWR,N,M,F)
DOUBLE PRECISION X(1024),Y(1024),C,D,FRINC,PWR,F

CALL DFT(X,Y,N,M)
DO 2 I=1, N
X(I)=X(I)/(N*F)
Y(I)=Y(I)/(N*F)
2 CONTINUE
CALL INTGRN(C,D,X,FRINC,PWR)
PWR=DABS(PWR)
RETURN
END
```

C***** SUBROUTINE 22 *****

```
SUBROUTINE BTFWSP(XO,YO,X2,Y2,C1,D1,FRINC,PFWMSP,N,M,F)
DOUBLE PRECISION XO(1024),YO(1024),X2(1024),Y2(1024)
DOUBLE PRECISION C1,D1,FRINC,PFWMSP,X(1024),Y(1024),F

DO 1 I =1, N
AA = XO(I)*X2(I)-YO(I)*Y2(I)
BB = XO(I)*Y2(I)+YO(I)*X2(I)
X(I)=AA
Y(I)=-BB
1 CONTINUE
CALL BEAT(X,Y,C1,D1,FRINC,PFWMSP,N,M,F)
RETURN
END
```

C***** SUBROUTINE 23 *****

```
SUBROUTINE BTSFWM(X1,Y1,X2,Y2,C1,D1,FRINC,PSFWM,N,M,F)
DOUBLE PRECISION X1(1024),Y1(1024),X2(1024),Y2(1024)
DOUBLE PRECISION X(1024),Y(1024),C1,D1,FRINC,PSFWM,F

DO 1 I =1, N
AA = X1(I)*X2(I)-Y1(I)*Y2(I)
BB = X1(I)*Y2(I)+X2(I)*Y1(I)
X(I)=AA
Y(I)=-BB
1 CONTINUE
CALL BEAT(X,Y,C1,D1,FRINC,PSFWM,N,M,F)
```

RETURN
END

C***** SUBROUTINE 24 *****

SUBROUTINE BTLOFWM(X2,Y2,X3,Y3,C2,D2,FRINC,PLOFWM,N,M,F)
DOUBLE PRECISION X2(1024),Y2(1024),X3(1024),Y3(1024)
DOUBLE PRECISION X(1024),Y(1024),C2,D2,FRINC,PLOFWM,F

DO 1 I =1, N
AA = X2(I)*X3(I)-Y2(I)*Y3(I)
BB = X2(I)*Y3(I)+X3(I)*Y2(I)
X(I)=AA
Y(I)=-BB
1 CONTINUE
CALL BEAT(X,Y,C2,D2,FRINC,PLOFWM,N,M,F)
RETURN
END

*

C***** SUBROUTINE 25 *****

*

SUBROUTINE PSDPN(DELNEW,FT,FIF,T,GPN)
DOUBLE PRECISION DELNEW,FT,GPN,PI,CC,CO,C1,FIF,AFT
DOUBLE PRECISION DENM1,DENM2,DENM,A1,T,DT

PI=22.0/7.0
DT=DELNEW*T
A1=DELNEW*(T**2.)/(2.0*PI)
GPN=A1/((FT**2.0)+(DT/2.0)**2)
WRITE(*,*)'GPN=',GPN,'FT','=',FT
RETURN
END

*

C***** SUBROUTINE 26 *****

*

SUBROUTINE TRANSF(X,Y,NSB,TS,M,T)
DOUBLE PRECISION X(1024),Y(1024),T,TS,FSA,F,AA

N=2**M
NQ=N/4
NH=N/2
C TS=T/NSB
FSA=1.0/TS
F=FSA/N

DO 2 I=NQ+2,NH+1
X(I)=0.0

```

      Y(I)=0.0
2     CONTINUE
      INC=1
      DO 4 I=NH+2,N
        J=I-2*INC
        X(I)=X(J)
        Y(I)=Y(J)
        INC=INC+1
C     WRITE(*,*) 'X=',X(I), 'Y=',Y(I)
4     CONTINUE
      CALL DFT(X,Y,N,M)
      DO 5 I=1,N
        X(I)=X(I)*F
        Y(I)=Y(I)*F
        AA=(X(I)**2+Y(I)**2)
C     WRITE(*,*) 'AA',I, '=',AA
5     CONTINUE
      RETURN
      END

*
***** SUBROUTINE 27 *****
*
      SUBROUTINE DFT(X,Y,N,M)

C     EMA X,Y,AX
      COMPLEX AX(1024),U,W,T
      DOUBLE PRECISION PI,X(1024),Y(1024)
      DO 4 I=1,N
        AX(I)= CMPLX(X(I),Y(I))
4     CONTINUE
C     N=2**M
      NV2=N/2
      NM1=N-1
      J=1
      DO 7 I=1,NM1
        IF(I .GE. J) GO TO 5
        T=AX(J)
        AX(J)=AX(I)
        AX(I)=T
5     K=NV2
6     IF(K .GE. J) GO TO 7
        J=J-K
        K=K/2
        GO TO 6
7     J=J+K
      PI=3.141592653589793
      DO 20 L=1,M

```

```

LE=2**L
LE1=LE/2
U= CMPLX(1.0,0.0)
W= CMPLX(COS(PI/LE1),SIN(PI/LE1))
DO 20 J=1,LE1
DO 10 I=J,N,LE
IP=I+LE1
T=AX(IP)*U
AX(IP)=AX(I)-T
10 AX(I)=AX(I)+T
20 U=U*W
DO 21 I=1,N
X(I)=REAL(AX(I))
Y(I)=AIMAG(AX(I))
21 CONTINUE
RETURN
END

```

```

*
***** SUBROUTINE 28 *****
*

```

```

SUBROUTINE INTGRN(C,D,Y,FRINC,PWR)
DOUBLE PRECISION Y(1024),C,D,DELY,FRINC,PWR

DELY=0.005
IMAXY=9
CALL SMPSNY(C,D,DELY,IMAXY,PWR,Y,FRINC)
C WRITE(50,*)'OUTPUT POWER=',PWR
RETURN
END

```

```

*
***** SUBROUTINE 29 *****
*

```

```

SUBROUTINE SMPSNY(C,D,DELY,IMAXY,SY,Y,FNINC)
DOUBLE PRECISION S11Y,SY,FUNHY,FUNC,FNINC
DOUBLE PRECISION SUMKY,FUND,FUNFTY,FUNYK,FT
DOUBLE PRECISION C,D,DC,DELY,HY,FRSTY,YK,Y(1024)

S11Y=0:0
SY=0.0
DC=D-C
IF(DC) 20,19,20
19 IERY1=1
RETURN
20 IF(DELY) 22,22,23
22 IERY1=2
RETURN
23 IF(IMAXY-1) 24,24,25

```

```

24   IERY1=3
      RETURN
25   HY=DC/2.0+C
      NHALFY=1
C    WRITE(*,*) 'HY=',HY,'FNINC=',FNINC
      I=ANINT(HY/FNINC)+1
C    WRITE(*,*) 'I=',I
      FUNHY=Y(I)
      SUMKY=FUNHY*DC*2.0/3.00
      I=ANINT(C/FNINC)+1
C    FUNC=Y(I)
C    WRITE(*,*) 'C=',C,'I=',I,'FNINC=',FNINC
      FUNC=Y(I)
      I=ANINT(D/FNINC)+1
      FUND=Y(I)
C    WRITE(*,*) 'D=',D,'I=',I
      SY=SUMKY+(FUNC+FUND)*DC/(6.00)
C    WRITE(*,*) 'SY=',SY,'SUMKY=',SUMKY,'FUNC=',FUNC,'FUND=',FUND
C    WRITE(*,*) 'IMAXY=',IMAXY
      DO 28 IY=2,IMAXY
      S11Y=SY
      SY=(SY-(SUMKY/2.))/2.0
      NHALFY=NHALFY*2
      ANHLFY=NHALFY
      FRSTY=C+(DC/ANHLFY)/2.0
      I=ANINT(FRSTY/FNINC)+1
      FUNFTY=Y(I)
      SUMKY=FUNFTY
      YK=FRSTY
C    WRITE(*,*) 'FRSTY=',FRSTY,'SUMKY=FUNFTY=',FUNFTY
      KLASTY=NHALFY-1
      FINCY=DC/ANHLFY
      DO 26 KY=1,KLASTY
      YK=YK+FINCY
      I=ANINT(YK/FNINC)+1
      FUNYK=Y(I)
      SUMKY=SUMKY+FUNYK
C    WRITE(*,*) 'FUNYK=',FUNYK,'FINCY=',FINCY,'YK=',YK
26   CONTINUE
      SUMKY=SUMKY*2.0*DC/(3.*ANHLFY)
C    WRITE(*,*) 'SUMKY=',SUMKY,'SY=',SY
      SY=SY+SUMKY
C    WRITE(*,*) 'SY=',SY,'S11Y=',S11Y
27   IF(ABS(SY-S11Y)-ABS(DELY*SY))29,28,28
28   CONTINUE
      SY=SY*2.0
C    WRITE(*,*) 'NO OF ITERATION IS MAX=',IMAXY

```

```

    IERY1=4
    GO TO 30
29  IERY1=0
    SY=SY*2.0
30  NOY=2*NHALFY
C   WRITE(*,*)'NO OF ITERATION IN Y=',NOY
    RETURN
    END

```

C***** SUBROUTINE 30 *****

```

SUBROUTINE PSD_FSK(FC,FT,DELTA,T,S_FSK)
DOUBLE PRECISION Ft,Fc,Gama,Delta,Sai,Alpha(2,2),B(2,2)
DOUBLE PRECISION T,S_FSK,S_norm,A1,A2,Product,SUM
DOUBLE PRECISION Theta1,Theta2

    Gama=Ft-Fc
    Theta1=Gama+Delta/2.0
    Theta2=Gama-Delta/2.0
    CALL SINC(Theta1,A1)
    CALL SINC(Theta2,A2)
C   WRITE(50,*)'THETA1=',THETA1,'A1=',A1

    SUM=0.0
    DO 12 j=1,2
    DO 13 k=1,2
C   CALL FUNB(j,k,gama,delta,B)
C   CALL FUNA(j,k,A1,A2,fun_aj,fun_ak)
    Product=B(j,k)*fun_aj*fun_ak
    SUM=SUM+Product
13  CONTINUE
12  CONTINUE
    S_norm=(A1+A2+sum)/8.0
    S_FSK=S_norm*T
C   WRITE(50,*)'S_FSK=',S_FSK,'FT=',FT
    RETURN
    END

```

C***** SUBROUTINE 31 *****

```

SUBROUTINE Sinc(Theta,Sinc_th)
DOUBLE PRECISION Theta,Sinc_th

    IF(Theta .EQ. 0.0) Then
    Sinc_th = 1.0
    Else
    D = Sin(Theta)

```



```
Sinc_th = D/Theta
ENDIF
RETURN
END
```

```
C***** SUBROUTINE 32 *****
```

```
SUBROUTINE PSDFSK(H,SFSK,FI,T)
DOUBLE PRECISION FI,H,SFSK,AN1,AN2
DOUBLE PRECISION Ih,DEL,OmegaT,T,ThetaP,ThetaM,ANUM,ADOM
DOUBLE PRECISION D1,D2,PI
```

```
PI=22.0/7.0
Ih = Anint (h)
DEL =h - Ih
OmegaT = 2.0*PI*FI*T
IF (DEL .EQ. 0.0 ) Then
AN1 = COS(OmegaT/2.0)
AN2 = (1.0/(fI-h/(2.0*T))) - (1.0/(fI+h/(2.0)))
SFSK = (AN1**2.0*AN2)/(8.0*PI*PI*T)
ELSE
```

```
Theta = PI*h
ThetaP = (OmegaT + Theta)/2.0
ThetaM = (OmegaT - Theta)/2.0
AN1 = T*(Theta**2.0)
```

```
CALL SINC(ThetaP,SincP)
CALL SINC(ThetaM,SincM)
```

```
ANUM = AN1*(SINCP**2.0)*(SINCM**2.0)
D1 = COS(Theta)
D2 = COS(OmegaT)
DNOM = 1.0 + D1**2.0 - 2.0*D1*D2
```

```
SFSK = ANUM / DNOM
```

```
ENDIF
RETURN
END
```

```
C***** FINISHED *****
```

